THE CHARACTERIZATION OF A NOVEL HUMAN CORE-SPECIFIC LYSOSOMAL

α1-6MANNOSIDASE INVOLVED IN N-GLYCAN CATABOLISM

by

CHAEHO PARK

(Under the Direction of Kelley W. Moremen)

ABSTRACT

In humans and rodents lysosomal catabolism of $Man_3GlcNAc_2$ core N-glycan structures results from the concerted actions of exoglycosidases including the broad specificity lysosomal α-mannosidase (LysMan), a core-specific α1-6mannosidase, and β-mannosidase, as well as the core chitobiose cleavage by an di-*N*-acetylchitobiase. In ungulates and carnivora, both the chitobiase and the α1-6mannosidase enzyme activities are absent suggesting a co-regulation of the two enzymes. We describe here the cloning, expression, purification and characterization of the human core-specific α1-6mannosidase with similarity to members of the glycosylhydrolase family 38. The recombinant enzyme had a pH optimum of 4.0, was potently inhibited by swainsonine and 1,4-dideoxy1,4-imino-D-mannitol, and was stimulated by Co^{+2}. NMR-based time course substrate specificity studies comparing the α1-6mannosidase with human LysMan revealed that the former enzyme selectively cleaved the α1-6mannose residue from $Man_3GlcNAc$, but not $Man_3GlcNAc_2$ or other larger high mannose structures, indicating the requirement for chitobiase action prior to α1-6mannosidase cleavage. In contrast, LysMan cleaved all of the α-linked mannose residues from $Man_{9-5}GlcNAc_2$, $Man_3GlcNAc_2$, or $Man_3GlcNAc$ structures except the core α1-6mannose residue.
Transcripts encoding the α1-6mannosidase were ubiquitously expressed in human tissues and expressed sequence tag searches in various mammalian species demonstrated a similar distribution in species-specific expression as the chitobiase. No expressed sequence tags were identified for bovine α1-6mannosidase despite the identification of two homologs in the bovine genome. The lack of conserved 5' flanking sequences for the bovine gene relative to the human α1-6mannosidase gene suggests that transcriptional gene silencing may account for the undetectable enzyme activity in bovine tissues similar to the transcriptional silencing previously identified for the bovine chitobiase gene.

INDEX WORDS: Human core-specific α1-6mannosidase, Broad specific lysosomal mannosidase, Chitobiase, N-Glycan

THE CHARACTERIZATION OF A NOVEL HUMAN CORE-SPECIFIC LYSOSOMAL α1-6MANNOSIDASE INVOLVED IN N-GLYCAN CATABOLISM

by

CHAEHO PARK

B.A., Sahmyook University, Korea, 1996

M.S., Hanyang University, Korea, 1998

A Dissertation Submitted to the Graduate Faculty of The University of Georgia in Partial Fulfillment of the Requirement for the Degree

DOCTOR OF PHILOSOPHY

ATHENS, GEORGIA

2005

© 2005

CHAEHO PARK

All Rights Reserved

THE CHARACTERIZATION OF A NOVEL HUMAN CORE-SPECIFIC LYSOSOMAL α1-6MANNOSIDASE INVOLVED IN N-GLYCAN CATABOLISM

by

CHAEHO PARK

Major Professor: Kelley W. Moremen

Committee: Michael Pierce
Debra Mohnen
William S.York

Electronic Version Approved:

Maureen Grasso
Dean of the Graduate School
The University of Georgia
May 2005

ACKNOWLEDGEMENTS

I would like to express acknowledge to my major professor, Kelley Moremen, and Steven Levery for their guidance in my work. The members of my lab, Lu, Yong, Narendra, Harminder, Alison, Steve, Heather, Gregg, Vitella and Trisha, have also been of great assistance in contributing to my doctorial research. Their encouragement and constant support pushed me forward, despite of challenging time. I would like to express appreciation to all committee members and the members of Dr. Pierce's lab.

I would like to thank to my family. They have provided love, encouragement, and support in Korea.

TABLE OF CONTENTS

Page

CHAPTER 1

LITERATURE REVIEW

I. Introduction

It has been estimated that >50% of the newly synthesized proteins in the endoplasmic reticulum are glycoproteins (1), and 90% of them are N-liked glycans (2). Glycoproteins have been shown to be essential in cell adhesion, development, and recognition events in metazoan organisms (3) as well as playing critical roles in protein folding, hormone action, immune surveillance, and acting as cell surface receptors (4).

The processing and maturation events during glycoprotein biosynthesis are sequentially ordered in the compartments of the secretory pathway including the endoplasmic reticulum (ER), intermediate compartment (IC), the Golgi complex, and trans-Golgi network (TGN) (5). The initial biosynthetic steps for N-glycan biogenesis occurs on the cytoplasmic face of the ER membrane and involves the synthesis of a polyisoprenoid lipid-linked precursor oligosaccharide. The glycan structure is extended by the addition of *N*-acetylglucosamine (GlcNAc) and mannose (Man) residues by the use of UDP-GlcNAc and GDP-Man activated sugar-nucleotide donors to form a $Man_5GlcNAc_2$-P-P-Dolichol structure, which subsequently flips into the luminal face of the ER membrane. On the luminal leaflet of the ER membrane, additional Man and Glc residues are added by the use of Dol-P-Man and Dol-P-Glc donors to produce the final mature $Glc_3Man_9GlcNAc_2$ structure covalently attached by pyrophosphoryl linkage to dolichol. The lipid-linked oligosaccharide is transferred to nascent polypeptide chains as they are extruded

through the ER membrane at their time of synthesis by the action of a multimeric complex, termed oligosaccharide transferase (OST). This complex enzyme transfers the intact glycan from the dolichol pyrophosphoryl intermediate to the amide side chains of Asn residues within the Asn-X-Ser/Thr consensus sequence on nascent polypeptide chains as they emerge from the Sec61 pore on the luminal side of the ER membrane (6, 7).

In the next steps of the N-glycan biosynthetic pathway, the oligosaccharides on the nascent polypeptides are immediately trimmed in the endoplasmic reticulum (ER). The three glucose residues are cleaved from the $Glc_3Man_9Glc_2$-Asn structure by ER glucosidases (Glucosidase I and II) (Fig. 1) (8). α1-2Mannosidases in the ER and Golgi subsequently catalyze the trimming of the four α1-2-linked mannose residues to form a $Man_5GlcNAc_2$ oligosaccharide intermediate (Fig.1). The action of GlcNAc transferase I in the medial Golgi complex then initiates the formation of complex and hybrid N-linked oligosaccharide by the addition of GlcNAc on the core Manα1-3Manβ1-4GlcNAcβ1-4GlcNAc-Asn branch to form the $GlcNAcMan_5GlcNAc_2$ intermediate. Golgi α-mannosidase II subsequently trims the final terminal α1-3 and α1-6 mannose residue to convert it to a $GlcNAcMan_3GlcNAc_2$ structure. Alternatively, maturation by another mannosidase, tentatively termed α-mannosidase III, may be capable of trimming $Man_5GlcNAc_2$ to $Man_3GlcNAc_2$ prior to the action of GlcNAc transferase I (Fig. 1) (8). The resulting $GlcNAcMan_3GlcNAc_2$ structure is further elaborated by Golgi glycosyltransferases to form the variety of complex N-glycans that are found on cellular and secreted glycoproteins (8).

In the early steps of the N-glycan biosynthetic pathway in humans, enzymatic defects resulting in incomplete lipid-linked oligosaccharide biosynthesis lead to an underglycosylation of cellular and secreted glycoproteins and the severe pathological consequences of congenital

disorders of glycosylation (CDG) type I (9, 10). There are two broad classes of enzymatic defects that lead to defects in glycosylation and lead to human disease, those that generate defective lipid-linked oligosaccharide precursors (termed CDG type I) (Table 1) and those that lead to incomplete processing of glycan structures attached to proteins (termed CDG type II) (Table 2)(11).

In addition, incomplete maturation of oligosaccharide structures by defects in terminal branching and capping reactions can result in variable consequences in development and pathology. Mouse models of enzymatic defects corresponding to human genetic diseases have also been generated to demonstrate the essential functions of specific enzymes in glycan maturation and development and have allowed the testing of additional hypotheses about the roles of specific glycan structural classes in human genetic disease (9, 12).

II. Classification of α-mannosidases

The varieties of α-mannosidases resident in different subcellular compartments have been divided into two broad classes based on their respective biochemical characteristics and positions of glycan cleavage. The two classes include enzymes that cleave single monosaccharides from the non-reducing terminus of the glycan structure (exo-α-mannosidase) and those that cleave internal mannose linkages (endo-α-mannosidases) (13). Golgi endo-α-mannosidase, the only member of the former class, cleaves $Glc_{3-1}Man_9GlcNAc_2$ structures by removal of $Glc_{3-1}Man$ to yield a $Man_8GlcNAc_2$ structure (14). The enzyme was initially identified in deoxynojirimycin and EDTA-treated rat liver Golgi membranes where glycan processing was blocked by the glucosidase inhibitor. Potential roles for the endo-α-mannosidase include the maturation of incompletely trimmed N-glycan structures once they reach the Golgi

complex as well as a potential role in glycan trimming during glycoprotein quality control in the ER (15). Endo-α-mannosidase has been purified by affinity chromatography from rat liver Golgi membranes (16), and pig liver microsomes (17). The enzyme is restricted to the chordate organisms, with the exception of several distinct classes of mollusca (18).

There are two subgroups of exo-mannosidases (19, 20); termed Class 1 and 2 mannosidases, which cleave Man residues from the non-reducing terminus of oligosaccharide structures. These enzymes are involved in either glycoprotein processing reactions or glycan catabolism. The Class 1 mannosidases (CAZY glycosylhydrolases 47, GH 47) (19) are involved in the biosynthesis and maturation of N-linked oligosaccharides on glycoproteins in the ER and Golgi as well as playing a role in targeting misfolded proteins for disposal as a part of the "quality control" process in the ER. The identification of Class 1 mannosidases is based on several biochemical criteria, such as similarities in a 440-510 amino acid catalytic domain sequence and a Ca^{2+} ion requirement for catalytic activity (19). This class of enzymes also have sensitivity to inhibition by the mannose glycone mimics, deoxymannojirimycin (dMNJ) and kifunensine (KIF), and have a substrate specificity for cleaving α1-2 mannose linkages involved in the maturation of N-linked oligomannose structures. ER mannosidase I, Golgi mannosidase IA, Golgi mannosidase IB, Golgi mannosidase IC, EDEM proteins, and fungal secreted mannosidases all belong to the Class 1 mannosidases (Fig. 2) (19).

The Class 2 mannosidases (CAZY glycosylhydrolases 38, GH 38) are a more heterogeneous collection of processing and catabolic mannosidases (19), but have additional homologs in a widely diverse array of organisms. Enzymes in this class can be distinguished by their activities toward the synthetic substrates, *p*-nitrophenyl-α-D-mannopyranoside (pNP-Man) and 4-methylumbelliferyl-α-D-mannopyranoside (4MU-Man), and some of the Class 2 α-

mannosidases may require divalent cations for catalytic activity (19). For instance, the structures of both the *Drosophila* Golgi α-mannosidase II and bovine broad specificity lysosomal α-mannosidase indicate that these enzymes contain a protein-bound Zn^{2+} ion within the active site involved in substrate binding (21, 22). In contrast, the soluble cytosolic α-mannosidase is stimulated by the addition of Co^{2+}, but not addition of Zn^{2+} ions (3, 19).

The size of the Class 2 enzymes are usually larger (110~135 kDa) than Class 1 mannosidases (73~76 kDa) (19). The Class 2 mannosidases are also highly sensitive to inhibition by the furanose transition state analogs swainsonine (SW) and 1,4-imino-1,4-imino-D-mannitiol (DIM) and less sensitive to the pyranose sugar mimics KIF and dMNJ (3). ER α-mannosidase II, Golgi α-mannosidase II, Golgi α-mannosidase IIx, cytosolic α-mannosidase, lysosomal α-mannosidase, and lysosomal α1-6mannosidase all belong to the Class 2 mannosidases (Fig. 3). Each enzyme can be distinguished by its unique characteristics of protein molecular weights, subcellular localization, pH optima, metal ion requirement, and substrate specificity (5).

The first identification of Golgi α-mannosidase II in mammalian systems was accomplished through the detection of an enzyme activity in Golgi membranes that cleaved pNP-α-Man (5, 23). This novel α-mannosidase was clearly distinguishable from the lysosomal or cytosolic α-mannosidases based on its pH optimum, kinetic properties, and molecular weight on SDS-PAGE (24). Subsequent studies using natural glycan substrates revealed a specificity for cleavage of two mannose residues from the $GlcNAcMan_5GlcNAc_2$ processing intermediate to a yield a $GlcNAcMan_3GlcNAc_2$ intermediate structure (25-27). Thus, the enzyme catalyzes the key final steps in *N*-glycan trimming essential for conversion of high mannose oligosaccharides to complex type mature oligosaccharides (28-30). Furthermore, immunoelectron microscopy has

demonstrated that Golgi α-mannosidase II is localized to the Golgi complex, but the sub-Golgi localization is variable in different cell types (31).

The *Drosophila*, mouse, and human forms of Golgi mannosidase II have been cloned and are characterized. They have been shown to be type II transmembrane proteins with a short NH_2-terminal cytoplasmic tail (five amino acids), a single transmembrane domain (21 amino acids), a short stem domain (1,124 amino acids) that is dispensable for stem catalytic activity, and a large luminal COOH-terminal catalytic domain (3). Other Golgi and ER processing mannosidases and glycosyltransferases involved in glycoprotein trimming and extension have this common structural topology (32). The greatest degree of sequence similarity among all of the Class 2 mannosidases is restricted to the luminal catalytic domain, particularly within the first ~300 amino acids of this domain (3, 5).

The broad-specificity lysosomal α-mannosidase that is involved in glycoprotein catabolism has been purified, cloned, and well characterized (33-37). It has a high degree of sequence similarity to Golgi α-mannosidase II despite its lower pH optimum and significantly broader substrate specificity (3). Unlike Golgi α-mannosidase II, the lysosomal α-mannosidase contains an NH_2-terminal signal sequence in place of the cytoplasmic tail, transmembrane domain, and stem region (3).

A soluble cytosolic α-mannosidase has also been purified, cloned, and partially characterized (38, 39). This enzyme has a more distant sequence similarity to the other Class 2 mannosidases and might contain a protein-bound Co^{2+} in the active site. This enzyme has been demonstrated to be involved in oligosaccharide catabolism of glycoproteins that have failed to fold in the lumen of the ER and have been retro-translocated into the cytoplasm for proteolytic

disposal. Consistent with its cytosolic localization, the enzyme does not appear to have cleavable signal sequence or transmembrane domain (40, 41).

Numerous additional related novel α-mannosidases have also been identified and the biochemical characteristics have been determined for partially purified enzymes from rat sperm plasma membranes or pig epididymis tissues (42-47). Cloning and further characterization of these novel mannosidases will be required to determine their respective roles in glycoprotein biosynthesis or catabolism.

III. Rat sperm mannosidase

The maturation and modification of rat sperm during capacitation within the epididymus involves many biochemical modifications to sperm surface glycoproteins by enzymes in the epididymal fluid. Among the enzymes proposed to be involved in these processes include a sperm surface α-mannosidase (42, 43).

The sperm plasma membrane α-mannosidase is clearly different from other α-mannosidases such as ER α-mannosidase, the cytosolic α-mannosidase, Golgi α-mannosidase I, and Golgi α-mannosidase II. It has been demonstrated that the rat sperm mannosidase does not cross-react with the polyclonal antibodies to the ER (48), cytosolic (38), and Golgi mannosidase II (49) mannosidases. The sperm surface enzyme is active at near neutral pH (between 6.2 and 6.5) (42) and its catalytic site is oriented towards the sperm surface (43, 44). The molecular weight of sperm mannosidase precursor forms (125 kDa and 135 kDa) is higher than the mature form (115 kDa) (44). The enzyme is activated by Co^{2+} and Mn^{2+} metal cations and has activity toward α1-2, α1-3, and α1-6mannose linkages to cleave $Man_{9-4}GlcNAc_2$ down to

$Man_{4-3}GlcNAc_2$ as well as cleaving mannose residues from [^{3}H]$Man_5GlcNAc$ and GlcNAc[^{3}H]$Man_5GlcNAc$ (42).

In an effort to identify the α-mannosidase activity in the germ cells, the enzyme was characterized from a detergent-solubilized germ cell extract where no cross-reactivity to antibodies to Golgi mannosidase IA were detected (24). In the cell extract, 25% of the total Man_9-mannosidase activity cross-reacted with an antibody raised to the rat sperm mannosidase. Enzyme assays performed in the presence dMNJ also resulted in a reduction of 25% of total mannosidase activity indicating the presence of the Class 1 enzymes in the detergent extract (42). This inhibitor does not affect sperm mannosidase activity. Thus, several α-mannosidases in addition to the sperm α-mannosidase, are also present in germ cells.

The sperm mannosidase is synthesized in the testis in a precursor form, which undergoes processing in the testicular germ cells to a smaller mature form. Western blots were used to demonstrate the presence of precursor forms (apparent molecular mass 125 kDa and 135 kDa) and a mature form (apparent molecular mass 115 kDa) on the testicular plasma membranes (44). Rat sperm plasma mannosidase appears to be an integral plasma membrane component of the rat sperm and immunolocalization indicates a peri-acrosomal localization on the sperm head (42, 44). Throughout rat spermatogenesis and sperm maturation, there appears to be a correlation between the increase of sperm α-mannosidase activity mediated by the conversion of the precursor form to generate a proteolytically-modified mature form, and the fertility of rat spermatozoa (44).

The initiation of proteolysis of the sperm mannosidase is elevated in the caput epididymis, and inclusion of trypsin inhibitors, such as benzamidine and aprotinin, largely prevent the conversion of the precursor form to the mature form (43) . Distribution of sperm α-

mannosidase in the germ cell plasma membrane fractions coincides with the plasma membrane marker enzyme, phosphodiesterase 1, confirming the subcellular localization. In these studies, the Man_9-mannosidase and the plasma membrane marker enzyme activities showed the highest relative activity in the plasma membrane fractions during cell fractionation (43).

The fertilization process requires a complex set of molecular events that enable the rat sperm to recognize and bind to the extracellular coat, or zona pellucida (ZP), of the egg (50, 51). Sperm-egg interaction is believed to involve a recognition process that involves species-specific carbohydrate recognition that depends on glycosidases and glycosyltransferases or lectin-like sugar binding proteins on the sperm plasma membrane (51-55). The role of the sperm plasma α-mannosidase in glycan modification and potential contributions to sperm-egg interactions remain to be resolved.

IV. Pig epididymal α-mannosidases

In an alternative set of studies, two distinctive of α-mannosidase activities (a lysosomal type α-mannosidase and the novel 135 kDa α-D-mannosidase) were purified from porcine cauda epididymal fluid (56). The lysosomal type α-mannosidase was synthesized and secreted in the distal caput and the proximal corpus epididymis (46, 56). The activity for hydrolysis of oligosaccharides significantly increased from proximal caput epididymis to distal caput epididymis. Using RT-PCR analysis, it was shown that the expression level of α-mannosidase mRNA was low in other parts of the epididymis and testicular tissue, but high in the distal caput epididymis (57). *In vitro*, the optimal pH for this enzyme to hydrolyze oligosaccharides is 3.5-4.0 (58). The purified enzyme is a tetramer shown to have an apparent molecular weight of 275 kDa and is composed of subunits of $[63\ kDa]_2 \cdot [51\ kDa]_2$ composition. It is likely derived from the

cleavage of an initial dimer of $[114\ kDa]_2$ composition (56). NH_2-terminal sequences of peptides derived from the porcine enzyme have the greatest similarity to the human, bovine and feline lysosomal α-mannosidases indicating that the epididymal enzyme is likely a secreted form of the porcine lysosomal α-mannosidase.

In a pH-dependency study, the epididymal lysosomal type α-mannosidase could cleave both pNP-Man and high-mannose oligosaccharides at pH 4.0. However, at lower pH (pH 3.0) the enzyme could not cleave oligosaccharides yet retained pNP-Man hydrolyzing activity. In contrast, the enzyme could cleave very little pNP-Man substrate at neutral pH, but glycan cleavage was still retained (59). The cause of these enzymatic differences is not clear.

In the acid extract of rat epididymis, the major acidic α-mannosidase was identified as equivalent to the broad-specificity lysosomal α-mannosidase (59). Rat lysosomal α-mannosidase hydrolyzes $Man_{9\text{-}5}$ high mannose oligosaccharides and linear Manα1-2Manα1-2Manα1-3Manβ1-4GlcNAc structures, but cleaves the branched trimannosyl core oligosaccharide (Manα1-6[Manα1-3]Manβ1-4GlcNAc) very slowly (59).

The lysosomal type α-mannosidase from the porcine epididymal fluid quickly hydrolyzes α1-2 mannose residues in high mannose oligosaccharides, but hydrolyzes $Man_5GlcNAc$ and the branched $Man_3GlcNAc$ oligosaccharides slowly (56). These results suggest differences in the substrate specificity between the rat and pig epididymal enzymes.

V. Alternate forms of epididymal α-mannosidase activity

In addition to the broad-specificity lysosomal-like mannosidase in epididymal fluid, a second activity was also detected and purified from porcine epididymal fluid (47) as a 135 kDa polypeptide that was proposed to be involved in sperm maturation. The purified porcine

epididymal mannosidase could cleave pNP-Man in the contrast to the inability of the rat sperm plasma membrane enzyme to cleave this substrate (47, 59). Both enzymes were able to cleave natural oligosaccharide substrates (47, 59). The purified enzyme from porcine epididymal fluid can weakly hydrolyze $Man_8GlcNAc_2$ down to $Man_6GlcNAc_2$ and has a optimum pH at 6.5 (46, 47, 60). The effects of alkaloid inhibitors such as SW, DIM, DMJ, and KIF have not been reported for either of the enzymes. The relationship between porcine epididymal mannosidase and rat sperm mannosidase has not been established.

Partial peptide sequence data were obtained from trypsin-digested purified 135 kDa epididymal α-mannosidase and the cDNA encoding the enzyme was cloned using oligonucleotide probes (47, 58). The resulting protein sequence had 25.7% amino acid sequence homology with the lysosomal α-mannosidase precursor from *Dictyostelium discoideum*. By Northern blot analysis, only corpus and cauda epididymis contains mRNA encoding the 135 kDa enzyme among all porcine tissues examined (brain, lung, liver, heart, spleen, kidney, muscle, and testis), thus this protein is expressed uniquely in porcine epididymis (47). Subsequent studies of the mouse homolog of the 135 kDa mannosidase revealed mRNA expression in testicular tissues by *in situ* hybridization, primarily in type A spermatogonia in stages IX-XI (57).

In contrast to the prior data, more recent studies have attempted to employ the promoter of the 135 kDa mannosidase for spermatogonia-specific transgenic protein expression. Northern blot studies revealed that the mouse homologue of the 135 kDa α-mannosidase is ubiquitously expression in virtually all mouse tissues (61). These data indicate that the tissue distribution of the mouse homologue (termed the MAN2B2 gene) is not exclusively expressed in epididymis tissues as previously proposed (61). Although a cDNA encoding pig 135 kDa α-mannosidase was isolated from a pig cDNA library (47), the identity of the rat sperm mannosidase from the

plasma membrane has not been determined. Therefore, the relationship of the latter enzyme to other Class 2 mannosidases remains to be resolved.

VI. Lysosomal mannosidase

Catabolism of the mannose linkages associated with the N-glycans on cellular and secreted glycoproteins is mainly accomplished by a broad specificity lysosomal α-mannosidase. The broad specificity lysosomal α-mannosidase is an exo-α-mannosidase catalyzing the hydrolysis of α1-2, α1-3, and α1-6mannosidic linkages present in complex, hybrid, and high-mannose Asn-linked glycans (5, 62). The enzyme is responsible for the catabolic degradation of N-linked glycans and release of free monosaccharides in the lysosomes of all eukaryotic organisms that have been examined (63) and the cDNA has been cloned, expressed, and the recombinant proteins have been purified and characterized from a number of species (33, 37, 64, 65).

The bovine, feline, and human lysosomal α-mannosidases have also been partially purified from liver tissues by using a combination of ammonium sulfate precipitation and Con A-Sepharose chromatography (63, 65-68). The enzymes release α1-2, α1-3, and α1-6 linked mannose residues from oligosaccharide substrates, $Man_{9-4}GlcNAc_2$ (65). The pentasaccharide, $Man_3GlcNAc_2$, was degraded by bovine liver lysosomal α-mannosidase, with rapid cleavage of the Manα1-3Man linkage and slow cleavage of the Manα1-6Man linkage. The end product is $ManGlcNAc_2$ core structure (Manβ1-4GlcNAcβ1-4GlcNAc). The digested oligosaccharide products are analyzed using TLC and HPLC (65).

The recent cloning of the lysosomal α-mannosidase from several species has allowed a comparison of the sequences and biochemical characteristics with other Class 2 glycohydrolases involved in glycoprotein biosynthesis and catabolism. The dendrogram shows four sequence clades for the GH 38 α-mannosidase from the respective species (Fig 3). Each of the four clades has a unique specificity and function in glycan processing or catabolism. The first clade is comprised of Golgi processing glycosidases, including Golgi α-mannosidase II and Golgi α-mannosidase IIx. The second clade is comprised of the broad specificity lysosomal α-mannosidases from various species. The third clade is a collection of enzymes from a broad assortment of species including bacteria, archaea, and eukaryota. The mammalian member of this clade is represented by the cytosolic mannosidase involved in glycan catabolism in the cytosol. The final clade is comprised of the α1-6mannosidases that are the subject of this dissertation.

The cloning of the cDNAs encoding the murine (37) and human (33) lysosomal α-mannosidases have allowed the expression, purification, and characterization of the recombinant expression products from the recombinant host, *Pichia pastoris*. These recombinant expression products were highly similar to the enzyme purified from mammalian sources (33, 37). The human and mouse lysosomal α-mannosidases have similar pH optima, K_m, and V_{max} values, are inhibited by swainsonine, and have activity toward natural substrates (37).

The murine cDNA encoding a lysosomal α-mannosidase was cloned, based on regions of protein sequence conservation between the lysosomal α-mannosidase from *Dictyostelium discoideum* and the murine Golgi α-mannosidase II (37). The coding region encoding the murine enzyme was 3.1 kb in length and encoded a polypeptide of 992 amino acids containing a putative NH_2-terminal signal sequence and 11 potential N-glycosylation sites. The deduced amino acid

sequence was 76.5% identical to the human lysosomal α-mannosidase and 38.1% identical to the lysosomal α-mannosidase from *D. discoideum* (69, 70).

VII. Genetic defect in the lysosomal α-mannosidase and accumulation of glycan structures

A genetic deficiency of the broad specificity lysosomal α-mannosidase, characterized by a defect in the coding region, causes the accumulation of undegraded oligosaccharides in the lysosomes of various animal models. Similar to other lysosomal storage diseases (Table 3), the genetic disease, termed α-mannosidosis, results in the inability to cleave glycans that are normally catabolically cleared from the lysosomal system. The result is a proliferation of distended lysosomes that eventually cause disease pathology. Human α-mannosdiosis patients are characterized by frequent infections, vomiting, coarse features, macroglossia, flat nose, large clumsy ears, widely spaced teeth, large head, big hands and feet, tall stature, slight hepatosplenomegaly, muscular hypotonia, lumbar gibbus, radiographic skeletal abnormalities, dilated cerebral ventricles, lenticular opacities, hypogammaglobulinemia, 'storage cells' in the bone marrow, and vacuolated lymphocytes in the bone marrow (71). Most affected patients die in early childhood (72).

The autosomal recessive human disorder (71), is characterized by massive accumulation of undegraded oligosaccharides, predominately extended linear structures containing a Manα1-3Manβ1-4GlcNAc core and variable extensions on the non-reducing terminal Man residue (63). Similar structures are accumulated in rodent models of the lysosomal storage disease. In contrast, oligosaccharides accumulating in the bovine and feline models of α-mannosdiosis contain a branched Manα1-3[Manα1-6]Manβ1-4GlcNAc$_2$ core that also contains two core GlcNAc residues. A linkage between catabolism of the reducing and non-reducing termini of N-glycan

core structures has been identified in studies on the substrate specificities of the respective catabolic enzymes as described below (73).

VIII. Catabolism of the N-glycan core structure by lysosomal α-mannosidases and chitobiase

The substrate specificity of broad specificity lysosomal α-mannosidases from human (63), rat (74), bovine and feline liver (65) involved in the catabolism of high mannose oligosaccharides results in the cleavage of α1-2, α1-3, and α1-6mannosidic linkages on N-linked glycans. Despite the broad linkage specificity of the major lysosomal α-mannosidase, the enzyme has poor efficiency for the cleavage of the final Manα1-6Man linkage in the Manα1-6Manβ1-4GlcNAc$_2$ core structure. The inefficiency in cleavage of this linkage, combined with the absence of the Manα1-6Man in the linear Manα1-3Manβ1-4GlcNAc series of glycans that accumulate in α-mannosidosis patients indicates that a separate enzyme must be involved the catabolism of this linkage. The presence of the residual unique α-mannosidase activity in cells of α-mannosidosis patients would account for the cleavage of the core Manα1-6Man linkage and the accumulation of linear glycans in the absence of the broad specificity α-mannosidase (75, 76).

At the reducing terminus of the N-glycan core, a chitobiase acts after the glycosylasparaginase to result in the sequential cleavage of the Asn residue and a single GlcNAc from the GlcNAcβ1-4GlcNAc core structure (77, 78). The chitobiase is active in humans and rodents, but no activity has been detected in cats, cattle, sheep, dogs, and pigs (62). In humans and rodents, core glycans containing a single GlcNAc accumulate in α-mannosidosis models. In contrast, cattle and cats accumulate glycans containing a GlcNAc$_2$ core (79, 80). These data

indicate that the presence or absence of this chitobiase can account for the differences in the core structures of the glycans in the various mammalian α-mannosidosis models.

VIII. The core-specific lysosomal α1-6mannosidase

The major urinary oligosaccharides in human α-mannosidosis patients are extended glycans based on the Manα1-3Manβ1-4GlcNAc core structure (81, 82). It was unexpected that glycans accumulating in the α-mannosidosis patients would lack the core Manα1-6Man linkage. In contrast, glycans that accumulates in cells or animals treated with SW (a potent lysosomal α-mannosidase inhibitor) accumulated structures containing a Manα1-3[Manα1-6]Manβ1-4GlcNAc core (75, 76). These data strongly suggest that an alternative enzyme must be responsible for the cleavage of the α1-6 linked mannose residue from core structure oligosaccharide in lysosomes and that this latter enzyme in sensitive to inhibition by SW (66-68).

A novel core-specific α-mannosidase capable of cleaving the α1-6mannose residue from Manα1-6Manβ1-4GlcNAc structures was initially identified in human α-mannosidase fibroblasts (67), since these cells were significantly reduced in the competing activity of the major broad-specificity α-mannosidase (67). The core-specific lysosomal α1-6mannosidase was initially difficult to characterize because of the small amounts of enzyme in human fibroblasts. In subsequent studies, the novel core-specific α-mannosidase was partially purified from normal human spleen (68) and rat liver (66), and the substrate specificity and characteristics of this enzyme were determined. The human lysosomal α1-6mannosidase was partially purified from human spleen using a combination of ammonium sulfate precipitation, concanavalin A-Sepharose, DEAE-Sephadex A50, and Sephacryl S-300 chromatography (68). This enzyme had a distinctive substrate specificity from the major broad-specificity lysosomal mannosidase,

hydrolyzing the α1-6mannose residue-linked to the core β1-4 linked mannose of N-glycan (68). Enzyme assays were performed using free glycan core structures and the enzymatic products were analyzed by using HPLC. The activity of lysosomal core-specific α1-6mannosidase was optimal at pH 4.0, and no activity was detected at neutral pH (68). The molecular weight was ~180 kDa determined by gel filtration on Sephacryl S-300 (68). Both Co^{2+} and Zn^{2+} cations stimulated the enzyme activity and SW and DIM both inhibited enzyme activity, but dMNJ had no effect on enzyme activity (68). When the activity toward pNP-Man was examined, the enzyme had poor activity toward the synthetic substrate (68).

The core-specific lysosomal α1-6mannosidase was also partially purified from rat liver (66). The enzyme substrate specificity was investigated using high mannose oligosaccharides and glycoasparagine glycans obtained from the tissues and urine of patients suffering from aspartylglucosaminuria (83). The $Man_3GlcNAc_2Asn$ structure is prepared from the urine of patient suffering from aspartylglucosaminuria (84), while the core oligosaccharides $Man_3GlcNAc_{2\text{-}1}$ and $Man_2GlcNAc_{2\text{-}1}$ structures were obtained by aspartly-N-acetyl-β-D-glucosaminidase and endo-N-acetyl-β-D-glucosaminidase digestions (66). The pattern of digestion products were identified by the thin layer chromatography (TLC) analysis demonstrating that hydrolysis of the α1-6Man linkage in the core oligosaccharide structure could only be accomplished with substrates containing a single GlcNAc residue at the core. These data indicated that the lysosomal α1-6mannosidase was dependent upon the prior action of the both glycosylasparaginase and chitobiase (66).

The novel α-mannosidase hydrolyzed the core α1-6mannosidic linkage of $Man_3GlcNAc$, however, cleavage of the α1-3 linked core mannose residue was extremely slow. In addition, the novel α1-6mannosidase did not catalyze the hydrolysis of other α-mannosyl residues on

$Man_{9\text{-}5}GlcNAc_{2\text{-}1}$ structures, even if structures contained α1-6Man residues at their non-reducing termini (62, 66-68). Since the human lysosomal mannosidase can not catalyze efficiently the hydrolysis of the α1-6 mannosidic linkage in the core structure, the α1-6mannosidase might have evolved to assist broad specificity lysosomal mannosidase for the efficient breakdown of the core N-glycan structures.

A hypothesis has also been proposed that the α1-6mannosidase and chitobiase are functionally linked based on two criteria. First, the α1-6mannosidase can only efficiently hydrolyze the N-glycan core α1-6mannose residue after the action of chitobiase and removal of a core GlcNAc residue. Second, the spectrum of species that express the α1-6mannosidase and the chitobiase enzyme activities are similar (62, 85).

The chitobiase gene is present in all mammalian species, but in some species (including ungulates, cats and dogs), transcripts encoding the chitobiase are suppressed by defective transcription resulting from alterations in the promoter sequences (86). The chitobiase gene from human and bovine sources have similar sizes, similar number of exons, and the translated proteins sequences are quite similar (86). In contrast, human upstream 5'-flanking regions differ significantly from the bovine genes. The human chitobiase at 5'-flanking region shows sequences characteristic of a housekeeping gene (86) including a TATA box and several highly GC-rich segments in the upstream 5'-flanking regions. There are also several Sp1 and AP-2 *cis* transcription factor binding sites in the upstream region (86). In contrast, the bovine chitobiase 5'-flanking regions contains no TATA box, but it does contain repetitive element sequences that would be predicted to impede transcription (79, 80, 86). In bovine tissues, the transcripts encoding the chitobiase are very low in abundance and enzyme activity is undetectable (86).

The sequence data on the bovine chitobiase gene suggests that, during mammalian evolution in the late Cretaceous and Paleocene period, the expression of chitobiase gene transcripts in unglulates and carnivora has likely been lost to result in an absence of the enzyme activity in these species. The data suggest that chitobiase gene expression is selectively inactivated through defects in promoter sequences in some mammalian species (cats, sheep, dogs, and pigs), but not others (humans rodents) (86). The core-specific α1-6mannosidase is also predicted to be active only in the latter mammalian species. Thus, it is possible that the two enzymes are genetically linked to accomplish the efficient catabolism of glycan structures in mammals.

If the hypothesis that the chitobiase and α1-6mannosidase function cooperatively and are commonly expressed in mammalian tissues to accomplish the efficient catabolism of glycan structures in mammals is correct, then it is possible that the two enzymes are genetically linked. It is a goal of this dissertation to determine if the α1-6mannosidase and chitobiase are similarly expressed in mammalian species, because the expression of latter gene transcripts has been lost in ungulates, cats, and dogs during the course of mammalian evolution (62). The studies in this dissertation will describe the cloning, expression, purification, and characterization of the human α1-6mannosidase and the determination of the transcript expression pattern in mammalian cells and tissues in an effort to resolve the issues relating to glycan catabolism and co-regulation with the chitobiase in a variety of mammalian species.

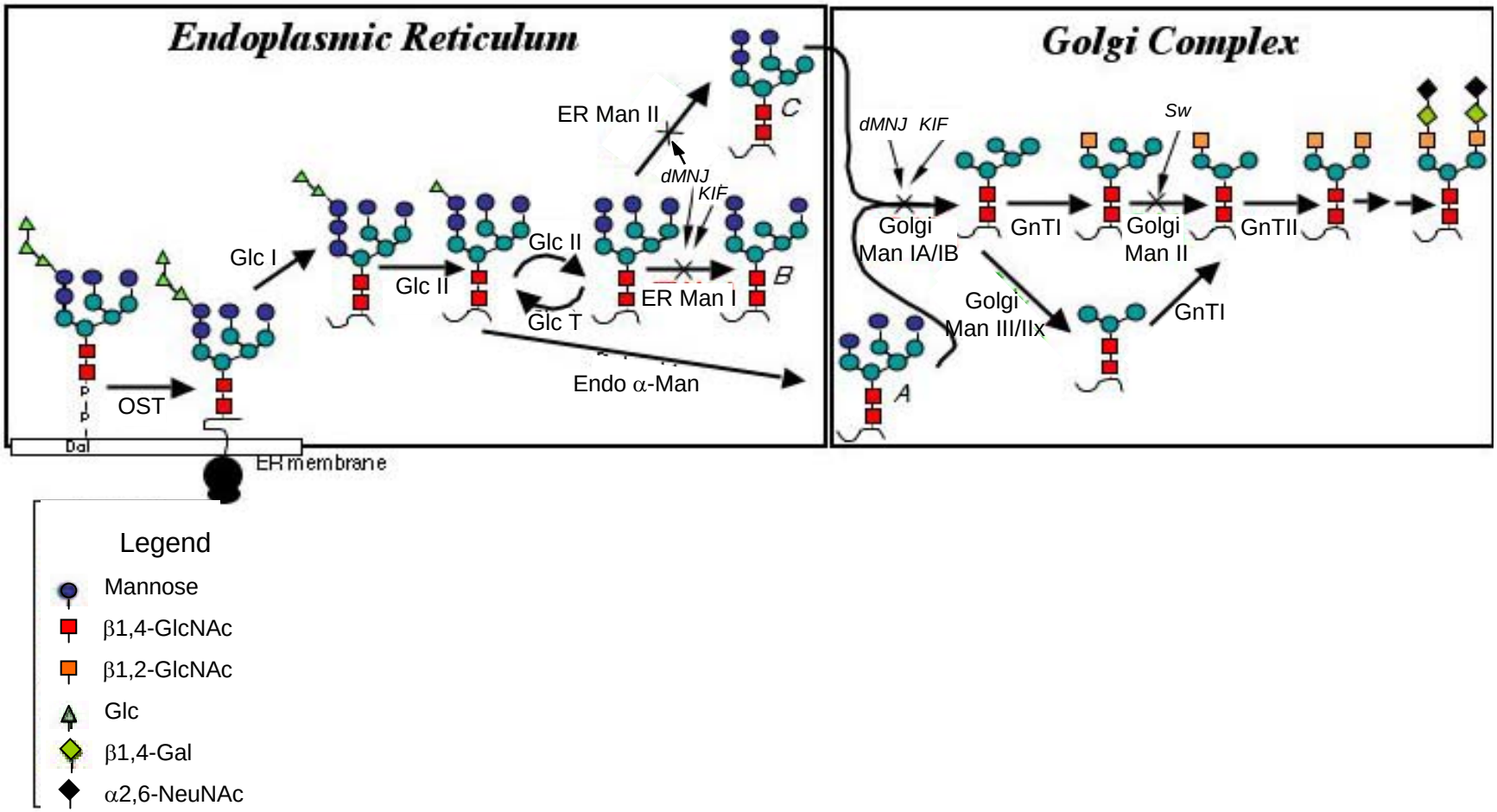

Fig. 1. The maturation of asparagine-linked oligosaccharides on nascent protein in the ER and Golgi. *(Moremen, Bichim. Biophys. Acta, 2002)*

Class 1 mannosidases

Glycosylhydrolase Family 47

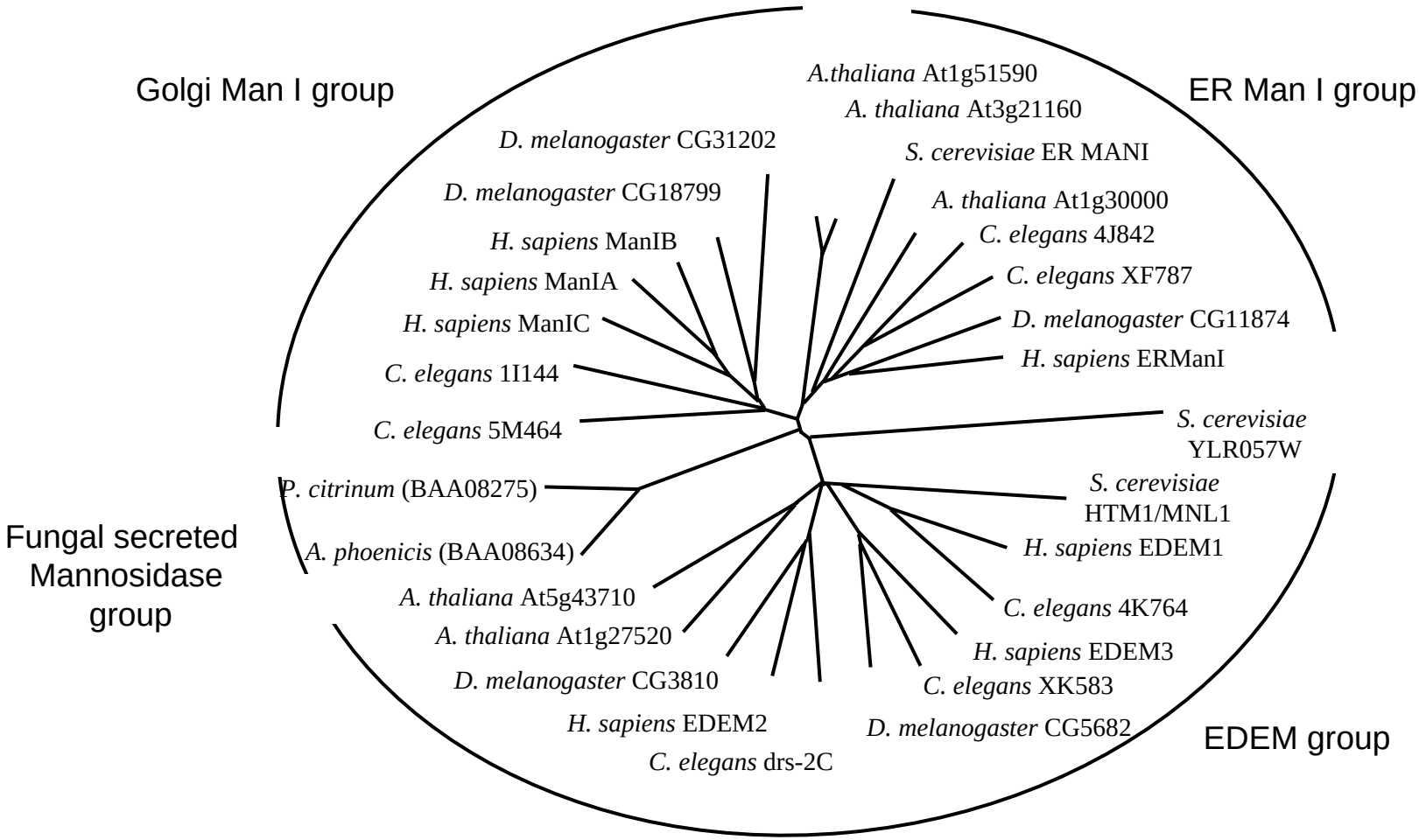

Fig. 2. Dendrogram representing the sequence similarity among Class 1 mannosidases.

S. W. Mast, K. Diekman, K. Karaveg, A. Davis, R.N, Sifers, and K. W. Moremen Glycobiology 2005

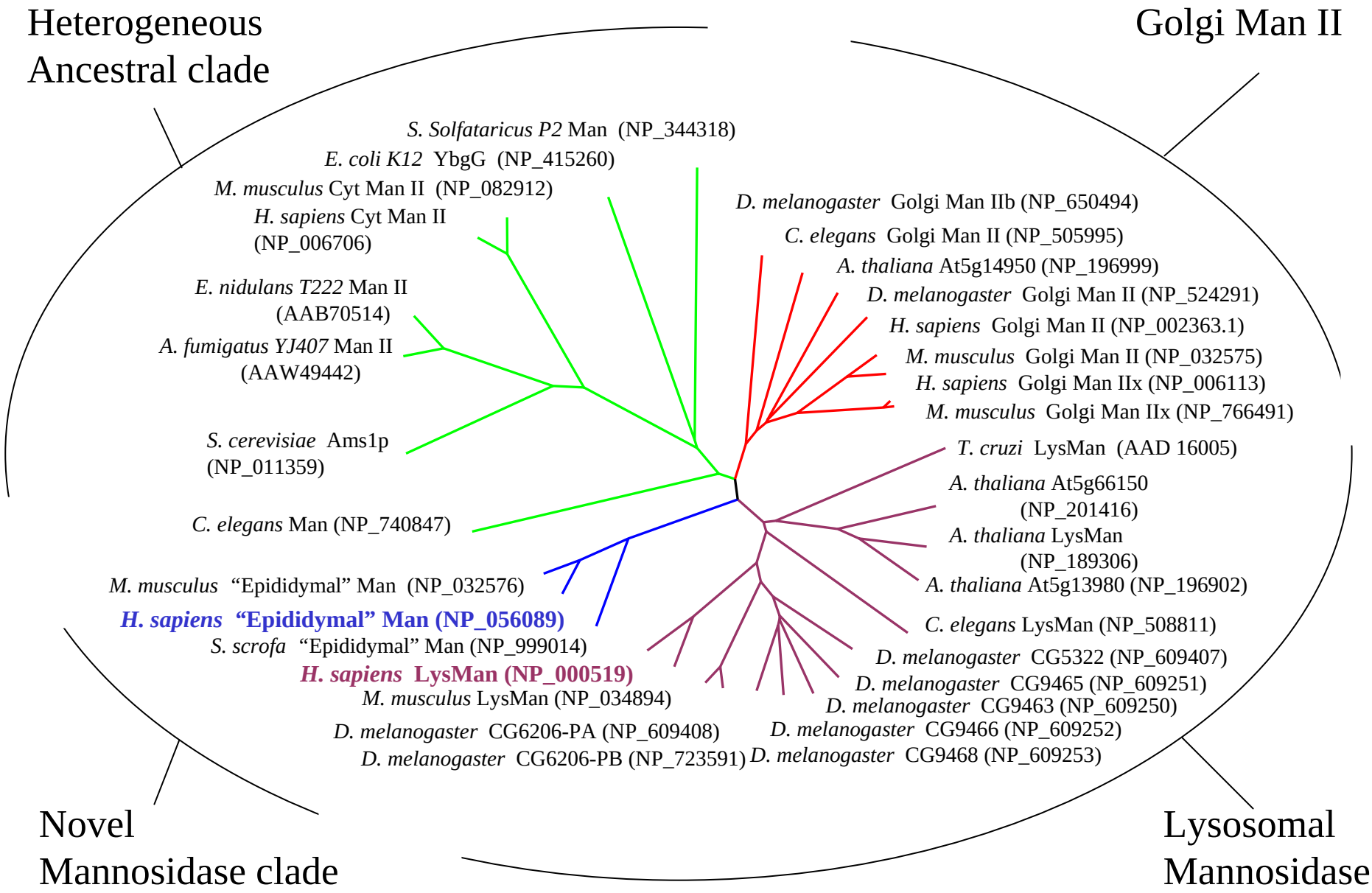

Fig. 3. Dendrogram representing the sequence similarity among Class 2 mannosidases.

Table 1. CDG type I human diseases, information provided in the "Encyclopedia of Biological Chemistry", from Elsevier Vol 1 pp34-39 and "Pediatric Neurology: Principles and Practice" 4th Edition.

Disorder	Gene	Enzyme	Key features
CDG-Ia	PMM 2	Phosphomannomutase II	Developmental delay, hypotonia, esotropia, lipodystrophy, cerebellar hypoplasia, stroke-like episodes, seizures
CDG-Ib	MPI	Phosphomannose Isomerase	Hepatic fibrosis, protein losing enteropathy, coagulopathy, hypoglycemia
CDG-Ic	ALG6	Glucosyltransferase I Dol-P-Glc: Man9GlcNAc2-PP-Dol Glucosyltransferase	Moderate developmental delay, hypotonia, esotropia, epilepsy
CDG-Id	ALG3	Dol-P-Man: Man5GlcNAc2-PP-Dol Mannosyltransferase	Profound psychomotor delay, optic atrophy, acquired microcephaly, iris colobomas; hypsarrhythmia
CDG-Ie	DPM 1	Dol-P-Man Synthase I GDP-Man: Dol-P-Mannosyltransferase	Profound psychomotor delay, severe developmental delay, optic atrophy, acquired microcephaly, epilepsy, hypotonia, mild dysmorphism, coagulopathy
CDG-If	MPDU1	MPDU1/Lec35	Short stature, icthyosis, psychomotor retardation, pigmentary retinopathy
CDG-Ig	ALG12	Dol-P-Man: Man7GlcNAc2PP-Dol Mannosyltransferase	Hypotonia, facial dysmorphism, psychomotor retardation, acquired microcephaly. Frequent infections
CDG-Ih	ALG8	Glucosyltransferase II Dol-P-Glc: Glc1Man9GlcNAc2-PP-Dol Glucosyltransferase	Hepatomegaly, protein-losing enteropathy, renal failure, hypoalbuminemia, edema, ascites
CDG-Ii	ALG2	Mannosyltransferase II GDP-Man: Man1GlcNAc2-PP-Dol Mannosyltransferase	Normal at birth; developmental delay, hypomyelination, intractable seizures, iris colobomas, hepatomegaly, coagulopathy
CDG-Ij	DPAGT1	UDP-GlcNAc: dolichol phosphate N-acetylglucosamine 1-phosphate transferase	Severe developmental delay, hypotonia, seizures, microcephaly, exotropia
CDG-Ik	ALG1	Mannosyltransferase I GDP-Man: GlcNAc2-PP-Dol Mannosyltransferase	Severe psychomotor retardation, hypotonia, acquired microcephaly, intractable seizures, fever, coagulopathy, nephrotic syndrome, early death
CDG-I*L*	ALG9	Mannosyltransferase Dol-P-Man: Man6 and 8GlcNAc2-PP-Dol Mannosyltransferase	Severe microcephaly, hypotonia, seizures, hepatomegaly

Table 2. CDG type I human diseases, information provided in the "Encyclopedia of Biological Chemistry", from Elsevier Vol 1 pp34-39 and "Pediatric Neurology: Principles and Practice" 4th Edition.

Disorder	Gene	Enzyme	Key features
CDG-IIa	MGAT2	GlcNAc-Transferase 2 (GnT II)	developmental delay, dysmorphism, stereotypies, seizures
CDG-IIb	GLS1	Glucosdase I	Dysmorphism, hypotonia, seizures, hepatomegaly, hepatic fiborsis (death at 2.5 months)
CDG-IIc	SLC35C1 /FUCT1	GDP-Fucose Transporter	Recurrent infections, persistent neutrophilia, developmental delay, microcephaly, hypotonia (normal Tf)
CDG-IId	B4GALT1	β1,4 galactosyltransferase	Hypotonia (myopathy), spontaneous hemorrhage, Dandy-Walker malformation
CDG-IIe	COG7	Conserved oligomeric Golgi complex subunit 7	Fatal in early infancy; dysmorphism, hypotonia, intractable seizures, hepatomegaly, progressive jaundice, recurrent infections, cardiac failure.
CDG-IIf	SLC35A1	CMP-Sialic acid transporter	Thrombocytopenia, no neurologic symptoms, normal Tf, abnormal platelet glycoproteins

Table 3. Lysosomal storage diseases

*Lysosomal Storage Diseases**

Disease Name	Omim #	Enzyme Defect	Substance Stored	Chromosome Location
A. Glycogenosis Disorders				
Pompe Disease	232300	Acid-α1, 4-Glucosidase	Glycogen α1-4 linked Oligosaccharides	17
B. Glycolipidosis Disorders				
GM1 Gangliodsidosis	230500	β-Galactosidase	GM1 Ganliosides	3
Tay-Sachs Disease	272800	β-Hexosaminidase A	GM2 Ganglioside	15
GM2 Gangliosidosis:	272750	GM2 Activator Protein	GM2 Ganglioside	5
Sandhoff Disease	268800	β-Hexosamindase A&B	GM2 Ganglioside	5
Fabry Disease	301500	α-Galactosidase A	Globosides	X
Gaucher Disease	230900	Glucocerebrosidase	Glucosylceramide	1
Metachromatic Leukodystrophy	250100	Arylsulfatase A	Sulphatides	22
Krabbe Disease	245200	Galactosylceramidase	Galactocerebroside	14
Niemann-Pick	257200	Acid Sphingomyelinase	Sphingomyelin	18
Niemann-Pick, Type C	257200	Cholesterol Esterification Defect	Sphingomyelin	18
Nieman-Pick, Type D	257250	Unknown	Sphingomyelin	18
Farber Disease	228000	Acid Ceramidase	Ceramide	?
Wolman Disease	278000	Acid Lipase	Cholesteryl Esters	10
C. Mucopolysaccharide Disorders				
Hurler Syndrome (MPS IH)	252800	α-L-Iduronidase	Heparan & Dermatan Sulfate	4
Scheie Syndrome (MPS IS)	252800	α-L-Iduronidase	Heparan & Dermatan Sulfate	4
Hurler-Scheie (MPS IH/S)	252800	α-L-Iduronidase	Heparan & Dermatan Sulfate	4
Hunter Syndrome (MPS II)	309900	Iduronate Sulfatase	Heparan & Dermatan Sulfate	X
Sanfilippo A(MPS IIIA)	252900	Heparan N-Sulfatase	Heparan Sulfate	17
Sanfilippo B(MPS IIIB)	252920	α-N-Acetylglucosaminidase	Heparan Sulfate	17
Sanfilippo C(MPS IIIC)	252930	Acetyl-CoA-Glucosaminide Acetyltransferase	Heparan Sulfate	14
Sanfilippo D(MPS IIID)	252940	N-Acetylglucosamine -6-Sulfatase	Heparan Sulfate	12
Morquio A(MPS IVA)	253000	Galactosamine-6-Sulfatase	Keratan Sulfate	16
Morquio B(MPS IVB)	253010	β-Galactosidase	Keratan Sulfate	3
Maroteaux-Lamy (MPS VI)	253200	Arylsulfatase B	Dermatan Sulfate	5
Sly Syndrome (MPS VII)	253220	β-Glucuronidase	?	7
D. Oligosaccharide/Glycoprotein Disorders				
α-Mannosidosis	**248500**	**α-Mannosidase**	**Mannose/Oligosaccharides**	**19**
β-Mannosidosis	248510	β-Mannosidase	Mannose/Oligosaccharides	4
Fucosidosis	230000	α-L-Fucosidase	Fucosyl Oligosaccharides	1
Asparylglucosaminuria	208400	N-Aspartyl-Asparylglucosamine β-Glucosaminidase	Asparagines	4
Sialidosis (Mucolipidosis I)	256550	α-Neuraminidase	Sialyloligosaccharides20	
Galactosialidosis (Goldberg Syndrome)	256540	Lysosomal Protective Protein Deficiency	Sialyloligosaccharides	20
Schindler Disease	104170	α-N-Acetyl-Galactosaminidase	?	22
E. Lysosomal Enzyme Transport Disorders				
Mucolipidosis II (I-Cell Disease)	252500	N-Acetylglucosamine-1-Phosphotransferase	Heparan Sulfate	4
F. Lysosomal Membrane Transport Disorders				
Cystinosis	219750	Cystine Transport Protein	Free Cystine	17
Salla Disease	269920	Sialic Acid Transport Protein	Free Sialic Acid and Glucuronic Acid	6
Infantile Sialic Acid Storage Disease	268740	Sialic Acid Transport Protein	Free Sialic Acid and Glucuronic Acid	6
G. Other				
Batten Disease (Juvenile Neuronal Ceroid Lipofuscinosis)	204200	Unknown	Lipofuscins	16
Infantile Neuronal Ceroid Lipofuscinosis	256730	Palmitoyl-Protein Thioesterase	Lipofuscins	1
Mucolipidosis IV	252650	Unknown	Gangliosides & Hyaluronic Acid	?
Prosaposin	176801	Saposins A, B, C or D		10

* From: www.geneticcentre.org/biochemical.htm

Fig. 4. Simplified scheme of glycoprotein biosynthesis and glycoprotein catabolism. Enzymes abbreviated as follows: OST, oligosaccharide transferase; GlcI, glucosidase I; Glc II, glucosidase II, Glc T, UDP-Glc: glycoprotein glucosyl-transferase; ER Man I, ER mannosidase I; Golgi Man IA/IB, Golgi mannosidases IA and IB; GnTI, GlcNAc transferase I; Golgi Man II, Golgi mannosidase II. Processing inhibitors block enzyme reactions indicated by an X and a thin arrow with the following abbreviations: dMNJ, 1-deoxymannojirimycin; KIF, kifunensine; Sw, swainsonine. Oligosaccharide structures are indicated in the legend in the lower left. Solid boxes indicate the membrane boundaries of the ER and Golgi as labeled in the figure.

Glycoprotein Biosynthesis

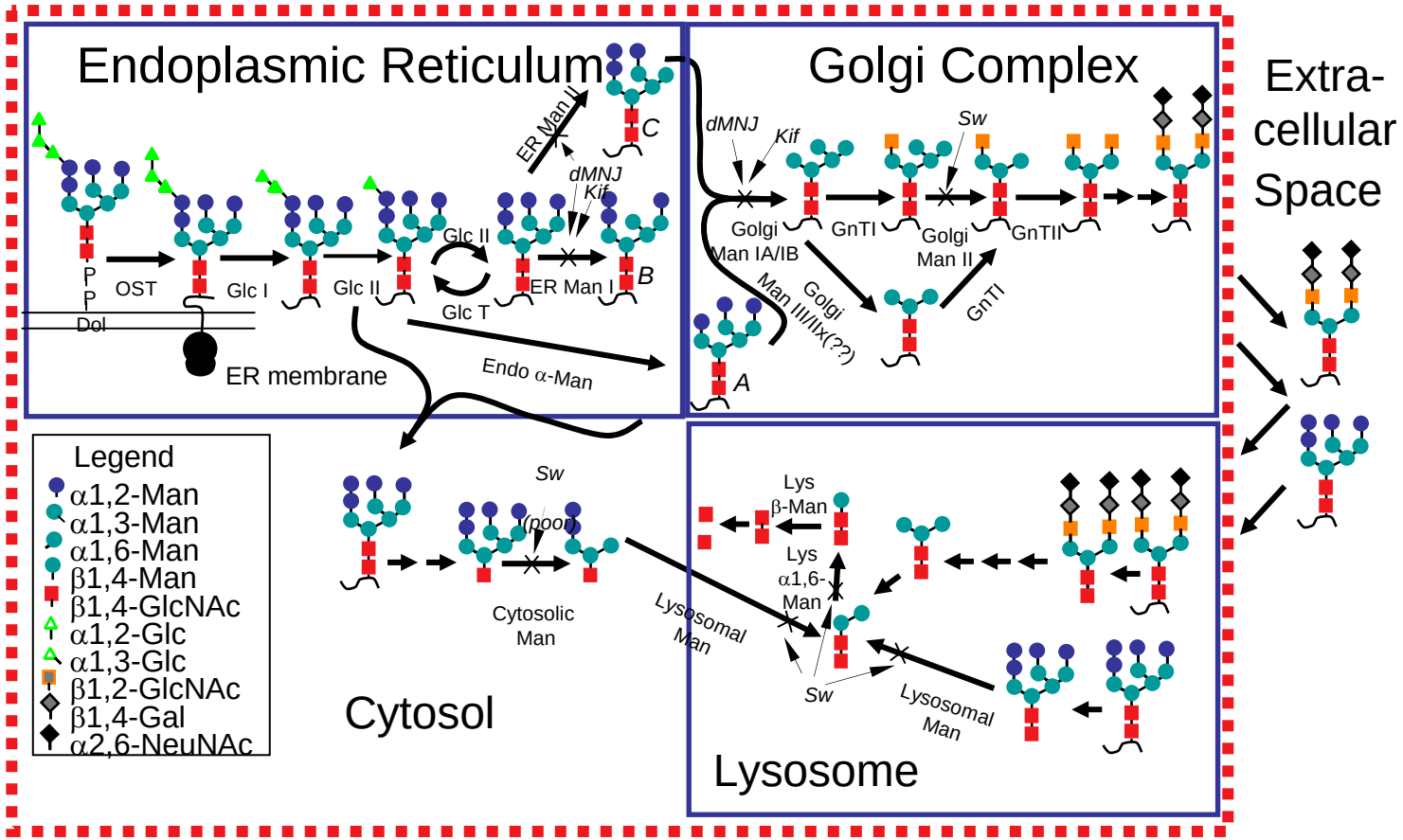

Glycoprotein Catabolism

(Moremen, Bichim. Biophys. Acta, 2002)

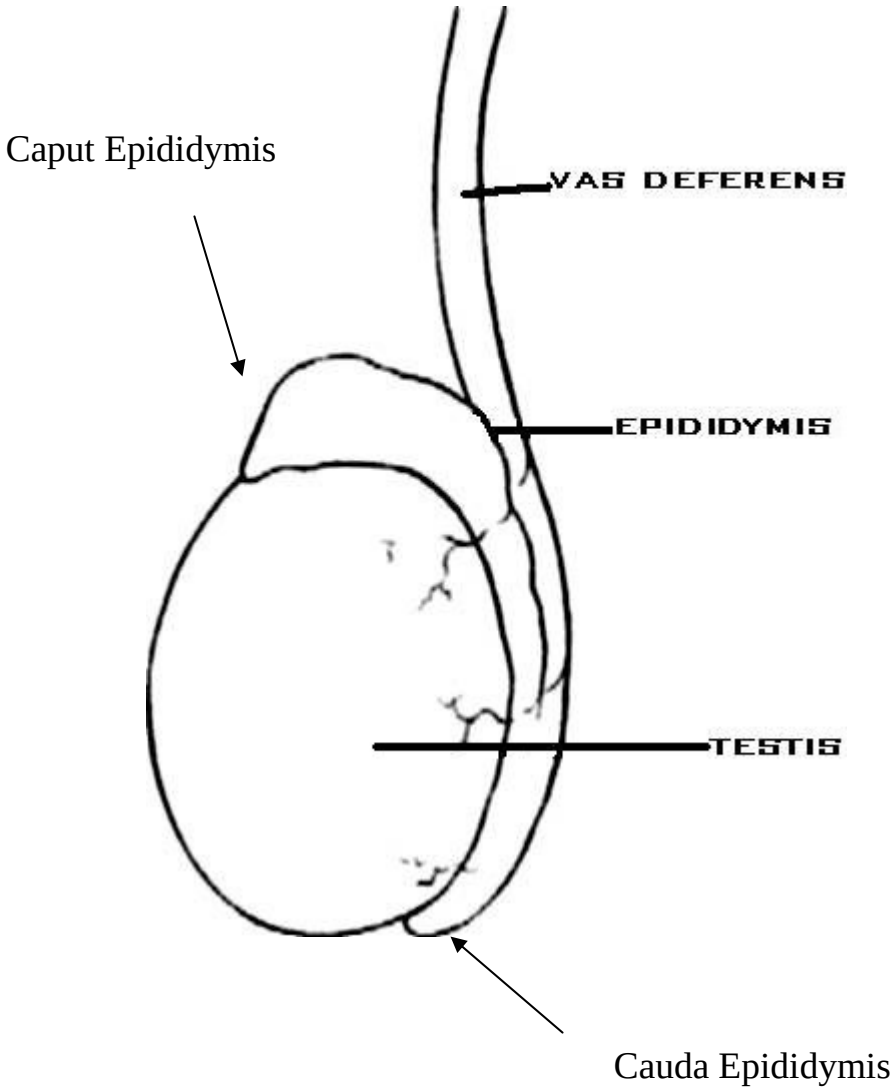

Fig. 5. Testis and Epididymis

http://www.ivf-infertility.com/ivf/pesa2.php

References:

1. Apweiler, R., Hermjakob, H., and Sharon, N. On the frequency of protein glycosylation, as deduced from analysis of the SWISS-PROT database. Biochim Biophys Acta, *1473:* 4-8, 1999.
2. Helenius, A. and Aebi, M. Roles of N-linked glycans in the endoplasmic reticulum. Annu Rev Biochem, *73:* 1019-1049, 2004.
3. Moremen, K. W. Golgi alpha-mannosidase II deficiency in vertebrate systems: implications for asparagine-linked oligosaccharide processing in mammals. Biochim Biophys Acta, *1573:* 225-235, 2002.
4. Cumming, D. A. Glycosylation of recombinant protein therapeutics: control and functional implications. Glycobiology, *1:* 115-130, 1991.
5. Moremen, K. W., Trimble, R. B., and Herscovics, A. Glycosidases of the asparagine-linked oligosaccharide processing pathway. Glycobiology, *4:* 113-125, 1994.
6. Knauer, R. and Lehle, L. The oligosaccharyltransferase complex from Saccharomyces cerevisiae. Isolation of the OST6 gene, its synthetic interaction with OST3, and analysis of the native complex. J Biol Chem, *274:* 17249-17256, 1999.
7. Silberstein, S. and Gilmore, R. Biochemistry, molecular biology, and genetics of the oligosaccharyltransferase. Faseb J, *10:* 849-858, 1996.
8. Kornfeld, R. and Kornfeld, S. Assembly of asparagine-linked oligosaccharides. Annu Rev Biochem, *54:* 631-664, 1985.
9. Schachter, H. Congenital disorders involving defective N-glycosylation of proteins. Cell Mol Life Sci, *58:* 1085-1104, 2001.

10. Jaeken, J., Matthijs, G., Barone, R., and Carchon, H. Carbohydrate deficient glycoprotein (CDG) syndrome type I. J Med Genet, *34:* 73-76, 1997.

11. Elsevier Encyclopedia of Biological Chemistry, p. 34-39: Elesevier.

12. Marth, J. D. Will the transgenic mouse serve as a Rosetta Stone to glycoconjugate function? Glycoconj J, *11:* 3-8, 1994.

13. Lubas, W. A. and Spiro, R. G. Golgi endo-alpha-D-mannosidase from rat liver, a novel N-linked carbohydrate unit processing enzyme. J Biol Chem, *262:* 3775-3781, 1987.

14. Lubas, W. A. and Spiro, R. G. Evaluation of the role of rat liver Golgi endo-alpha-D-mannosidase in processing N-linked oligosaccharides. J Biol Chem, *263:* 3990-3998, 1988.

15. Jakob, C. A., Burda, P., Roth, J., and Aebi, M. Degradation of misfolded endoplasmic reticulum glycoproteins in Saccharomyces cerevisiae is determined by a specific oligosaccharide structure. J Cell Biol, *142:* 1223-1233, 1998.

16. Hiraizumi, S., Spohr, U., and Spiro, R. G. Ligand affinity chromatographic purification of rat liver Golgi endomannosidase. J Biol Chem, *269:* 4697-4700, 1994.

17. Bause, E. and Burbach, M. Purification and enzymatic properties of endo-alpha 1, 2-mannosidase from pig liver involved in oligosaccharide processing. Biol Chem, *377:* 639-646, 1996.

18. Dairaku, K. and Spiro, R. G. Phylogenetic survey of endomannosidase indicates late evolutionary appearance of this N-linked oligosaccharide processing enzyme. Glycobiology, *7:* 579-586, 1997.

19. Moremen, K. in Oligosaccharides in Chemistry and Biology: A Comprehensive Handbook, Vol. II, p. 81-117. New York: John Wiley and Sons, Inc.,, 2000.

20. Henrissat, B. and Bairoch, A. Updating the sequence-based classification of glycosyl hydrolases. Biochem J, *316:* 695-696, 1996.

21. Heikinheimo, P., Helland, R., Leiros, H. K., Leiros, I., Karlsen, S., Evjen, G., Ravelli, R., Schoehn, G., Ruigrok, R., Tollersrud, O. K., McSweeney, S., and Hough, E. The structure of bovine lysosomal alpha-mannosidase suggests a novel mechanism for low-pH activation. J Mol Biol, *327:* 631-644, 2003.

22. van den Elsen, J. M., Kuntz, D. A., and Rose, D. R. Structure of Golgi alpha-mannosidase II: a target for inhibition of growth and metastasis of cancer cells. Embo J, *20:* 3008-3017, 2001.

23. Dewald, B. and Touster, O. A new alpha-D-mannosidase occurring in Golgi membranes. J Biol Chem, *248:* 7223-7233, 1973.

24. Tulsiani, D. R. and Touster, O. The purification and characterization of mannosidase IA from rat liver Golgi membranes. J Biol Chem, *263:* 5408-5417, 1988.

25. Tulsiani, D. R., Hubbard, S. C., Robbins, P. W., and Touster, O. alpha-D-Mannosidases of rat liver Golgi membranes. Mannosidase II is the GlcNAcMAN5-cleaving enzyme in glycoprotein biosynthesis and mannosidases Ia and IB are the enzymes converting Man9 precursors to Man5 intermediates. J Biol Chem, *257:* 3660-3668, 1982.

26. Tabas, I. and Kornfeld, S. The synthesis of complex-type oligosaccharides. III. Identification of an alpha-D-mannosidase activity involved in a late stage of processing of complex-type oligosaccharides. J Biol Chem, *253:* 7779-7786, 1978.

27. Harpaz, N. and Schachter, H. Control of glycoprotein synthesis. Processing of asparagine-linked oligosaccharides by one or more rat liver Golgi alpha-D-mannosidases

dependent on the prior action of UDP-N-acetylglucosamine: alpha-D-mannoside beta 2-N-acetylglucosaminyltransferase I. J Biol Chem, *255:* 4894-4902, 1980.

28. Turco, S. J. and Robbins, P. W. The initial stages of processing of protein-bound oligosaccharides in vitro. J Biol Chem, *254:* 4560-4567, 1979.

29. Tabas, I., Schlesinger, S., and Kornfeld, S. Processing of high mannose oligosaccharides to form complex type oligosaccharides on the newly synthesized polypeptides of the vesicular stomatitis virus G protein and the IgG heavy chain. J Biol Chem, *253:* 716-722, 1978.

30. Kornfeld, S., Li, E., and Tabas, I. The synthesis of complex-type oligosaccharides. II. Characterization of the processing intermediates in the synthesis of the complex oligosaccharide units of the vesicular stomatitis virus G protein. J Biol Chem, *253:* 7771-7778, 1978.

31. Velasco, A., Hendricks, L., Moremen, K. W., Tulsiani, D. R., Touster, O., and Farquhar, M. G. Cell type-dependent variations in the subcellular distribution of alpha-mannosidase I and II. J Cell Biol, *122:* 39-51, 1993.

32. Paulson, J. C. and Colley, K. J. Glycosyltransferases. Structure, localization, and control of cell type-specific glycosylation. J Biol Chem, *264:* 17615-17618, 1989.

33. Liao, Y. F., Lal, A., and Moremen, K. W. Cloning, expression, purification, and characterization of the human broad specificity lysosomal acid alpha-mannosidase. J Biol Chem, *271:* 28348-28358, 1996.

34. Nilssen, O., Berg, T., Riise, H. M., Ramachandran, U., Evjen, G., Hansen, G. M., Malm, D., Tranebjaerg, L., and Tollersrud, O. K. alpha-Mannosidosis: functional cloning of the

lysosomal alpha-mannosidase cDNA and identification of a mutation in two affected siblings. Hum Mol Genet, *6:* 717-726, 1997.

35. Tollersrud, O. K., Berg, T., Healy, P., Evjen, G., Ramachandran, U., and Nilssen, O. Purification of bovine lysosomal alpha-mannosidase, characterization of its gene and determination of two mutations that cause alpha-mannosidosis. Eur J Biochem, *246:* 410-419, 1997.

36. Berg, T., King, B., Meikle, P. J., Nilssen, O., Tollersrud, O. K., and Hopwood, J. J. Purification and characterization of recombinant human lysosomal alpha-mannosidase. Mol Genet Metab, *73:* 18-29, 2001.

37. Merkle, R. K., Zhang, Y., Ruest, P. J., Lal, A., Liao, Y. F., and Moremen, K. W. Cloning, expression, purification, and characterization of the murine lysosomal acid alpha-mannosidase. Biochim Biophys Acta, *1336:* 132-146, 1997.

38. Shoup, V. A. and Touster, O. Purification and characterization of the alpha-D-mannosidase of rat liver cytosol. J Biol Chem, *251:* 3845-3852, 1976.

39. Bischoff, J., Moremen, K., and Lodish, H. F. Isolation, characterization, and expression of cDNA encoding a rat liver endoplasmic reticulum alpha-mannosidase. J Biol Chem, *265:* 17110-17117, 1990.

40. Duvet, S., Labiau, O., Mir, A. M., Kmiecik, D., Krag, S. S., Verbert, A., and Cacan, R. Cytosolic deglycosylation process of newly synthesized glycoproteins generates oligomannosides possessing one GlcNAc residue at the reducing end. Biochem J, *335:* 389-396, 1998.

41. Grard, T., Herman, V., Saint-Pol, A., Kmiecik, D., Labiau, O., Mir, A. M., Alonso, C., Verbert, A., Cacan, R., and Michalski, J. C. Oligomannosides or oligosaccharide-lipids as

potential substrates for rat liver cytosolic alpha-D-mannosidase. Biochem J, *316:* 787-792, 1996.

42. Tulsiani, D. R., Skudlarek, M. D., and Orgebin-Crist, M. C. Novel alpha-D-mannosidase of rat sperm plasma membranes: characterization and potential role in sperm-egg interactions. J Cell Biol, *109:* 1257-1267, 1989.

43. Pereira, B. M., Abou-Haila, A., and Tulsiani, D. R. Rat sperm surface mannosidase is first expressed on the plasma membrane of testicular germ cells. Biol Reprod, *59:* 1288-1295, 1998.

44. Tulsiani, D. R., NagDas, S. K., Skudlarek, M. D., and Orgebin-Crist, M. C. Rat sperm plasma membrane mannosidase: localization and evidence for proteolytic processing during epididymal maturation. Dev Biol, *167:* 584-595, 1995.

45. Tulsiani, D. R., Skudlarek, M. D., Nagdas, S. K., and Orgebin-Crist, M. C. Purification and characterization of rat epididymal-fluid alpha-D-mannosidase: similarities to sperm plasma-membrane alpha-D-mannosidase. Biochem J, *290:* 427-436, 1993.

46. Okamura, N., Dacheux, F., Venien, A., Onoe, S., Huet, J. C., and Dacheux, J. L. Localization of a maturation-dependent epididymal sperm surface antigen recognized by a monoclonal antibody raised against a 135-kilodalton protein in porcine epididymal fluid. Biol Reprod, *47:* 1040-1052, 1992.

47. Okamura, N., Tamba, M., Liao, H. J., Onoe, S., Sugita, Y., Dacheux, F., and Dacheux, J. L. Cloning of complementary DNA encoding a 135-kilodalton protein secreted from porcine corpus epididymis and its identification as an epididymis-specific alpha-mannosidase. Mol Reprod Dev, *42:* 141-148, 1995.

48. Bischoff, J. and Kornfeld, R. Evidence for an alpha-mannosidase in endoplasmic reticulum of rat liver. J Biol Chem, *258:* 7907-7910, 1983.

49. Novikoff, P. M., Tulsiani, D. R., Touster, O., Yam, A., and Novikoff, A. B. Immunocytochemical localization of alpha-D-mannosidase II in the Golgi apparatus of rat liver. Proc Natl Acad Sci U S A, *80:* 4364-4368, 1983.

50. O'Rand, M. G. Sperm-egg recognition and barriers to interspecies fertilization. Gamete Res, *19:* 315-328, 1988.

51. Kligman, I., Glassner, M., Storey, B. T., and Kopf, G. S. Zona pellucida-mediated acrosomal exocytosis in mouse spermatozoa: characterization of an intermediate stage prior to the completion of the acrosome reaction. Dev Biol, *145:* 344-355, 1991.

52. Wassarman, P. M. Mammalian fertilization: egg and sperm (glyco)proteins that support gamete adhesion. Am J Reprod Immunol, *33:* 253-258, 1995.

53. Dell, A., Morris, H. R., Easton, R. L., Panico, M., Patankar, M., Oehniger, S., Koistinen, R., Koistinen, H., Seppala, M., and Clark, G. F. Structural analysis of the oligosaccharides derived from glycodelin, a human glycoprotein with potent immunosuppressive and contraceptive activities. J Biol Chem, *270:* 24116-24126, 1995.

54. Yonezawa, N., Aoki, H., Hatanaka, Y., and Nakano, M. Involvement of N-linked carbohydrate chains of pig zona pellucida in sperm-egg binding. Eur J Biochem, *233:* 35-41, 1995.

55. Miller, D. J., Macek, M. B., and Shur, B. D. Complementarity between sperm surface beta-1,4-galactosyltransferase and egg-coat ZP3 mediates sperm-egg binding. Nature, *357:* 589-593, 1992.

56. Jin, Y. Z., Dacheux, F., Dacheux, J. L., Bannai, S., Sugita, Y., and Okamura, N. Purification and properties of major alpha-D-mannosidase in the luminal fluid of porcine epididymis. Biochim Biophys Acta, *1432:* 382-392, 1999.

57. Hiramoto, S., Tamba, M., Kiuchi, S., Jin, Y. Z., Bannai, S., Sugita, Y., Dacheux, F., Dacheux, J. L., Yoshida, M., and Okamura, N. Stage-specific expression of a mouse homologue of the porcine 135kDa alpha-D-mannosidase (MAN2B2) in type A spermatogonia. Biochem Biophys Res Commun, *241:* 439-445, 1997.

58. Okamura, N., Kiuchi, S., Tamba, M., Kashima, T., Hiramoto, S., Baba, T., Dacheux, F., Dacheux, J. L., Sugita, Y., and Jin, Y. Z. A porcine homolog of the major secretory protein of human epididymis, HE1, specifically binds cholesterol. Biochim Biophys Acta, *1438:* 377-387, 1999.

59. Tulsiani, D. R., Coleman, V. D., and Touster, O. Rat epididymal alpha-D-mannosidase: purification, carbohydrate composition, substrate specificity, and antibody production. Arch Biochem Biophys, *267:* 60-68, 1988.

60. Ohata, K., Okamura, N., Kojima, M., and Yasue, H. Assignment of alpha-mannosidase gene (MAN2B2) to swine chromosome 8p23-pter by fluorescence in situ hybridization. Mamm Genome, *8:* 158-159, 1997.

61. Tascou, S., Nayernia, K., Engel, W., and Burfeind, P. Refinement of the expression pattern of a mouse homologue of the porcine 135-kDa alpha-d-mannosidase (MAN2B2). Biochem Biophys Res Commun, *272:* 951-952, 2000.

62. Daniel, P. F., Winchester, B., and Warren, C. D. Mammalian alpha-mannosidases--multiple forms but a common purpose? Glycobiology, *4:* 551-566, 1994.

63. al Daher, S., de Gasperi, R., Daniel, P., Hall, N., Warren, C. D., and Winchester, B. The substrate-specificity of human lysosomal alpha-D-mannosidase in relation to genetic alpha-mannosidosis. Biochem J, *277:* 743-751, 1991.

64. Gonzalez, D. S., Kagawa, Y., and Moremen, K. W. Isolation and characterization of the gene encoding the mouse broad specificity lysosomal alpha-mannosidase1. Biochim Biophys Acta, *1445:* 177-183, 1999.

65. DeGasperi, R., al Daher, S., Daniel, P. F., Winchester, B. G., Jeanloz, R. W., and Warren, C. D. The substrate specificity of bovine and feline lysosomal alpha-D-mannosidases in relation to alpha-mannosidosis. J Biol Chem, *266:* 16556-16563, 1991.

66. Haeuw, J. F., Grard, T., Alonso, C., Strecker, G., and Michalski, J. C. The core-specific lysosomal alpha(1-6)-mannosidase activity depends on aspartamidohydrolase activity. Biochem J, *297:* 463-466, 1994.

67. Daniel, P. F., Evans, J. E., De Gasperi, R., Winchester, B., and Warren, C. D. A human lysosomal alpha(1----6)-mannosidase active on the branched trimannosyl core of complex glycans. Glycobiology, *2:* 327-336, 1992.

68. De Gasperi, R., Daniel, P. F., and Warren, C. D. A human lysosomal alpha-mannosidase specific for the core of complex glycans. J Biol Chem, *267:* 9706-9712, 1992.

69. Champion, M. J. and Shows, T. B. Mannosidosis: assignment of the lysosomal alpha-mannosidase B gene to chromosome 19 in man. Proc Natl Acad Sci U S A, *74:* 2968-2972, 1977.

70. Bachinski, L. L., Krahe, R., White, B. F., Wieringa, B., Shaw, D., Korneluk, R., Thompson, L. H., Johnson, K., and Siciliano, M. J. An informative panel of somatic cell

hybrids for physical mapping on human chromosome 19q. Am J Hum Genet, *52:* 375-387, 1993.

71. Ockerman, P. A. The diagnosis of glycogen storage disease in clinical practice. Isr J Med Sci, *3:* 494-497, 1967.

72. Sun, H. and Wolfe, J. H. Recent progress in lysosomal alpha-mannosidase and its deficiency. Exp Mol Med, *33:* 1-7, 2001.

73. Stinchi, S., Lullmann-Rauch, R., Hartmann, D., Coenen, R., Beccari, T., Orlacchio, A., von Figura, K., and Saftig, P. Targeted disruption of the lysosomal alpha-mannosidase gene results in mice resembling a mild form of human alpha-mannosidosis. Hum Mol Genet, *8:* 1365-1372, 1999.

74. Michalski, J. C., Haeuw, J. F., Wieruszeski, J. M., Montreuil, J., and Strecker, G. In vitro hydrolysis of oligomannosyl oligosaccharides by the lysosomal alpha-D-mannosidases. Eur J Biochem, *189:* 369-379, 1990.

75. Cenci di Bello, I., Dorling, P., and Winchester, B. The storage products in genetic and swainsonine-induced human mannosidosis. Biochem J, *215:* 693-696, 1983.

76. Winchester, B. Role of alpha-D-mannosidases in the biosynthesis and catabolism of glycoproteins. Biochem Soc Trans, *12:* 522-524, 1984.

77. Kuranda, M. J. and Aronson, N. N., Jr. A di-N-acetylchitobiase activity is involved in the lysosomal catabolism of asparagine-linked glycoproteins in rat liver. J Biol Chem, *261:* 5803-5809, 1986.

78. DeGasperi, R., Li, Y. T., and Li, S. C. Presence of two endo-beta-N-acetylglucosaminidases in human kidney. J Biol Chem, *264:* 9329-9334, 1989.

79. Song, Z. W., Li, S. C., and Li, Y. T. Absence of endo-beta-N-acetylglucosaminidase activity in the kidneys of sheep, cattle and pig. Biochem J, *248:* 145-149, 1987.

80. Aronson, N. N., Jr. and Kuranda, M. J. Lysosomal degradation of Asn-linked glycoproteins. Faseb J, *3:* 2615-2622, 1989.

81. Yamashita, K., Tachibana, Y., Mihara, K., Okada, S., Yabuuchi, H., and Kobata, A. Urinary oligosaccharides of mannosidosis. J Biol Chem, *255:* 5126-5133, 1980.

82. Matsuura, F., Nunez, H. A., Grabowski, G. A., and Sweeley, C. C. Structural studies of urinary oligosaccharides from patients with mannosidosis. Arch Biochem Biophys, *207:* 337-352, 1981.

83. Akasaki, M., Sugahara, K., Funakoshi, I., Aula, P., and Yamashina, I. Characterization of a mannose-containing glycoasparagine isolated from urine of a patient with aspartylglycosylaminuria (AGU). FEBS Lett, *69:* 191-194, 1976.

84. Tachibana, Y., Yamashita, K., Kawaguchi, M., Arashima, S., and Kobata, A. Digestion of asparagine-linked oligosaccharides by endo-beta-N-acetylglucosaminidase in the human skin fibroblasts obtained from fucosidosis patients. J Biochem (Tokyo), *90:* 1291-1296, 1981.

85. Winchester, B. Lysosomal metabolism of glycoproteins. Glycobiology, *15:* 1R-15R, 2005.

86. Liu, B., Ahmad, W., and Aronson, N. N., Jr. Structure of the human gene for lysosomal di-N-acetylchitobiase. Glycobiology, *9:* 589-593, 1999.

CHAPTER 2

CHARACTERIZATION OF A NOVEL HUMAN CORE-SPECIFIC LYSOSOMAL α1-6MANNOSIDASES INVOLVED IN N-GLYCAN CATABOLISM

Chaeho Park, Lu Meng, Leslie Stanton, Robert Collins, Steven Mast, Xiaobing Yi, Heather Strachan, and Kelley W. Moremen. To be submitted to Journal of Biological Chemistry. 2005

ABSTRACT

In humans and rodents lysosomal catabolism of $Man_3GlcNAc_2$ core N-glycan structures results from the concerted actions of exoglycosidases including the broad specificity lysosomal α-mannosidase (LysMan), a core-specific α1-6mannosidase, and β-mannosidase, as well as the core chitobiose cleavage by a di-*N*-acetylchitobiase. In ungulates and carnivora, both the chitobiase and the α1-6mannosidase are absent suggesting a co-regulation of the two enzymes. We describe here the cloning, expression, purification and characterization of the human core-specific α1-6mannosidase with similarity to members of the glycosylhydrolase family 38. The recombinant enzyme had a pH optimum of 4.0, was potently inhibited by swainsonine and 1,4-dideoxy1,4-imino-D-mannitol, and was stimulated by Co^{+2}. NMR-based time course substrate specificity studies comparing the α1-6mannosidase with human LysMan revealed that the former enzyme selectively cleaved the α1-6mannose residue from $Man_3GlcNAc$, but not $Man_3GlcNAc_2$ or other larger high mannose structures, indicating the requirement for chitobiase action prior to α1-6mannosidase cleavage. In contrast, LysMan cleaved all of the α-linked mannose residues from $Man_{9-5}GlcNAc_2$, $Man_3GlcNAc_2$, or $Man_3GlcNAc$ structures except the core α1-6mannose residue.

Transcripts encoding the α1-6mannosidase were ubiquitously expressed in human tissues and expressed sequence tag searches in various mammalian species demonstrated a similar distribution in species-specific expression as the chitobiase. No expressed sequence tags were identified for bovine α1-6mannosidase despite the identification of two homologs in the bovine genome. The lack of conserved 5' flanking sequences for the bovine gene relative to the human α1-6mannosidase gene suggests that synthesis of the bovine α1-6mannosidase transcripts may

be defective as a result of altered promoter sequences, similar to the altered promoter element sequences previously identified for the bovine chitobiase gene.

INTRODUCTION

Eukaryotes contain a variety of α-mannosidases resident in different subcellular compartments, where they cleave mannose residues either as part of N-glycan biosynthesis in the secretory pathway or as a part of N-glycan catabolism in the cytosol or lysosomes. There are two broad families of α-mannosidases in mammalian cells that can be distinguished by their distinctive substrate specificities, responses to inhibitors, cation requirements, protein molecular weights, subcellular localizations, and enzyme mechanisms (1). The Class 1 α-mannosidases (CAZy glycosylhydrolase family 47, GH47 (2, 3)) are largely restricted to the early secretory pathway where they are involved in glycoprotein maturation and quality control (4, 5). The Class 2 α- mannosidases (CAZy glycosylhydrolase family 38, GH38 (2, 3)) are found in the Golgi complex, lysosomes, and in the cytosol where they are involved in either glycoprotein biosynthesis or catabolism (2, 6).

The broad specificity lysosomal α-mannosidase (LysMan) is a GH38 enzyme involved in glycan catabolism where it cleaves α1-2, α1-3, and α1-6Man linkages in N-linked glycans (7, 8). The critical role of this enzyme in lysosomal catabolism is indicated by the severe clinical phenotypes for the lysosomal storage disease, α-mannosidosis, where the enzymatic defect results in glycan accumulation and subsequent pathology in humans (9) cattle (10), cats (11, 12), mice (13) and guinea pigs (14). α-Mannosidosis models in various mammalian species reveal a remarkable variation in the glycan structures that are accumulated. Vertebrate α-mannose-containing structures include both high mannose N-glycans as well as the tri-mannosyl core (Manα1-3[Manα1-6]Manβ1-4GlcNAcβ1-4GlcNAc) of complex type structures. In humans and rodents, a deficiency of LysMan causes the predominant accumulation of the major linear storage product, Manα1-3Manβ1-4GlcNAc, along with other extended products on the Manα1-

3-branch (15-17), suggesting that an alternate enzyme is responsible for the cleavage of the α1-6Man residue from the tri-mannosyl core structure. In contrast, cattle and cats with α-mannosidosis accumulate glycans that contain both a $GlcNAc_2$ core structure (18)and a α1-6Man residue linked to the core β1-4Man, suggesting an association between cleavage of the chitobiosyl core and the cleavage of the core Manα1-6Man linkage.

An explanation for the linkage between the two distinct cleavage events was revealed with the identification of an enzyme with specificity for cleavage of the core α1-6Man linkage (15, 19, 20). This latter enzyme was initially identified in human α-mannosidosis fibroblasts (21) and partially purified from human spleen (22) and rat liver (23), but the cDNA encoding this enzyme activity has not been identified. The substrate specificities for the core-specific human and rat lysosomal α1-6mannosidases were found to be dependent on the prior action of the lysosomal enzymes, aspartyl-*N*-acetyl-beta-D-glucosaminidase and di-*N*-acetyl-chitobiase, which yield a Manα1-3[Manα1-6]Manβ1-4GlcNAc core structure (16, 23, 24). Rat liver lysosomal α1-6mannosidase was shown to preferentially act on the core $Man_3GlcNAc$ structure, but not $Man_3GlcNAc_2$ suggesting that there is a strict requirement for glycan release from the peptide backbone via aspartylglucosaminidase action and cleavage of the chitobiosyl core by chitobiase (16, 23-25).

Surprisingly, chitobiase gene expression is selectively inactivated through alterations in promoter element sequences in some mammalian species (cats, cattle, sheep, dogs and pigs), but not others (humans, mice), and the core-specific α1-6mannosidase is predicted to be active only under the latter conditions. Thus, the presence of chitobiase activity in some mammalian species and not others can at least partially account for the differences in accumulated oligosaccharides in the α-mannosidosis models. A further parallel between the enzymes was revealed when α1-

6mannosidase activity could also only be detected in tissue extracts of humans and rodents, but not from cattle, cats, or dogs (16) suggesting a similar expression pattern as the chitobiase.

While, the α1-6mannosidase was initially thought of as redundant with the activity of the broad specificity LysMan for N-glycan catabolism, detailed substrate specificity studies have revealed that LysMan has very poor efficiency for cleavage of the Manα1-6Man linkage in the N-glycan tri-mannosyl core. Thus, a model was proposed that the chitobiase and core-specific α1-6mannosidase work in functional collaboration to provide the full and efficient catabolism of N-glycans in the lysosomes of some mammalian species, but the accessory activities of the chitobiase and possibly the α1-6mannosidase have been lost through alterations in promoter sequences leading to defective transcription in ungulates, cats and dogs (16). The absence of a clearly identified gene or cDNA encoding the core specific α1-6mannosidase has made it difficult to establish the genetic relationship between the expression and transcriptional inactivation of chitobiase versus the core-specific α1-6mannosidase.

In an independent line of investigation, an α-mannosidase of 135 kDa was previously isolated from porcine epididymal fluid that was proposed to be involved in sperm maturation (26, 27). A cDNA encoding this enzyme was isolated from a pig cDNA library derived from the porcine proximal corpus epididymis (26) and a mouse homolog was subsequently cloned from a testis cDNA library (28). Northern blots indicated that the cDNAs were expressed in male reproductive tissues in pigs and mice (26, 28, 29), but no recombinant enzyme expression data were presented for the equivalent enzyme from any species. Subsequent studies by Tascou et al (30) and by our lab (see below) indicated that the enzyme was a ubiquitously expressed in animal tissues in contrast to the more restricted expression data in the prior studies.

In the present work, we have cloned a human cDNA encoding a novel α-mannosidase with sequence similarity to the pig and mouse 135 kDa "epididymal" α-mannosidases. The novel human α-mannosidase cDNA was expressed in human embryonic kidney cells (HEK293), purified, and characterized for substrate specificity toward a series of high mannose oligosaccharides in comparison with the broad specificity LysMan. Our data indicate that the cDNA encodes the core specific α1-6mannosidase involved in lysosomal catabolism of N-glycans in mammalian cells. Transcripts encoding the enzyme are expressed in a similar subset of mammalian species as the chitobiase and comparison of the 5'-flanking regions for the bovine and human α1-6mannosidase genes indicates that alterations in promoter element sequences that could account for the loss of transcript expression in bovine tissues.

EXPERIMENTAL PROCEDURES

Cloning and expression of a novel human α-mannosidase: The human cDNA homolog of the pig/mouse 135 kDa α-mannosidase was identified by sequence searching of a cloned cDNA library (GenBank accession no. AL553663, human placenta, Invitrogen Inc.) and the cDNA in the pCMV script vector was fully sequenced to confirm that it matched the corresponding GenBank reference sequence (NM_015274). Primers were designed to amplify a ~1.3 kb fragment at the 3' end of the coding region in order to eliminate the termination codon and append a sequence that would contain a 6xHis tag and an HA tag, followed by a new termination codon and a *Not*I site. The 5' primer annealed to position 1810-1839 relative to the ATG initiation codon, just upstream from an *Eco*RI site at position 1846-1851. The 3' primer annealed to position 2998-3027 at the end of the coding region followed by a 5' extension containing the tag sequences, termination codon, and *Not*I site. The amplification was performed in a 25 μl

reaction volume containing 20 ng plasmid DNA, 1.0 mM $MgCl_2$, 30 mM Tris-HCl (pH 8.5), 7.5 mM $(NH_4)_2SO_4$, 200 μM each dNTP, 0.5 μM 5' and 3' primer, 2.5 units of *Pfu* polymerase in a thermal cycler programmed for a preincubation at 94°C, (1 min) followed by a temperature cycle of 94°C (30 sec), 65°C (30 sec) and 72°C (4 min) for 30 cycles. After PCR, the resulting 1.3 kb amplimer was subcloned into an *Eco*RI/*Not*I cut pBSSK vector (Stratagene) and sequenced. The modified 3' end of the coding region was then ligated to the 1.9 kb EcoRI fragment corresponding to the front portion of the coding region and transferred to a mammalian expression vector (pEAK10, Edge Biosystems, Gaithersburg, MD) as a *Hin*dIII/*Not*I fragment. For the human LysMan construct, a similar modification of the 3' end to append a 6xHis and HA tag sequence was accomplished by PCR amplification of a 740 bp fragment at the 3' end of the coding region. The 5' primer annealed to position 2401-2470, upstream of an *Sac*I site and the 3' primer annealed to position 3052-3081 with a 5' extension on the latter primer containing the tag sequences, termination codon, and *Not*I site. The amplimer was subcloned into a *Sac*I/*Not*I cut pBSSK vector (Stratagene) and sequenced. The modified COOH-terminus of the coding region was then ligated to an *Eco*RI/*Sac*I fragment corresponding to the front portion of the coding region and transferred to the pEAK10 expression vector as a *Hin*dIII/NotI fragment. For the generation of stable transfectants in HEK293 cells, the cells were grown to 50% ~ 80% confluency in 100 mm tissue culture dishes in DMEM/10% FCS (Sigma). Transfection was performed using 20 μg of the respective expression plasmid construct and 10 μl lipofectamine 2000 (Invitrogen) according to the method of Wu et al (31). Following transfection the cells were allowed to grow at 37 ˚C for 24 h before selection with 1 μg/ml puromycin. After growth to confluency, the cultures were split 1:5 and the antibiotic selection was increased to 2 μg/ml puromycin for subsequent growth. For enzyme production, the transfected cells were grown in

T175 flasks to confluency and the medium was replaced with DMEM/10%FCS/1.5% DMSO to allow cell cycle arrest. Subsequently the cultures were grown for an additional 3 weeks at 37 ˚C prior to harvesting the conditioned medium.

Purification of a novel human α-mannosidase: The conditioned medium from the transfected cultures expressing LysMan or the novel α-mannosidase was clarified by centrifugation at 2800 × g for 30 min prior to purification using an identical protocol for both enzymes. The respective clarified culture medium was brought to a final concentration of 0.4 M ammonium sulfate solution and the solutions were applied to a Phenyl-Sepharose column (Pharmacia, 32 mm x 140 mm). The columns were washed with 60 ml of phosphate buffer containing 400 mM ammonium sulfate, and α-mannosidase activity was eluted over a 900 ml decreasing linear gradient of 0.4-0 M ammonium sulfate and a 0-40 % increasing gradient of ethylene glycol in sodium phosphate buffer (pH 7.5). Fractions containing the enzyme activity were pooled and dialyzed overnight against 50 mM sodium phosphate buffer (pH 7.5) at 4 ˚C. The dialyzed samples were then applied to cobalt-chelating Sepharose column (16 mm x 100 mm). The column was washed with 30 ml of sodium phosphate buffer (pH 7.5) and enzyme activity was eluted with a linear gradient of 0-300 mM NaCl at a flow rate of 3 ml/min. Peak fractions of α-mannosidase activity were pooled and concentrated by ultrafiltration through a YM-100 membrane (Amicon, Inc., Beverly, MA). The concentrated enzyme preparations were further purified by loading onto a Superdex 200 gel filtration column (16 mm × 700 mm, Amersham Pharmacia Biotech) pre-equilibrated with 50 mM HEPES (pH 7.5) and 200 mM NaCl. Fractions containing α-mannosidase activity were pooled.

Identification of proteins by SDS-PAGE and mass spectrometry: An aliquot of the purified recombinant enzyme (50 μg) was subjected to SDS-PAGE and stained with Coomassie Blue G-250. The protein band was excised, reduced, alkylated, and digested in-gel with modified trypsin (32) (Worthington, Freehold, NJ) as described previously (33). The tryptic peptides from the digested protein were resolved by capillary C18 reverse phase high pressure liquid chromatography with in-line tandem MS/MS on a Thermo Finnigan LTQ linear ion-trap mass spectrometer. The spectra were analyzed using TurboSequest (Thermo Finnigan) and stringently filtered to identify the protein of interest (34). A total of seven tryptic peptides were identified with a minimum of 30% coverage of the human α-mannosidase sequence encoded by the expression construct.

Northern blot analysis: Northern blots containing poly (A^+) RNA from various human tissues were purchased from Clonetech Laboratories. The blots were prehybridized, hybridized, and washed as described previously (35) using radiolabeled probes derived from the 740 bp or 1.3 kb amplimers of human LysMan and the novel α-mannosidase coding regions, respectively. The blots were subsequently hybridized with a radiolabeled human β-actin control probe (Clonetech) to act as an RNA load control for the blots. ^{32}P-Labeled DNA probes were generated using [^{32}P]dCTP (Amersham Pharmacia Biotech) and the Ready-To-Go labeling system (Amersham Pharmacia Biotech). Blots were visualized with a PhosphorImager (Molecular Dynamics) after a 1-day exposure.

α-Mannosidase activity assays with 4-methylubelliferyl-α-D-mannopyranoside (4MU-Man) and inhibition studies: Hydrolysis of 4MU-Man (Sigma) was assayed at 37˚C using 5 μl of

the enzyme sample in a final volume of 50 µl containing 100 mM sodium acetate (pH 4.0), 3 mM 4MU-Man, and 1 mM $CoCl_2$. Reactions were stopped by the addition of 150 µL of sodium carbonate to a final concentration of 150 mM. Fluorescence was quantitated on a Spectramax Gemini XS fluorescence reader. All fluorescence values were compared to a 4MU-Man standard curve. For inhibition studies, swainsonine (SW), 1,4-dideoxy-1,4-imino-D-mannitol (DIM), kifunensine (KIF), and 1-deoxymannojirimycin (dMNJ) were prepared as stock solutions in water. Inhibitor data were collected in triplicate. Lineweaver Burk plots and Dixon plots were used to transform the kinetic data into values of K_m and K_i as previously described (7, 36, 37).

Metal and pH Studies: To examine the effects of the metal cations on enzyme activity, the enzymes were first preincubated with 5 mM EDTA for 2 hours, and then passed through a HiTrap desalting column (16 mm x 50 mm, Amersham Pharmacia Biotech) to remove any dissociable divalent cations. Aliquots of the enzyme preparation were then preincubated at various times with 1 mM concentrations of either $CoCl_2$, $CuCl_2$, $FeCl_2$, $MgCl_2$, $MnCl_2$, $NiCl_2$, $ZnCl_2$, or EDTA in 200 mM HEPES buffer, pH 7.0, at 37 ˚C. The enzyme samples were then brought to pH 4.0 with McIlvaine buffer (38), 4MU-Man was added to a final concentration of 3 mM, and the mixture was then incubated at 37 ˚C for 1 h for the enzyme assays. To determine the influence of pH on enzyme activity, enzyme assays were performed using McIlvaine buffer in the indicated pH ranges.

Mannosidase activity assays with high mannose substrate: Various pyridylamine (PA)-tagged glycans, including $Man_9GlcNAc_2$-PA, $Man_8GlcNAc_2$-PA, $Man_7GlcNAc_2$-PA, $Man_6GlcNAc_2$-PA, $Man_5GlcNAc_2$-PA, and $GlcNAcMan_5GlcNAc_2$-PA were isolated as

previously described (7) and incubated with the novel human α-mannosidase or human LysMan in 100 mM sodium acetate buffer (pH 4.0) for 24 hours at 37 ˚C. The reaction products were then incubated at 100˚C for 5 min and then resolved on a Hypersil APS2 NH_2 HPLC column as previously described (7, 39).

^{1}H-NMR analysis of the oligosaccharide digestion products: Enzyme reactions containing 20 μg of $Man_3GlcNAc_2$ (V-LABS, Inc) were digested with human LysMan, or the novel human α1-6mannosidase, either with or without prior digestion with recombinant human chitobiase (kind gift of Dr. Nathan Aronson, Univ. S. Alabama) in 100mM sodium acetate buffer (D_3, 99%) (pH 4.0). Oligosaccharide samples were removed at the indicated time points, deuterium exchanged by repeated evaporation from D_2O (99.95%, Cambridge Isotope Labs, Inc.) under vacuum, and then dissolved in 500 μl D_2O. ^{1}H-NMR analysis of the oligosaccharides in D_2O or sodium acetate buffer (D_3, 99%, Cambridge Isotope Labs, Inc.) were performed at 25 or 37 °C on a Varian Unity Inova 600 or 800 MHz spectrometer using standard acquisition software available in the Varian VNMR software package.

Sequence analysis and graphical representation: GH 38 sequences were identified in the the GenBank sequence database by TBLASTN searches (40) using the human LysMan protein sequence (GenBank accession no. NP_000519) as the query sequence and the resulting sequences were edited to reflect the Glyco_hydro_38 PFAM motif (41). Multiple sequence alignments were performed using the ClustalX program (42) and a neighbor-joining tree was generated within this program using 1000 bootstrap trials. Dendrograms was displayed as a radial unrooted tree using the program Treeview (43). Species-specific DNA sequence searches

of EST databases were performed by BLASTN searches of species-filtered EST databases using the web-based resource of the National Center for Biotechnology Information (www.ncbi.nlm.nih.gov/BLAST). Comparative pairwise analysis of DNA sequences was accomplished using the Compare and DotPlot subroutines (44) of the University of Wisconsin Genetics Computer Group (GCG software, version 10.2) using a window of 21 residues and a stringency of 14.

RESULTS

Isolation of a human cDNA homolog of the pig and mouse 135 kDa "epididymal" mannosidase: Previous studies on a partially purified α-mannosidase from human spleen and rat liver identified a unique enzyme activity capable of cleaving the Manα1-6Man linkage in the $Man_3GlcNAc$ core of mammalian N-glycan structures (22, 23). The enzyme has several characteristics that are similar to other GH38 α-mannosidases, including size (180 kDa), pH optimum (pH ~4.0), and sensitivity to inhibition by SW and DIM (22). Since the cDNA encoding this enzyme has not yet been identified, we examined sequences related to the GH38 α-mannosidases in order to discover potential candidates that might encode this catalytic activity. Members of the GH38 α-mannosidase family from a number of fully sequenced genomes were analyzed for their sequence relationships. Two signature peptide sequences have been identified as PFAM motifs for the GH 38 α-mannosidases (41), termed Glyco_hydro_38 for a 327 amino acid NH_2-terminal motif and Glyco_hydro_38C for a 487 amino acid COOH-terminal motif (Fig. 1). Sequences containing the Glyco_hydro_38 motif were analyzed from human and mouse sources, as well as other representative species (*Drosophila melanogaster*, *Caenorhabditis elegans*, and *Arabidopsis thaliana*, *Saccharomyces cerevisiae*, and *E. coli*) and

were used to generate an unrooted dendrogram for this multigene family. The dendrogram (Fig. 2) shows four sequence clades for the GH38 α-mannosidases from the respective species. One of the clades represents members known to be involved in glycoprotein biosynthesis (Golgi α-mannosidase II and Golgi α-mannosidase IIx from humans and mice (2, 6, 45, 46) as well as orthologs from *Drosophila melanogaster*, *Caenorhabditis elegans*, and *Arabidopsis thaliana*). A second clade contains the broad specificity lysosomal α-mannosidase involved in glycoprotein catabolism (LysMan from humans and mice (7, 36) as well as multiple orthologs in *Drosophila melanogaster*, *Caenorhabditis elegans*, and *Arabidopsis thaliana*). The third clade is a heterogeneous collection of enzymes represented by the mammalian ER/cytosolic α-mannosidase involved in dolichol-oligosaccharide turnover and the catabolism of glycans on glycoproteins that failed ER quality control and were translocated into the cytosol in mammalian species (2, 4, 5, 47). Several orthologs within this latter clade were found in other diverse organisms classes (i.e. fungi, archaea, and bacteria) suggesting an ancestral origin of this clade. Surprisingly, this latter clade does not contain members from *Drosophila melanogaster* or *Arabidopsis thaliana* suggesting that there may be selective loss of this gene in some species. Finally, a relatively restricted set of vertebrate sequences comprise the fourth GH38 clade (species and GenBank accession numbers include: human [NP_056089], orangutan [Q5RDJ3], chimpanzee [XP_51709], mouse [NP_032576], rat [AAP92617], pig [NP_999014], cow [XP_610717], dog [XP_545897], chicken [XP_420805], and fish (Tetraodon nigroviridis) [CAG04580]; human, mouse, pig peptide sequences are shown in Fig. 2). Noteworthy is the lack of sequence homologs within this latter clade from *Drosophila melanogaster*, *Caenorhabditis elegans*, *Arabidopsis thaliana,* or any other non-vertebrate source. The cDNAs encoding the pig and mouse homologs have been previously cloned (26, 28), but recombinant

enzyme expression has not been accomplished. A sequence alignment of the human, mouse, and pig sequences from this clade is shown in Fig. 1, along with the addition of the human LysMan sequence as reference. The sequence alignment also illustrates the secondary structure features derived from the bovine LysMan structure (PDB 1O7D, (48)) below the sequence alignment indicating that the most conserved regions among members of this clade are predominately restricted to segments of secondary structure, while more divergent sequences are found in the intervening loop regions. All of the members of this novel vertebrate clade also retain the conserved catalytic acid/base (Asp^{290}) and nucleophile (Asp^{151}) proposed from the structure of Golgi α-mannosidase II (PDB 1HWW) (49), as well as the residues that are involved in Zn^{2+} coordination (His^{36}, His^{419}, and Asp^{38}) in the catalytic sites of both bovine LysMan (48) and *Drosophila* Golgi α-mannosidase II (49) (numbering based on the novel human α-mannosidase sequence, colored boxes, Fig. 1). The human sequence homolog of this novel GH38 α-mannosidase subgroup was further examined here as a representative of the enzymes in this latter clade to determine its catalytic characteristics, oligosaccharide substrate specificity, and transcript expression patterns.

Recombinant protein expression in HEK293 cells: A recombinant form of the novel human α-mannosidase was overexpressed and isolated as a secreted protein from the conditioned media of a stably transfected HEK293 cell line. Parallel expression and purification of the human LysMan from transfected HEK293 cells was accomplished in order to compare the catalytic characteristics of the two enzymes. The conditioned media from the respective cell lines were harvested and the enzymes were purified by a combination of Phenyl-Sepharose, cobalt chelating-Sepharose, and Superdex-200 gel filtration chromatography (Fig. 3) using 4MU-Man

as a substrate to monitor enzyme activity during purification. The bulk of the serum proteins were removed from the enzyme preparations on the cobalt chelating-Sepharose column. Surprisingly, neither the His tag or the HA tag appended to the COOH-terminus of the α-mannosidase coding region appeared to be retained by the recombinant proteins as determined by immunoblotting with the respective anti-epitope antibodies. To confirm that the enzymes that we isolated corresponded to the coding regions that we cloned and expressed, the purified enzyme preparations after Superdex-200 chromatography were resolved by SDS-PAGE, stained with Coomassie-G250, excised, digested with trypsin, and sequenced by LC-MS/MS as described in "Experimental Procedures". The peptide sequences that were identified corresponded to the protein sequence encoded by our respective expression constructs confirming the identity of the recombinant protein product and suggesting that the tag sequences had been removed by proteolytic cleavage during or subsequent to secretion of the enzyme into the culture medium.

pH and metal activation studies: Enzyme assays performed with 4MU-Man as substrate revealed that both the novel human α-mannosidase and human LysMan had a pH optimum of ~4.0 (Fig. 4) consistent with a potential lysosomal localization for the former enzyme. Both *Drosophila* Golgi α-mannosidase II and bovine LysMan are proposed to contain an enzyme bound Zn^{2+} ion in their respective active sites involved in direct interactions with glycone substrate hydroxyl residues. To test the influence of various metal cations on the respective α-mannosidase enzyme activities, both the novel human α-mannosidase and human Lysman were stripped of dissociable cations by treatment with EDTA, followed by desalting to remove the chelating agent. The enzyme preparations were then incubated with cations or EDTA for varied

periods of time followed by enzyme assays with 4MU-Man as substrate. The novel human α-mannosidase activity was stimulated by the addition of $CoCl_2$, with greatest stimulation (9-fold) occurring after 1 h preincubation with the cation. Stimulation by $MnCl_2$, $MgCl_2$ and $ZnCl_2$ were 2-4-fold, while preincubation with the other cations or EDTA were inhibitory (Fig. 5A). In particular, $CuCl_2$, $FeCl_2$, and $NiCl_2$ inhibited most significantly after preincubation suggesting either a slow exchange of the cation into the active site or an inhibitory effect of the cation on enzyme stability. Surprisingly, human LysMan activity was not stimulated by the addition of $ZnCl_2$, nor was the enzyme inactivated by more than ~40% by prolonged incubation with EDTA. The effects of incubation with $MnCl_2$, $MgCl_2$, $ZnCl_2$ or $NiCl_2$ were similar to the effects of EDTA treatment, with the exception that the enzymes were less stable with prolonged incubation with $MnCl_2$ and $ZnCl_2$. Incubation with $CoCl_2$, $CuCl_2$, and $FeCl_2$ were more inhibitory than the other cations, especially following preincubation (Fig 5B).

Inhibition studies on the novel human α-mannosidase and human LysMan: The novel human α-mannosidase and human LysMan were examined for their inhibitor profiles using 4MU-Man as substrate. Both enzymes followed normal Michaelis-Menten kinetics with K_m values of 7.6 mM and 0.52 mM on the substrate 4MU-Man, respectively (Table 2). SW and DIM, characteristic Class II mannosidase inhibitors, had similar effects on both enzymes, resulting in sub-micromolar K_i values. The Class 1 α-mannosidase inhibitors, KIF and dMNJ, had less inhibitory effects on both enzymes, with the former compound resulting in K_i values in the low micromolar range and the latter compound inhibiting the enzymes in the 60-200 μM range. Thus, the novel human α-mannosidase had a similar response to the inhibitors as the

human LysMan, while the K_m for the 4MU-Man synthetic substrate was considerably higher for the former enzyme.

Substrate specificity studies with larger oligosaccharide substrates: The substrate specificities of the novel human α-mannosidase and human LysMan were examined using a collection of high mannose N-glycan substrates tagged at their reducing terminus with pyridylamine. Similar amounts of the two enzymes, based on 4MU-Man activity assays, were incubated with the respective substrates for 24 h at 37 °C and resolved by HPLC to examine the degree of glycan trimming. The novel human α-mannosidase was unable to cleave $Man_{9\text{-}6}GlcNAc_2$-PA or $GlcNAcMan_5GlcNAc_2$-PA (Fig. 6, Panels b, e, h, k, and q), but the enzyme weakly cleaved $Man_5GlcNAc_2$-PA to $Man_4GlcNAc_2$-PA (60% conversion, Fig. 6, Panel n) only after prolonged incubation. By contrast, human LysMan hydrolyzed $Man_{9\text{-}5}GlcNAc_2$-PA down to $Man_2GlcNAc_2$-PA, (Fig. 6, Panels c, f, i, l, and o) but would not cleave the $GlcNAcMan_5GlcNAc_2$-PA glycan processing intermediate (Fig. 6, Panel r). These results confirm that human LysMan can hydrolyze a variety of glycan substrates containing terminal α1-2-, α1-3-, and α1-6-linked mannose residues, whereas the novel α-mannosidase is unable to recognize these larger high mannose structures as substrates for hydrolysis.

Substrate specificity studies of the novel human α-mannosidase and human LysMan toward Man_3 core-mannosyl oligosaccharides by ^{1}H-NMR: In an effort to determine whether the novel α-mannosidase has a substrate specificity similar to the core-specific α1-6mannosidase (16, 21-23), we performed a series of time course studies for the digestion of $Man_3GlcNAc_{2\text{-}1}$ glycans and examined the reaction products by ^{1}H-NMR. $Man_3GlcNAc$ was generated from

$Man_3GlcNAc_2$ by digestion with human chitobiase and spectra of both glycans were obtained for the assignment of the resonances of the anomeric protons for each substrate. The spectra shown in Fig. 7B, indicating the digestion of $Man_3GlcNAc_2$ by chitobiase, also contains the novel human α-mannosidase (time zero for the novel human α-mannosidase digestion). As a result there is a slight reduction in the peak signal for the α1-6-linked Man residue (***Man4'***) because of a partial digestion of this linkage (compare Fig. 7A and 7B). Digestion of Manα1-6[Manα1-3]Manβ1-4GlcNAcβ1-4GlcNAc by chitobiase resulted in the shift of a GlcNAc H-1 (***GlcNAc1***) resonance from δ=4.591 ppm to δ=5.191 ppm indicative of the generation of a free GlcNAc α-anomer enzymatic product. Each of the two substrates was then used to generate a time course digestion profile with either the novel human α-mannosidase or human LysMan as the enzyme source. A 12 h digestion of the $Man_3GlcNAc$ substrate by the novel human α-mannosidase resulted in the disappearance of the α1-6Man residue (***Man4'*** H-1 resonance at δ=4.902 ppm, Fig. 7C) and the appearance of a free mannose α-anomer resonance at δ=5.152 ppm (Fig. 7C). Confirmation of the cleavage of the ***Man4'*** residue was indicated by the loss of the H-2 resonance for ***Man4'*** at δ=4.162 ppm, but retention of the H-1 and H-2 signals for ***Man4***, ***Man3***, and ***GlcNAc2*** (Fig. 7C). The time course of $Man_3GlcNAc$ cleavage by the novel human α-mannosidase or the human LysMan indicated that both enzymes could remove a single monosaccharide from the glycan substrate, but each enzyme cleaved a different residue (Fig. 8). As indicated from the 12 h digestion in Fig. 7C, the novel human α-mannosidase rapidly cleaved the α1-6Man residue (***Man4'*)** from the Manα1-6[Manα1-3]Manβ1-4GlcNAc substrate (Fig. 8B), whereas the human LysMan cleaved the α1-3Man residue (***Man4*)** (Fig. 8H) without further cleavage. A similar result was obtained when the human LysMan was incubated with the $Man_3GlcNAc_2$ substrate, only the α1-3Man residue (***Man4*)** was cleaved (Fig. 8K). In contrast,

no cleavage occurred when the novel human α-mannosidase was incubated with $Man_3GlcNAc_2$ substrate (Fig. 8E). These data indicate that the novel α-mannosidase can cleave only the α1-6Man residue from the Man_3 core glycan structure after the action of chitobiase to yield a Manα1-3Manβ1-4GlcNAc structure, a characteristic previously identified for the lysosomal core-specific α1-6mannosidase (16, 21-23). Hereafter we will refer to this enzyme as the human core-specific α1-6mannosidase.

Tissue distribution of mRNA transcripts for human LysMan and human core-specific α1-6mannosidase: Transcript levels of human LysMan and the human core-specific α1-6mannosidase were determined in human tissues by Northern blot analysis. A major transcript of ~4.5 kb was found in all tissues (Fig. 9), consistent with the size of the human GenBank reference sequence (NM_015274, 4242 bp), including ~37 bp of 5' untranslated region, a coding region of 3027 bp, ~1.2 kb 3' untranslated sequence, and a poly(A) tail. The transcripts encoding human LysMan and the novel human α-mannosidase were similarly expressed in most human tissues, with the exception of brain where human LysMan had lower expression levels and skeletal muscle and kidney where the α1-6mannosidase had slightly lower transcript levels.

Comparison of core-specific α1-6mannosidase and chitobiase transcript expression in mammalian species – Previous studies have indicated that the chitobiase and the core-specific α1-6mannosidase may be expressed in a similarly restricted set of mammalian species (16, 24). In particular, human and rodent species express transcripts encoding the chitobiase. However, ungulates, cats and dogs have the chitobiase gene, but transcripts are not expressed as a result of

alterations in the 5' promoter sequences that cause defective gene transcription (16, 25). Core-specific α1-6mannosidase activity was also detected in human and rodent tissues, but no activity was detected from extracts of cow, dog, or cat tissues (16). To determine if the absence of core-specific α1-6mannosidase activity resulted from defective transcription, we identified cDNA or genomic sequences encoding the human, mouse, cow, dog, and pig versions of the core-specific α1-6mannosidase as well as the corresponding chitobiase sequences by cross-species TBLASTN searching of the GenBank sequence database (Table 3). Coding region DNA sequences were subsequently employed for searching the respective species-specific expressed sequence tag (EST) databases and the numbers of exact match EST sequences were tallied as a surrogate measure for the relative transcript abundance in each species (Table 3). As a control, EST sequences encoding LysMan were tallied in each species, since this latter lysosomal enzyme has been shown to be expressed in each of the respective species (7, 8, 48, 50, 51). The total number of EST sequences with identity to LysMan varied widely, largely as a result of the variable number of the EST sequence entries in the GenBank database for each species (Table 3). When the number of EST sequences identified for the chitobiase and α1-6mannosidase were compared to the LysMan-specific ESTs in human and mouse, the abundance was consistently lower (42% and 25% for human and mouse α1-6mannosidase and 23% and 8% for human and mouse chitobiase, respectively, compared to LysMan). The total number of ESTs identified for LysMan was <100 for the dog, pig, and cow transcripts reflecting a ≥10-fold lower number of ESTs in the respective databases. Pig ESTs encoding the chitobiase were surprisingly numerous (88% of the number of LysMan ESTs), whereas the number of α1-6mannosidase-specific ESTs in the pig database numbered only two (8% of the number of LysMan ESTs), despite the original identification of the enzyme and the cDNA encoding the α1-6mannosidase in this species (26).

In contrast, dog ESTs encoding the α1-6mannosidase were numerous (95% of the number of LysMan ESTs), while the chitobiase ESTs in dog were in relatively low abundance (10% of the number of LysMan ESTs). In the bovine EST database no sequences were detected with identity to either the chitobiase or the α1-6mannosidase, despite the identification of >70 LysMan-specific EST sequences in this species. In the case of the α1-6mannosidase, two partial gene sequences with high similarity to human α1-6mannosidase were identified within the incompletely sequenced bovine genome (Table 3), but in neither instance were ESTs encoded by these genes detected in database searches. These data indicate that transcripts encoding both the chitobiase and core-specific α1-6mannosidase are variable in abundance in dogs and pigs, but in all cases they are generally less abundant than LysMan-specific transcripts. However, despite the presence of the respective genes in the bovine genome, transcripts encoding both the chitobiase and core-specific α1-6mannosidase appear to be absent from bovine tissues.

In prior work examining the defective transcription of the bovine chitobiase it was noted that the coding sequence was highly conserved between the human and bovine enzymes, whereas the 5'-flanking sequences were completely divergent between the two species (25). This contrasted with a comparison of the 5'-flanking sequences of human and bovine LysMan, which retained considerable sequence conservation (58% identity (25)) in the upstream sequences. This loss of sequence similarity and the inclusion of a repetitive element sequence within the bovine chitobiase 5'-flanking sequence were used as an explanation for the absence of bovine transcripts for the chitobiase. We performed a similar pairwise sequence analysis between the human α1-6mannosidase 5'-flanking sequence and the corresponding flanking sequences of the two putative partial bovine α1-6mannosidase genes. The dotplot analysis revealed no appreciable sequence similarity in the 5'-flanking sequences (Fig. 10A and 10B) similar to the results of the

pairwise comparison of the human and bovine chitobiase genes (Fig. 10C). In contrast, the sequence similarity in the 5' flanking sequences of the human and bovine LysMan was clearly evident in the dotplot analysis (Fig. 10D). These data suggest that the lack of transcripts encoding the α1-6mannosidase in bovine tissues is likely a result from defective transcription, analogous to the defective transcription for the chitobiase, through alterations in 5' flanking sequences that lead to disruptions of promoter elements necessary for transcript synthesis.

DISCUSSION

The catabolism of N-glycosylated proteins in mammalian lysosomes occurs through a bidirectional process (52). Polypeptides are digested by lysosomal proteases and the associated N-glycans are released from Asn side chains at their reducing termini by a glycosylasparaginase action. Glycan structures are also cleaved from their non-reducing termini by a collection of exoglycosidases to result in trimming down to the glycan core. Complex type and high mannose N-glycans are differentiated by the array of enzymes required for cleavage to the glycan core, but both processes yield a $Man_3GlcNAc_2$ structure that must be further degraded to monosaccharides in lysosomes. The same enzyme responsible for the broad specificity cleavage of α1-2, α1-3, and α1-6mannose residues in high mannose structures, LysMan, initiates the cleavage of the $Man_3GlcNAc_2$ core (Fig. 8K). This enzyme has the ability to cleave the core α1-3Man residue, but the final α1-6Man residue is largely resistant to cleavage by this enzyme. In humans and rodents, the further catabolism of the Manα1-6Manβ1-4$GlcNAc_2$ core requires a complex interplay between cleavage at both the reducing and non-reducing termini of the glycan structure (16, 52)**.** Exoglycosidase cleavage of the Manα1-6Man linkage by α1-6mannosidase requires the prior action of the chitobiase to cleave the GlcNAcβ1-4GlcNAc core. Finally, the lysosomal β-

mannosidase cleaves the Manβ1-4GlcNAc linkage to complete glycan catabolism. Surprisingly, the chitobiase gene is found predominately in mammalian species as well chickens and slime mold, however the corresponding enzyme activity was not found in ungulates and carnivora despite the presence of the corresponding gene in the respective genomes (52). Characterization of the bovine chitobiase gene indicated that selective alterations in the 5'-flanking sequences could account for the absence of transcripts and chitobiase enzyme activity. *In vitro* assays of cell and tissue extracts for the core-specific α1-6mannosidase in several mammalian species indicated an absence of the latter enzyme activity in a similar set of species as the chitobiase. Species that do not contain appreciable chitobiase or α1-6mannosidase activities presumably accomplish glycan catabolism solely through exoglycosidase action following oligosaccharide release by glycosylasparaginase. In these latter species it is not clear how the cleavage of the Manα1-6Man linkage is efficiently accomplished in the absence of α1-6mannosidase action.

While molecular studies on the chitobiase have effectively characterized the nature of the species distribution and expression of this enzyme, parallel studies on the α1-6mannosidase have been restricted to *in vitro* assays from crude tissue and cell extracts or partially purified enzyme preparations (21-23). Identification of the cDNA or gene encoding the enzyme was hampered by difficulties in enzyme purification from crude tissue extracts and the complexity of assaying the enzyme with small oligosaccharide substrates. Initial studies also indicated a high K_m for the enzyme with synthetic pNP- or 4MU-Man substrates. We decided to take an alternate approach for the identification of the cDNA encoding the α1-6mannosidase. The characteristics of the core-specific α1-6mannosidase from crude extracts were similar in several respects to other GH38 enzymes, including pH optimum, response to inhibitors, large size, stimulation by divalent cations, and ability to cleave α1-6Man linkages. Among the various GH38 sequences from

vertebrate and non-vertebrate sources, four subgroups were detected by phylogenetic analysis. Members of three of those subgroups had well defined functions in glycan biosynthesis or catabolism. The fourth subgroup was uniquely restricted to vertebrates and none of the known members of this latter group had been expressed or characterized for detailed oligosaccharide substrate specificity. As candidates for the α1-6mannosidase activity, we chose to clone, express, purify, and characterize the human member of this subgroup and compare its substrate specificity with the well-characterized human LysMan, which we had previously cloned and expressed (7). Consistent with the hypothesis that members of this subgroup exhibit core-specific α1-6mannosidase activity, all of the characteristics of the recombinant enzyme, including low pH optimum, potent sensitivity to SW and DIM, stimulation by Co^{2+} and Zn^{2+}, and cleavage of the α1-6Man linkage in a $Man_3GlcNAc$ substrate were in agreement with prior data on the partially purified α1-6mannosidase (22, 23).

Prior data on the mouse and pig orthologs of the α1-6mannosidase indicated a tissue-restricted expression pattern. The enzyme was initially isolated from porcine caudal epididymal fluid and Northern blots indicated transcript expression restricted to the border of the caput and corpus epididymis (26). Mouse transcripts encoding the enzyme were found exclusively in type A spermatogonia at stages IX-XI of spermatogenesis (28). In contrast, subsequent studies have shown that transcripts encoding the murine ortholog of the α1-6mannosidase are not restricted to reproductive tissues, but they are ubiquitously expressed, consistent with our present data demonstrating a ubiquitous expression of transcripts encoding the human enzyme. Northern blots and *in situ* hybridizations for the pig and mouse α1-6mannosidase employed oligonucleotide probes in the initial transcript studies (26, 28), while the more recent studies ((30) and Fig. 9) have used larger, high stringency probes to clearly demonstrate a ubiquitous pattern of transcript

expression. A broadly distributed transcript expression profile for the core-specific α1-6mannosidase is also indicated by the identification of numerous ESTs encoding the α1-6mannosidase from a wide variety of mammalian tissues and cells.

While prior data on the substrate specificity of the purified porcine "epididymal" enzyme detected weak cleavage of Man_8GlcNA_2-PA to Man_6GlcNA_2-PA, our data on the recombinant α-mannosidase showed no detectable cleavage of larger PA-tagged N-glycans except for a weak activity toward Man_5GlcNA_2-PA. Incomplete cleavage of the glycan and insufficient quantities of the Man_5GlcNA_2-PA substrate precluded the further characterization of this enzymatic product. However, high activity was found for the cleavage of the Manα1-6Man linkage on a Manα1-3[Manα1-6]Manβ1-4GlcNAc substrate as characterized in ^{1}H-NMR time-course studies. The rate of cleavage of this substrate was comparable to the rate of cleavage of the Manα1-3Man linkage in the $Man_3GlcNAc$ substrate by LysMan. Prior data on the purified porcine α1-6mannosidase ortholog also indicated that the enzyme had a pH optimum of ~6.5 in contrast to the acidic pH optimum (pH ~4.0) for the recombinant human α1-6mannosidase. One possible explanation for the discrepancy for the activity would be a contaminating enzyme in the porcine α-mannosidase preparation, since the activity of the human α1-6mannosidase toward the 4MU-Man substrate is low as a result of the high K_m toward this substrate, especially in the absence of added Co^{2+}.

The low pH optimum and the prior data indicating a lysosomal localization for the core-specific α1-6mannosidase (16, 24) strongly suggests that the human α1-6mannosidase characterized here is involved in lysosomal N-glycan catabolism. The absence of any detectable activity toward $Man_3GlcNAc_2$ substrates or larger high mannose substrates would likely preclude

a role for this enzyme in the modification of sperm-surface glycoproteins in the epididymus or testis as originally proposed for the porcine and murine forms of the enzyme (26, 28, 29).

Analysis of transcript expression levels in various mammalian species indicate that transcripts encoding LysMan are expressed in human, mouse, cow, dog, and pig tissues, as previously described (15-17, 53). In contrast, chitobiase ESTs were identified from human and mouse sources, low transcript abundance was indicated for chitobiase in the dog EST database, and no ESTs were detected from bovine sources. These data are consistent with the model for a conserved chitobiase gene within genomes of all vertebrate, but selective alterations in promoter sequences leading to defective transcription within ungulates and carnivora. Surprisingly, numerous chitobiase-specific ESTs were identified from pig sources, despite prior data indicating that the enzyme activity was absent in this species. The abundance of α1-6mannosidase-specific ESTs was similar in several respects to the abundance of ESTs encoding chitobiase. Numerous ESTs were identified in the human and mouse databases, but no ETS were detectable in the bovine database. EST abundance differed in dog and pigs, where α1-6mannosidase ESTs were highly abundant in the dog database but are rare in the pig database. The absence of any detectable sequence similarity in the 5' flanking sequences between the human and bovine α1-6mannosidase genes, similar to the loss of promoter sequences for bovine chitobiase, indicated that the two genes are likely to be inactivated by a similar mechanism in the cow.

The functional linkage of chitobiase and α1-6mannosidase activities suggests a co-evolution of the enzymes for the full and efficient catabolism of the N-glycan core structures despite their presence on different chromosomes in humans (chromosome 4p16.1 for α1-6mannosidase and 1p22 for chitobiase) and mice (chromosome 3H3 for α1-6mannosidase

and 5B2 for chitobiase). The common occurrence of both enzymes in the same species is also correlated with the structures of glycans that accumulate in species lacking the broad specificity LysMan. Human and rodent species predominately accumulate structures based on a core Manα1-3Manβ1-4GlcNAc structure in the absence of LysMan as a result of the presence of both lysosomal chitobiase and α1-6mannosidase. Ungulates and cats accumulate structures based on the Manα1-3[Manα1-6]Manβ1-4GlcNAc$_2$ core structure based on the absence of these latter enzymes. Presumably the two enzymes act in tandem to provide an efficient catabolism of the core N-glycans in mammalian lysosomes. Surprisingly, even species that do not express chitobiase and core-specific α1-6mannosidase express a LysMan activity that is relatively inefficient for the cleavage of the core Manα1-6Man linkage. The manner by which glycan catabolism is accomplished under these circumstances is not understood. Thus, the benefit of the "accessory" hydrolase functions of the chitobiase and α1-6mannosidase are achieved in only a restricted subset of mammals for glycan catabolism. The manner by which these enzymes were recruited and maintained through vertebrate evolution will be an ongoing area of research in the future.

*FOOTNOTES:

This work was supported by National Institutes of Health Research Grants GM47533, CA91295, and RR05351 (to K.W.M.).

We wish to thank Dr. Nathan Aronson (University of So. Alabama) for his kind gift of recombinant human chitobiase and Dr. Lance Wells for his assistance in performing the LC-MS/MS sequencing analysis of the recombinant proteins.

[1]The abbreviations used are: ER, endoplasmic reticulum; LysMan, lysosomal mannosidase; SW, swainsonine; DIM, 1,4-dideoxy-1,4-imino-D-mannitol; dMNJ, 1-deoxymannojirimycin; Kif, kifunensine; 4MU, 4-methylumbelliferyl-; pNP-, p-Nitrophenyl-; NMR, nuclear magnetic resonance; HPLC, high performance liquid chromatography; GH, glycosylhydrolase, EST, expressed sequence tag

Fig. 1: **Sequence alignments of GH38 members from a novel clade of α-mannosidases.** A diagrammatic representation of the coding region for GH38 mannosidases is shown at the top of the figure, indicated by the gray line, with the two characteristic PFAM motifs highlighted by the large colored boxes (Glyco_hydro_38 highlighted in orange and Glyco_hydro_38C highlighted in green). GH38 α-mannosidase sequences from pig (Pig, GenBank NP_999014), mouse (Mouse, NP_032576), and human (Human, NP_056089, the sequence studied here) sources as well as the broad specificity human LysMan sequence (Human_Lys, NP_000519) are shown in the sequence alignment. Identical sequences are shown with dark blue highlighting, while similar sequences are displayed with light blue highlighting. The two signature PFAM motifs are highlighted in the sequence (Glyco_hydro_38, orange line over the sequence alignment, and Glyco_hydro_38C, green line over the sequence alignment). The positions of predicted secondary structure are indicated below the sequence alignment based on the structure of the bovine LysMan (PDB 1O7D, (48)). α-Helical segments are represented by colored helices below the sequence alignment, while segments of β-sheet structure are indicated by solid black arrows. The putative conserved catalytic acid/base (Asp^{290}, green box) and nucleophile (Asp^{151}, orange box) are indicated based on the assignment of these roles in *Drosophila* Golgi α-mannosidase II (49). Residues involved in Zn^{2+} coordination (His^{36}, His^{419}, Asp^{38}, red boxes) are highlighted based on the structures of *Drosophila* Golgi α-mannosidase II (49) and bovine LysMan (48).

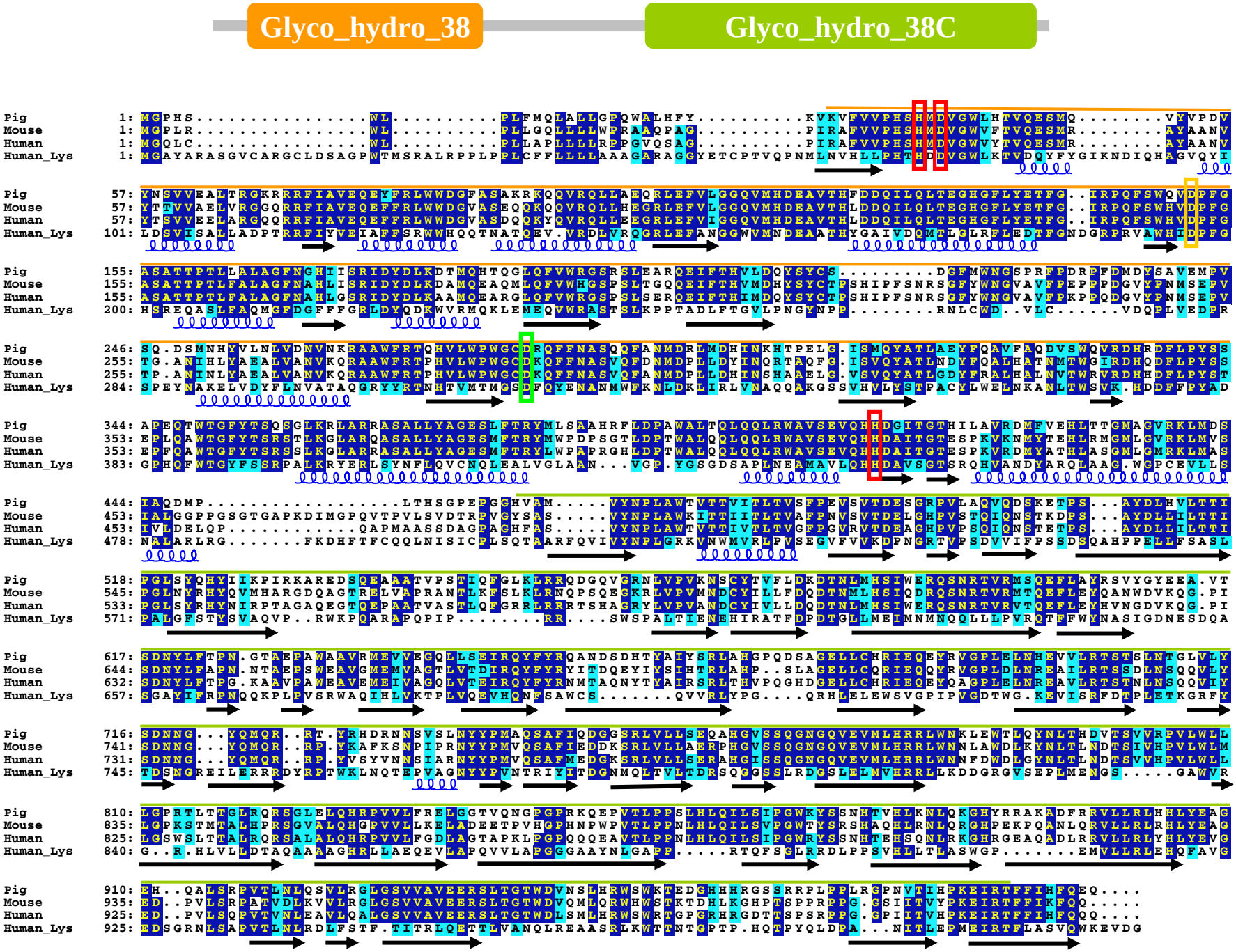
Glyco_hydro_38
Glyco_hydro_38C
Pig
Mouse
Human
Human_Lys

Fig. 2: **Dendrogram of GH38 α-mannosidases shows four sequence clades**. GH38 members from *Homo sapiens, Mus musculus, Drosophila melanogaster*, *Caenorhabditis elegans*, *Arabidopsis thaliana* were identified by TBLASTN searches (40) of the GenBank database. Selected fungal, bacterial, archaeal and pig sequences were also included where indicated. The respective sequences were edited to reflect the Glyco_hydro_38 PFAM motif (41), multiple sequence alignments were performed using the ClustalX program (42), and a neighbor-joining tree was generated within this program using 1000 bootstrap trials. The tree was displayed as a radial unrooted dendrogram using the program Treeview (43). Sequence and species designations and their corresponding GenBank accession numbers (in parentheses) are indicated at the end of each branch. The outer oval with the indicated labels show the designations of the subgroups within the GH38 α-mannosidase family based on the sequence similarity analysis. The four clades represent Golgi mannosidase II, lysosomal mannosidase, a heterogeneous ancestral clade, and a clade represented by a collection of novel vertebrate α-mannosidase sequences.

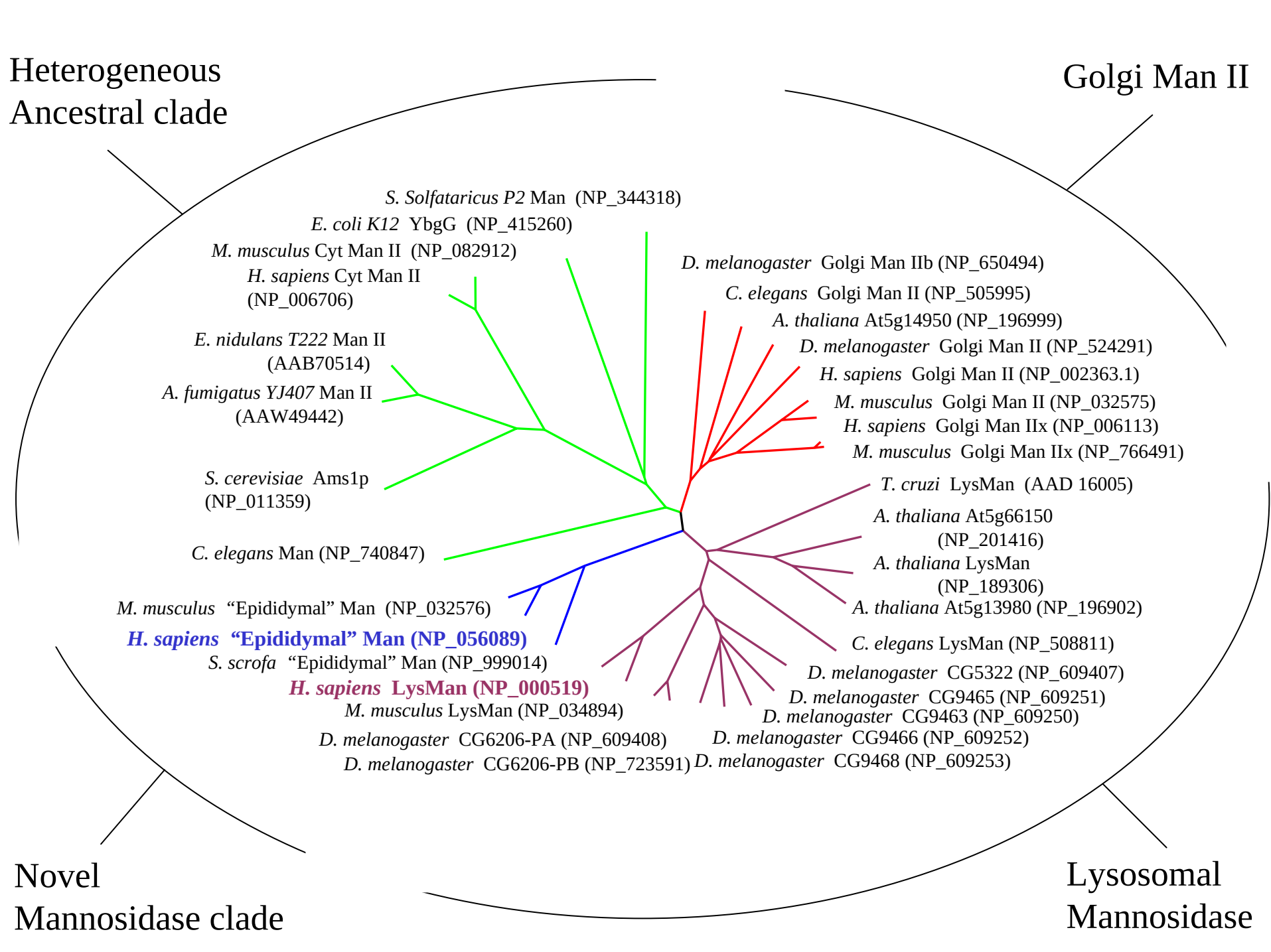
Heterogeneous
Ancestral clade
Golgi Man II
S. Solfataricus P2 Man (NP_344318)
E. coli K12 YbgG (NP_415260)
M. musculus Cyt Man II (NP_082912)
H. sapiens Cyt Man II
(NP_006706)
E. nidulans T222 Man II
(AAB70514)
A. fumigatus YJ407 Man II
(AAW49442)
S. cerevisiae Ams1p
(NP_011359)
C. elegans Man (NP_740847)
M. musculus "Epididymal" Man (NP_032576)
H. sapiens "Epididymal" Man (NP_056089)
S. scrofa "Epididymal" Man (NP_999014)
H. sapiens LysMan (NP_000519)
M. musculus LysMan (NP_034894)
D. melanogaster CG6206-PA (NP_609408)
D. melanogaster CG6206-PB (NP_723591)
D. melanogaster Golgi Man IIb (NP_650494)
C. elegans Golgi Man II (NP_505995)
A. thaliana At5g14950 (NP_196999)
D. melanogaster Golgi Man II (NP_524291)
H. sapiens Golgi Man II (NP_002363.1)
M. musculus Golgi Man II (NP_032575)
H. sapiens Golgi Man IIx (NP_006113)
M. musculus Golgi Man IIx (NP_766491)
T. cruzi LysMan (AAD 16005)
A. thaliana At5g66150
(NP_201416)
A. thaliana LysMan
(NP_189306)
A. thaliana At5g13980 (NP_196902)
C. elegans LysMan (NP_508811)
D. melanogaster CG5322 (NP_609407)
D. melanogaster CG9465 (NP_609251)
D. melanogaster CG9463 (NP_609250)
D. melanogaster CG9466 (NP_609252)
D. melanogaster CG9468 (NP_609253)
Novel
Mannosidase clade
Lysosomal
Mannosidase

Fig. 3: **Purification of the novel recombinant human α-mannosidase and human LysMan from the culture medium HEK293 cells**. The conditioned medium from stably transfected HEK293 cells expressing the novel human α-mannosidase was successively chromatographed over Phenyl-Sepharose (panel A), cobalt chelating-Sepharose (panel B), and Superdex-200 (panel C). Column fractions were assayed for α-mannosidase activity (open squares) and absorbance at 280 nm (solid squares). The pooled fractions from each chromatography step are indicated by the bar above the corresponding plot. The final enzyme preparations of the novel human α-mannosidase (D) and human LysMan (E) were resolved by SDS-PAGE and stained with Coomassie Blue G-250. The purified human LysMan on SDS-PAGE appears as a band at ~120 kDa for the full length enzyme and two bands at ~72 kDa and ~50 kDa that result from selective proteolysis as described previously (51).

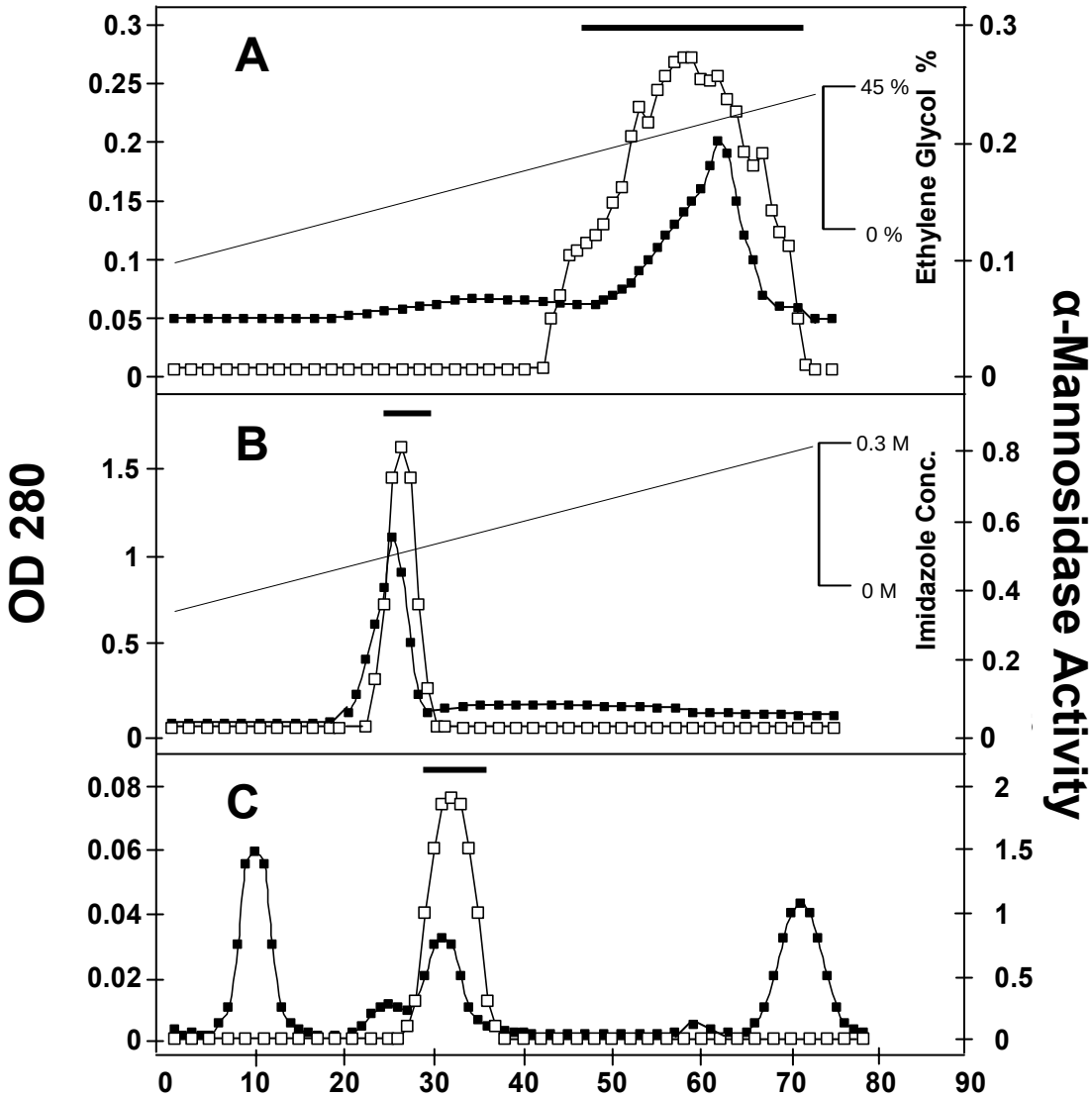
A
B
C
OD 280
α-Mannosidase Activity
45 %
0 %
Ethylene Glycol %
0.3 M
0 M
Imidazole Conc.
0.3
0.25
0.2
0.15
0.1
0.05
0
1.5
1
0.5
0.8
0.6
0.4
0.08
0.06
0.04
0.02
2
1.5
1
0.5
0
10
20
30
40
50
60
70
80
90

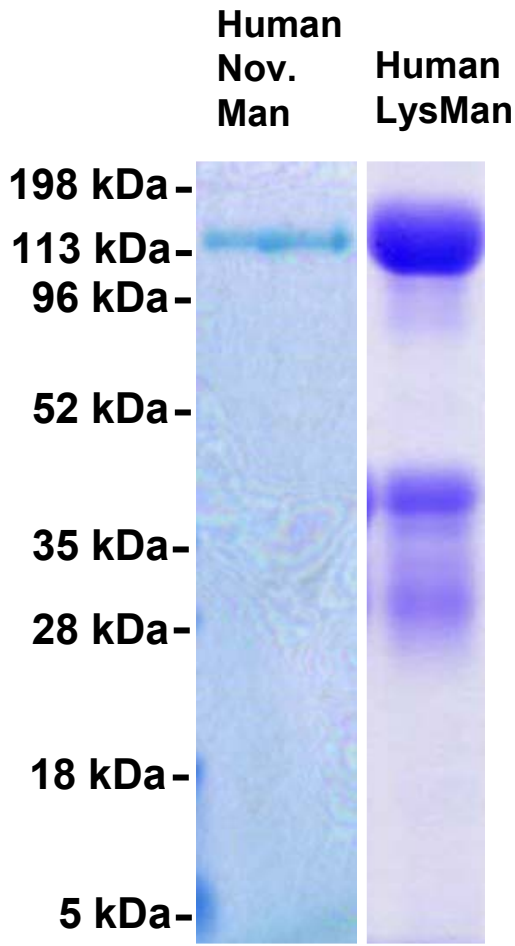
Human
Nov.
Man
Human
LysMan
198 kDa
113 kDa
96 kDa
52 kDa
35 kDa
28 kDa
18 kDa
5 kDa

Table 1: Purification of recombinant human novel α-mannosidase from conditioned medium of stably transfected HEK293 cells.

Step	Protein	Activity	Specific Activity	Enrichment	Yield
	(mg)	*(units)*	*(units/mg)*	*(-fold)*	*(%)*
Phenyl Sepharose	96	23.64	0.24	1	100
Co^{2+}-Chelate Affinity	0.19	3.47	18.26	74.1	15
Superdex 200	0.017	2.5	144.50	586	11

Fig. 4: **Influence of pH on the novel human α-mannosidase and human LysMan enzyme activity**. The novel human α-mannosidase (open triangles) and human LysMan (close squares) activities were assayed using 4MU-Man as substrate at the indicated pH values as described in "Experimental Procedures."

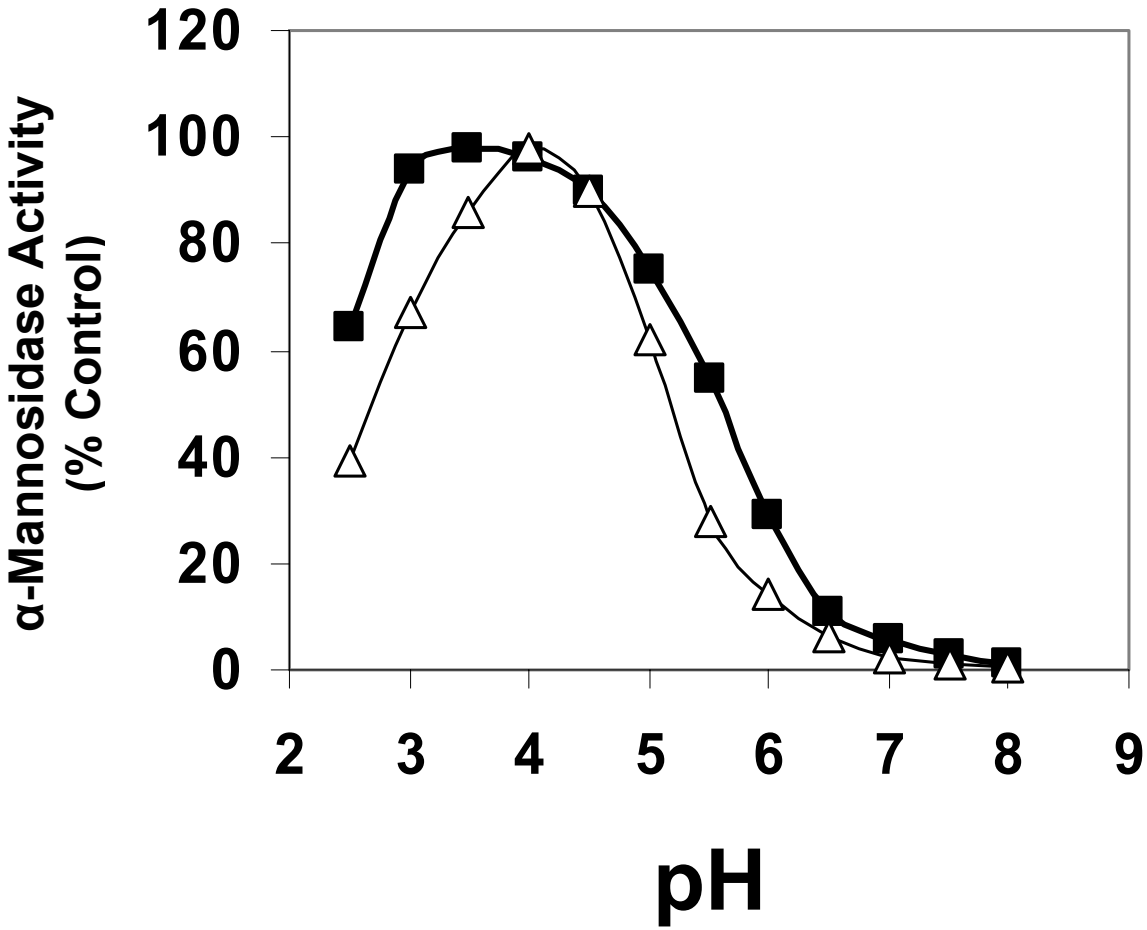
α-Mannosidase Activity
(% Control)
120
100
80
60
40
20
0
2
3
4
5
6
7
8
9
pH

Fig. 5: **The effect of divalent cations on the novel human α-mannosidase and human LysMan enzyme activities.** The novel human α-mannosidase (Panel A) and human LysMan (Panel B) were stripped of divalent cations by treatment with EDTA, desalted to remove the chelator, and then incubated for the indicated time in the presence of various divalent cations ($CoCl_2$, $CuCl_2$, $FeCl_2$, $MgCl_2$, $MnCl_2$, $NiCl_2$, and $ZnCl_2$), EDTA, or control conditions in the presence of buffer alone at pH 7.0 at 37°C. The pH was then adjusted to 4.0 and the enzyme activities were assayed with the 4MU-Man substrate. Activity levels are expressed as percentages of the level measured in control assays containing no metal cations. The color key in the figure indicates the time of incubation at 37 °C before the enzyme assay.

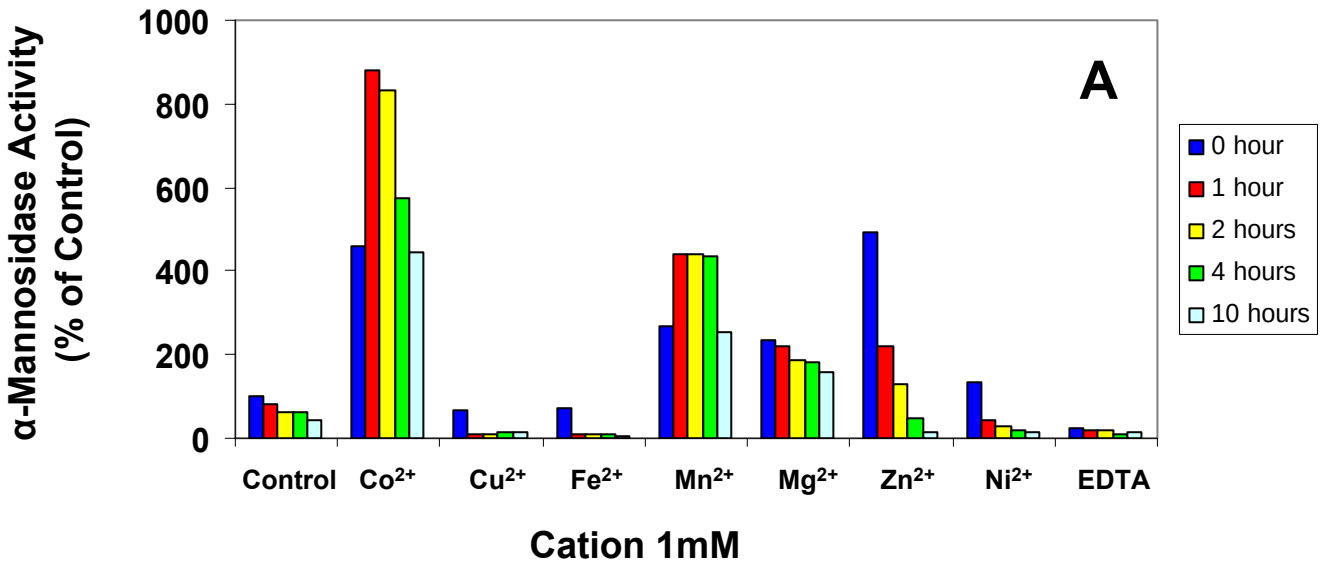
α-Mannosidase Activity
(% of Control)
1000
800
600
400
200
0
A
0 hour
1 hour
2 hours
4 hours
10 hours
Control
Co2+
Cu2+
Fe2+
Mn2+
Mg2+
Zn2+
Ni2+
EDTA
Cation 1mM

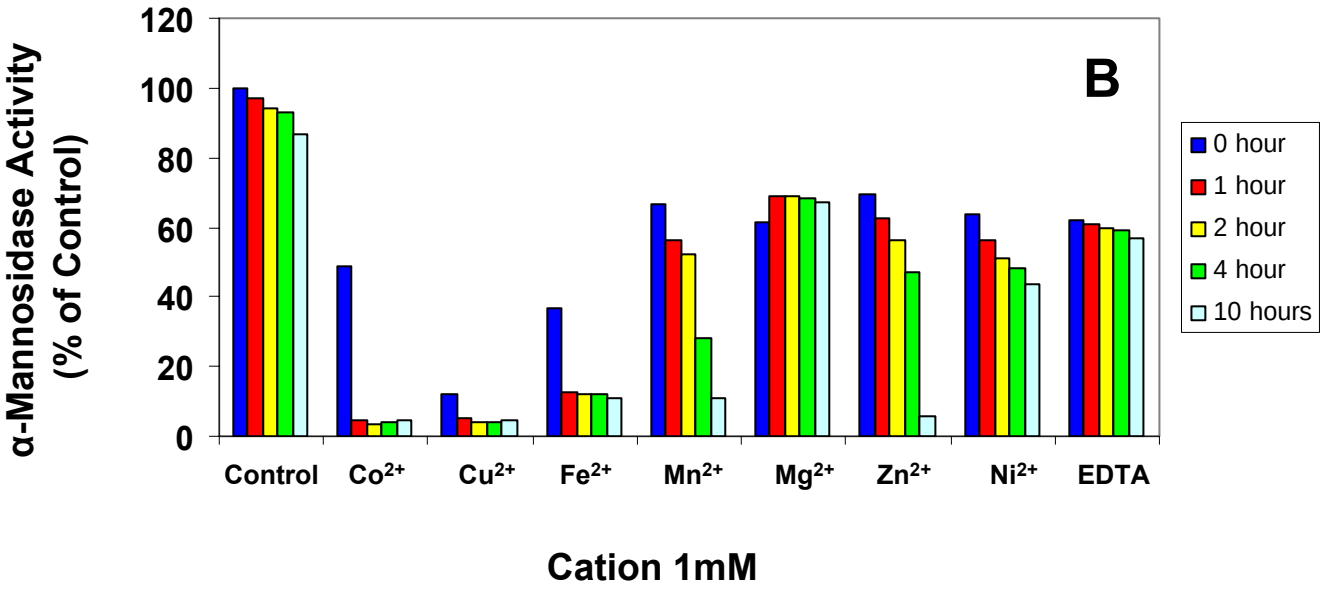
B
α-Mannosidase Activity
(% of Control)
120
100
80
60
40
20
0
Control
Co2+
Cu2+
Fe2+
Mn2+
Mg2+
Zn2+
Ni2+
EDTA
Cation 1mM
0 hour
1 hour
2 hour
4 hour
10 hours

Table 2: Comparison of inhibitor profiles for the novel human α-mannosidase and human LysMan.

Inhibitors	Novel human α-mannosidase[a]	Human LysMan[a]
	K_i	K_i
	(μM)	*(μM)*
SW	0.121	0.076
DIM	0.720	0.349
KIF	13	19
dMNJ	202	65

[a] The K_m values for the novel human α-mannosidase and human LysMan using 4MU-Man substrate were 7.6 mM and 0.52 mM, respectively.

Fig. 6: **Digestion of high mannose oligosaccharide substrates by the novel human α-mannosidase and human LysMan**. Pyridylamine-tagged (PA) oligosaccharide substrates ($Man_9GlcNAc_2$-PA, **M9**; $Man_8GlcNAc_2$-PA, **M8**; $Man_7GlcNAc_2$-PA, **M7**; $Man_6GlcNAc_2$-PA, **M6**; $Man_5GlcNAc_2$-PA, **M5**; $GlcNAcMan_5GlcNAc_2$-PA, **GnM5)** were subjected to enzymatic cleavage with the novel human α-mannosidase or human LysMan for 24 hours at 37 ˚C and resolved on a Hypersil APS2 NH_2-column. Left panels, standard oligosaccharide substrates with elution positions indicated by the respective labels; center panels, digestion of respective oligosaccharide substrates by the novel human α-mannosidase; right panels, digestion of respective oligosaccharide substrates by human LysMan. Peaks were identified by comparison to PA-tagged standards of known structure (left panel).

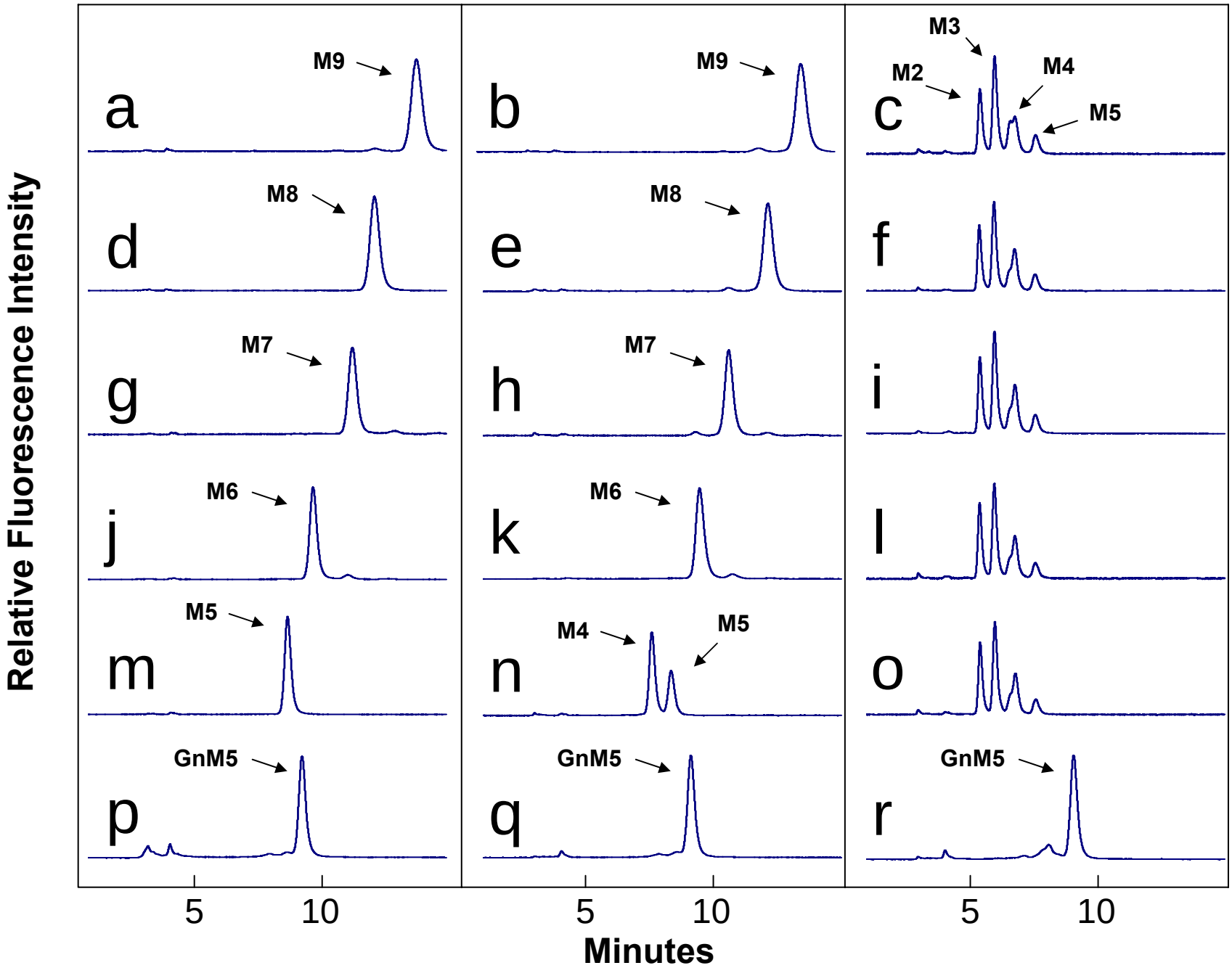
Relative Fluorescence Intensity
a
M9
b
M9
c
M3
M2
M4
M5
d
M8
e
M8
f
g
M7
h
M7
i
j
M6
k
M6
l
m
M5
n
M4
M5
o
p
GnM5
q
GnM5
r
GnM5
5
10
5
10
5
10
Minutes

Fig. 7: **^{1}H-NMR analysis of $Man_3GlcNAc_{2\text{-}1}$ oligosaccharide substrates and the product of $Man_3GlcNAc$ digestion by the novel human α-mannosidas.** Downfield sections of the 1-D ^{1}H-NMR spectra are shown for the mannosyl oligosaccharides, $Man_3GlcNAc_2$ (Panel A), $Man_3GlcNAc$ (following the digestion of $Man_3GlcNAc_2$ by chitobiase, Panel B), and $Man_2GlcNAc$ (following digestion of $Man_3GlcNAc$ by the novel human α-mannosidase, Panel C). The assignments of H-1 and H-2 resonances in the ^{1}H-NMR spectra are indicated by the color-coded labels relative to the structures shown at the top of each panel. The spectra of the $Man_3GlcNAc$ structure generated by chitobiase digestion (Panel B) indicates a shift of the GlcNA1 H-1 resonance from δ=4.591 ppm to δ=5.191 ppm indicative of the generation of a free GlcNAc α-anomer enzymatic product. Digestion of the $Man_3GlcNAc$ structure by the novel human α-mannosidase resulted in the disappearance of the α1-6Man residue (***Man4'*** H-1 resonance at δ=4.902 ppm) and the appearance of a free mannose α-anomer resonance at δ=5.152 ppm (Panel C). The β-anomers of the monosscharide products were obscured by the water peak in Panels B and C. The H-2 resonance for ***Man4'*** at δ=4.162 ppm was also lost from the spectrum in Panel C, but the H-1 and H-2 signals for ***Man4***, ***Man3***, and ***GlcNAc2*** were unchanged indicating the cleavage of a single mannose residue with the formation of a Manα1-3Manβ1-4GlcNAc product by the novel human α-mannosidase.

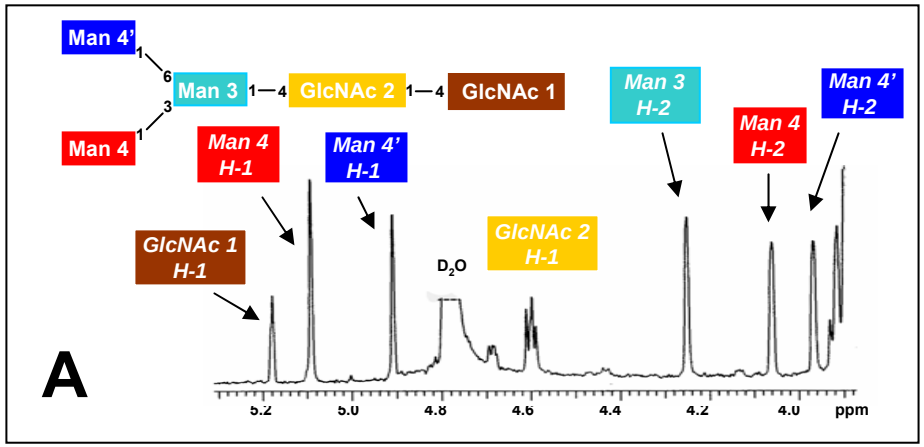
Man 4'
Man 3
GlcNAc 2
GlcNAc 1
Man 4
Man 4 H-1
Man 4' H-1
GlcNAc 1 H-1
D2O
GlcNAc 2 H-1
Man 3 H-2
Man 4 H-2
Man 4' H-2
A
5.2
5.0
4.8
4.6
4.4
4.2
4.0
ppm

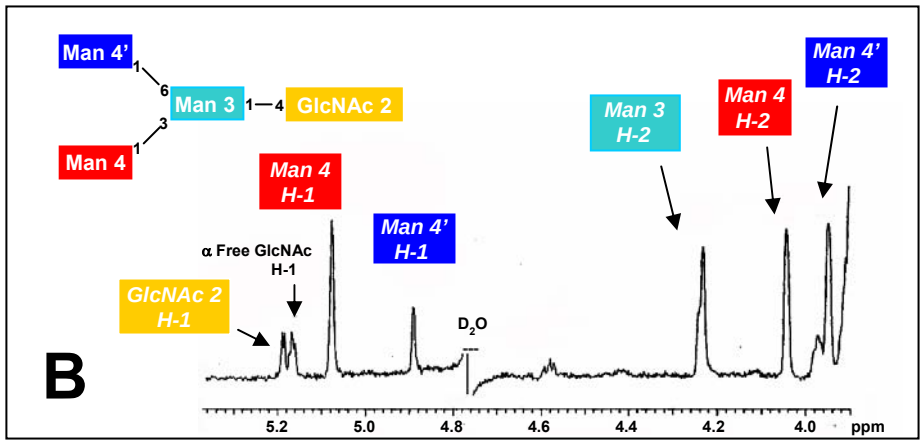
Man 4'
Man 3
GlcNAc 2
Man 4
Man 4 H-1
Man 4' H-1
α Free GlcNAc H-1
GlcNAc 2 H-1
D2O
Man 3 H-2
Man 4 H-2
Man 4' H-2
B
5.2
5.0
4.8
4.6
4.4
4.2
4.0
ppm

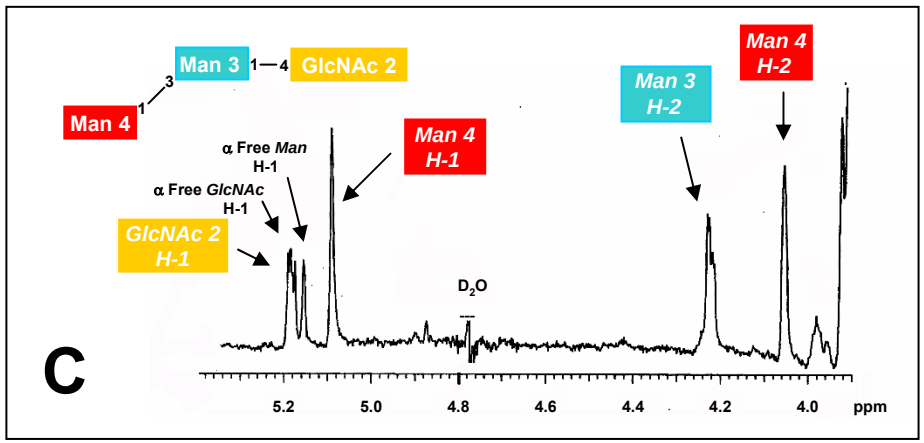
Man 3
GlcNAc 2
Man 4
α Free Man H-1
α Free GlcNAc H-1
Man 4 H-1
GlcNAc 2 H-1
D2O
Man 3 H-2
Man 4 H-2
C
5.2
5.0
4.8
4.6
4.4
4.2
4.0
ppm

Fig. 8: **Time course studies of hydrolysis of $Man_3GlcNAc_2$ and $Man_3GlcNAc$ by the novel human α-mannosidase and human LysMan**. The novel human α-mannosidase was incubated with $Man_3GlcNAc$ (Panels A-C) or $Man_3GlcNAc_2$ (Panels D-F) for defined time points. Aliquots of the digestion reaction were removed at each time point and prepared for ^{1}H-NMR spectroscopy as described in "Experimental Procedures". ^{1}H-NMR spectra of the individual time points are shown in Panels B and E for the digestion of $Man_3GlcNAc$ and $Man_3GlcNAc_2$, respectively. Quantitation of the peak areas for the resonances of the ***Man4*** and ***Man4'*** residues, as well as the sum of the peak areas for the α-and β-anomers of the released free mannose residue are indicated in the plots in Panels C and F (***Man4*** residue, red boxes; ***Man4'*** residue, blue boxes; free mannose, green boxes). The time course data indicated that only the ***Man4'*** residue is cleaved from the $Man_3GlcNAc$ substrate by the novel α-mannosidase (Panel A), but no significant cleavage of either residue was detected with the $Man_3GlcNAc_2$ substrate (Panel B), demonstrating that the novel α-mannosidase was a core-specific α1-6mannosidase. Similar studies were performed with human LysMan (Panels G-L), where digestion of $Man_3GlcNAc$ (Panels G-I) or $Man_3GlcNAc_2$ (Panels J-L) both resulted in the cleavage of residue ***Man4*** (Panels H and K). No appreciable cleavage of residue ***Man4'*** was detected (Panels G and J) with either substrate.

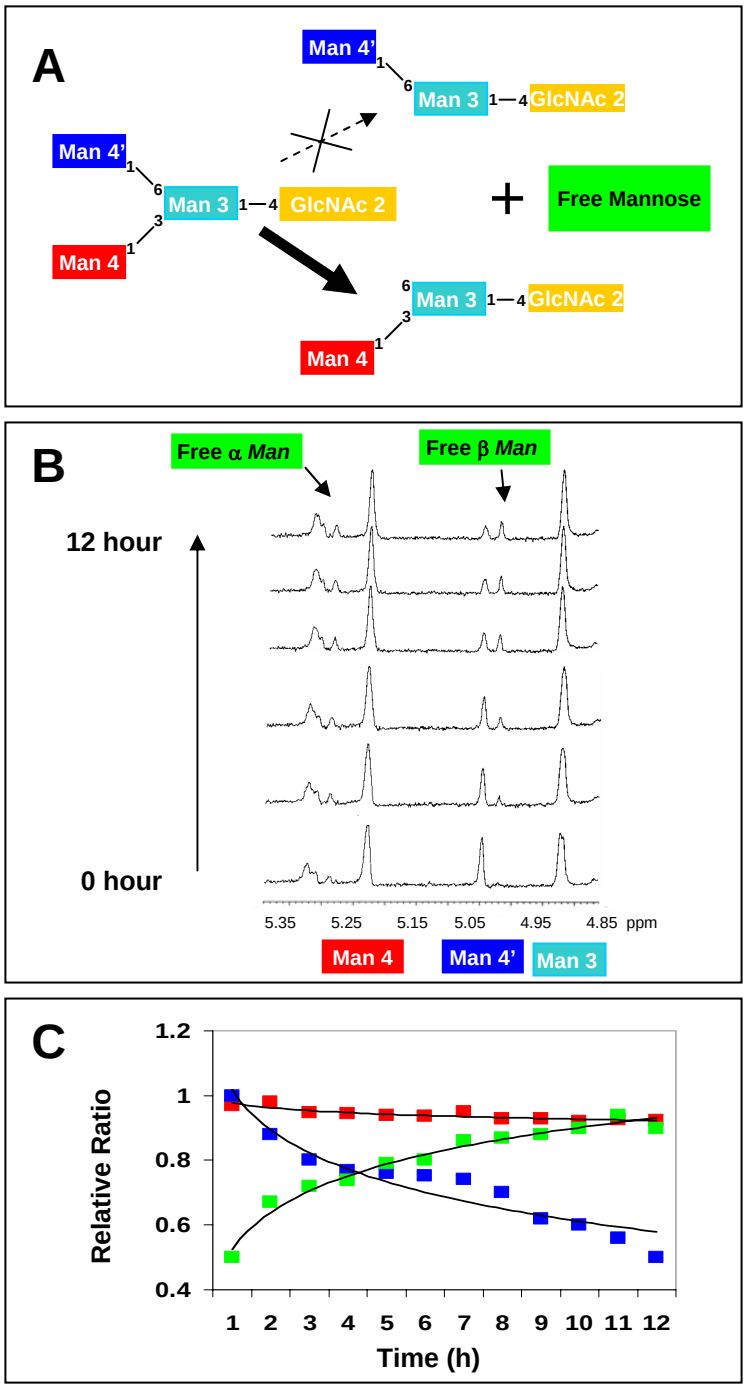
A
Man 4'
1
6
Man 3
1—4
GlcNAc 2
Man 4'
1
6
Man 3
1—4
GlcNAc 2
3
1
Man 4
+
Free Mannose
6
Man 3
1—4
GlcNAc 2
3
1
Man 4
B
Free α Man
Free β Man
12 hour
0 hour
5.35
5.25
5.15
5.05
4.95
4.85
ppm
Man 4
Man 4'
Man 3
C
Relative Ratio
1.2
1
0.8
0.6
0.4
1
2
3
4
5
6
7
8
9
10
11
12
Time (h)

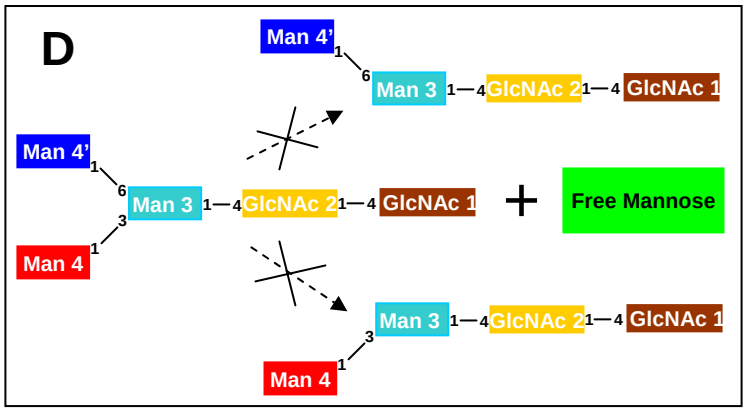
D
Man 4'
1
6
Man 3
1—4
GlcNAc 2
1—4
GlcNAc 1
Man 4'
1
6
Man 3
1—4
GlcNAc 2
1—4
GlcNAc 1
3
Man 4
1
+
Free Mannose
Man 3
1—4
GlcNAc 2
1—4
GlcNAc 1
3
Man 4
1

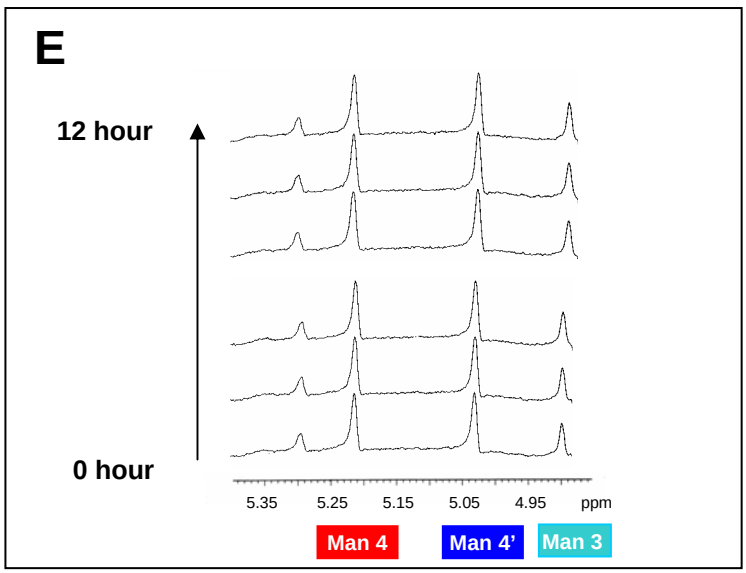
E
12 hour
0 hour
5.35
5.25
5.15
5.05
4.95
ppm
Man 4
Man 4'
Man 3

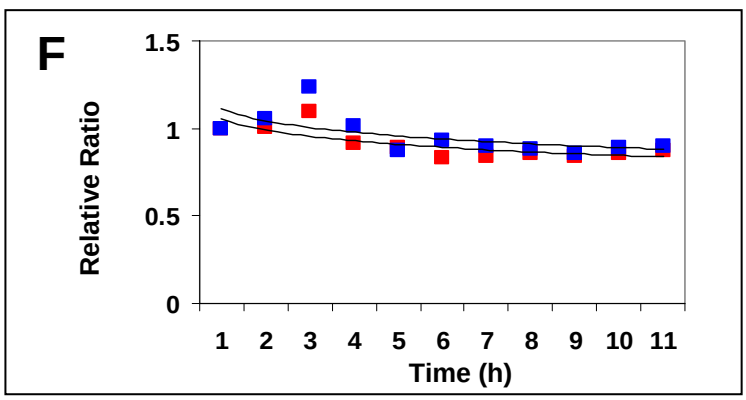
F
Relative Ratio
1.5
1
0.5
0
1
2
3
4
5
6
7
8
9
10
11
Time (h)

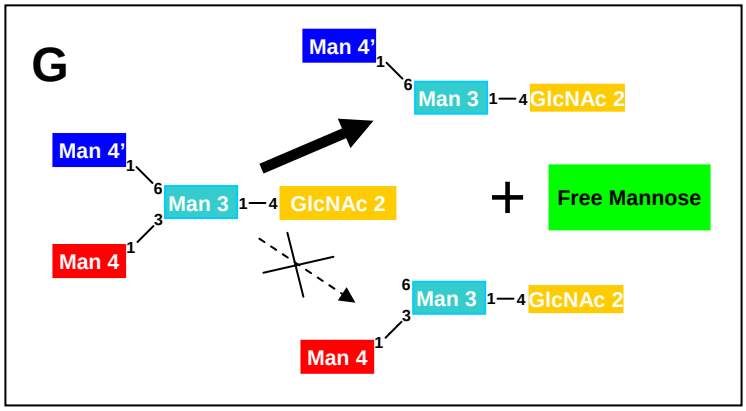
G
Man 4'
1
6
Man 3
1—4
GlcNAc 2
Man 4'
1
6
Man 3
1—4
GlcNAc 2
3
Man 4
1
+
Free Mannose
6
Man 3
1—4
GlcNAc 2
3
Man 4
1

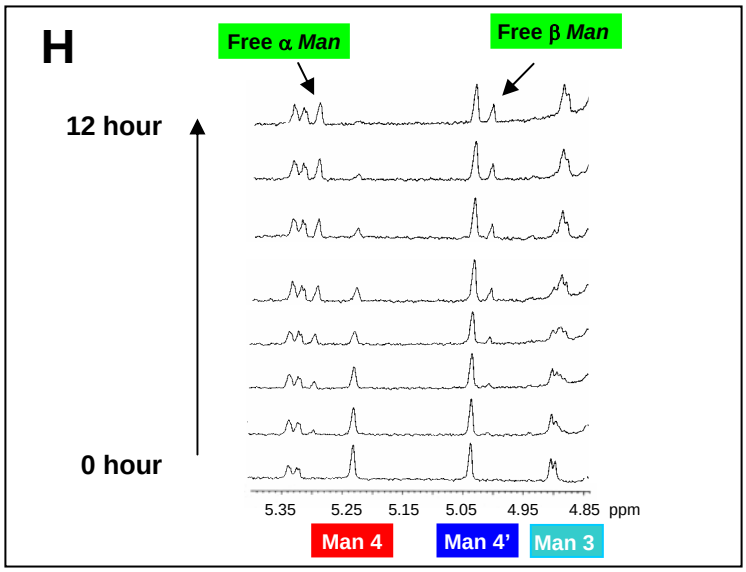
H
Free α Man
Free β Man
12 hour
0 hour
5.35
5.25
5.15
5.05
4.95
4.85
ppm
Man 4
Man 4'
Man 3

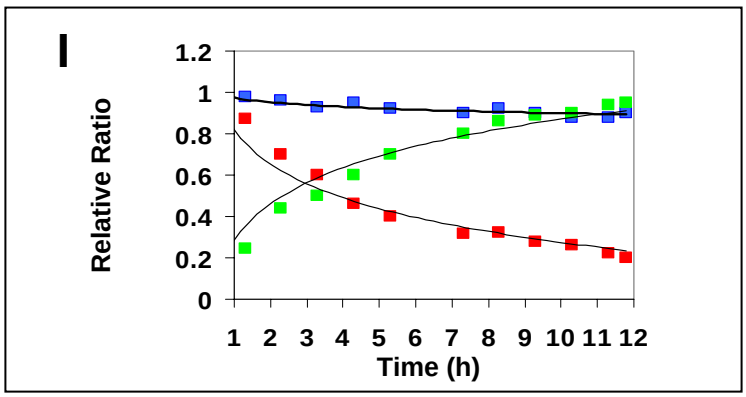
I
Relative Ratio
1.2
1
0.8
0.6
0.4
0.2
0
1
2
3
4
5
6
7
8
9
10
11
12
Time (h)

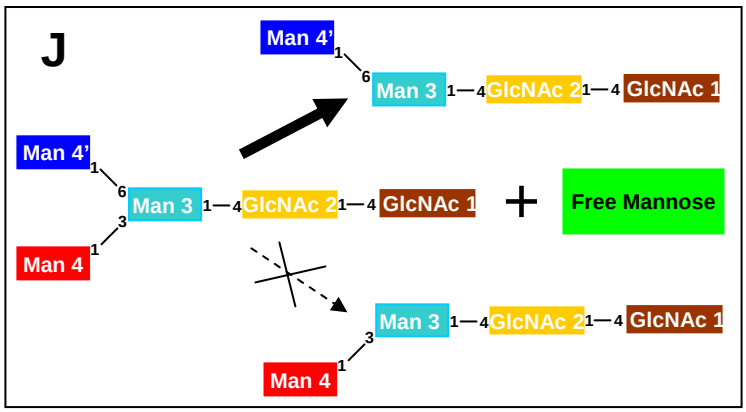
J
Man 4'
1
6
Man 3
1—4
GlcNAc 2
1—4
GlcNAc 1
Man 4'
1
6
Man 3
1—4
GlcNAc 2
1—4
GlcNAc 1
3
1
Man 4
+
Free Mannose
Man 3
1—4
GlcNAc 2
1—4
GlcNAc 1
3
1
Man 4

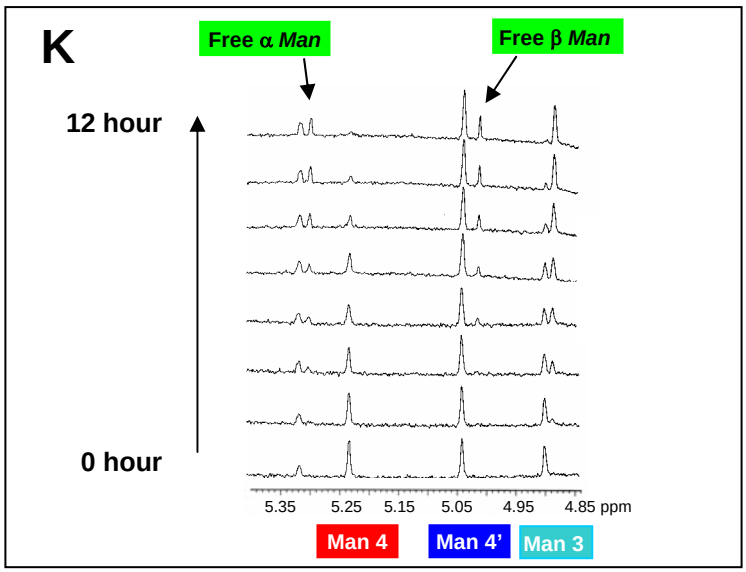
K
Free α Man
Free β Man
12 hour
0 hour
5.35
5.25
5.15
5.05
4.95
4.85 ppm
Man 4
Man 4'
Man 3

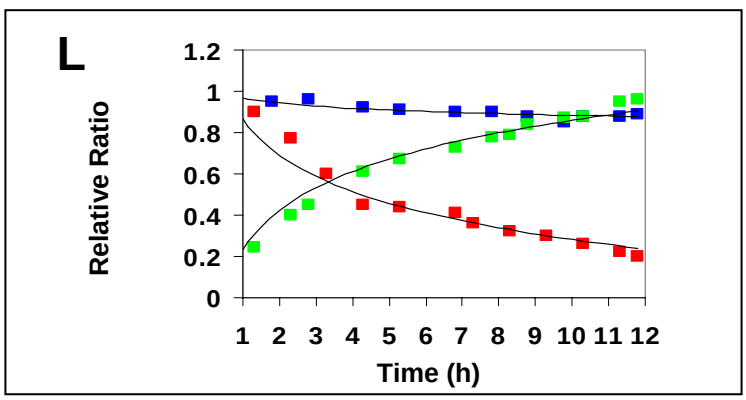
L
Relative Ratio
1.2
1
0.8
0.6
0.4
0.2
0
1 2 3 4 5 6 7 8 9 10 11 12
Time (h)

Fig. 9: **Tissue distribution of mRNA transcripts for the human core-specific α1-6mannosidase and human LysMan.** A Northern blot of human tissue poly(A+) RNAs was hybridized with radiolabeled probes from the coding regions of human LysMan (*top panel*) or human core-specific α1-6mannosidase (*middle panel*) as described in "Experimental Procedures". The blot was rehybridized with β-actin cDNA as a control (*bottom panel*). Lanes on the blot represent the RNA isolated from the tissues indicated at the top (PBL, peripheral blood leukocytes). The sizes of the transcripts indicated by the arrows were estimated based on the electrophoretic mobility of radiolabeled RNA standards.

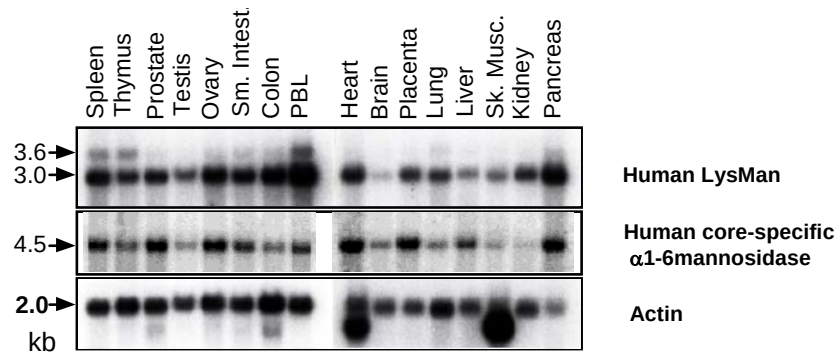
Spleen
Thymus
Prostate
Testis
Ovary
Sm. Intest.
Colon
PBL
Heart
Brain
Placenta
Lung
Liver
Sk. Musc.
Kidney
Pancreas
3.6
3.0
4.5
2.0
kb
Human LysMan
Human core-specific
α1-6mannosidase
Actin

Fig. 10: **Dotplot analysis comparing the 5'-flanking sequences and partial coding regions for human and bovine core-specific α1-6mannosidase, chitobiase and Lysman.** Two partial bovine homologs of the core-specific α1-6mannosidase gene were identified by BLAST searches of bovine genomic sequences in the GenBank sequence database (Accession numbers XM_606608 and XM_601622). Sequences corresponding to the first 375 bp of the respective enzyme coding regions (numbering starting at 1 with the ATG translation start site) and as much as 1 kb of 5'-flanking sequence (negative numbering relative to the translation start site) were identified for the human and bovine LysMan (1 kb of 5'-flanking sequence for each), human and bovine chitobiase (1 kb and 660 bp, respectively, for each), and the human and two bovine core-specific α1-6mannosidase homologs (1 kb each for human and bovine XM_606608 homolog sequences and 910 bp for the bovine XM_601622 homolog sequence). A pairwise sequence comparison of the corresponding bovine and human sequences for each gene were performed and displayed as a dotplot diagram where each dot in the corresponding two-dimensional plot indicates a sequence identity of at least 14 residues over a sliding window of 21 residues (see Experimental Procesures"). A diagonal line indicates an extended sequence similarity between the two sequences. In each plot, the upper right quadrant corresponds to the first 375 bp of the respective coding region. The lower left quadrant corresponds to the respective 5'-flanking regions. An extended diagonal line is detected in the upper right quadrant in each plot, but the dotplot corresponding to a comparison of the bovine and human LysMan sequences contains an extended diagonal line into the lower left quadrant indicating an extended sequence similarity in the 5'-flanking sequences for these two sequence homologs.

A

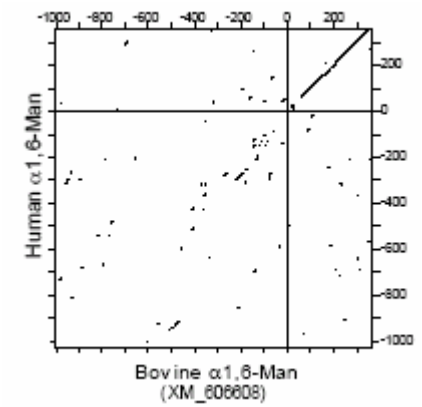
Human α1,6-Man
Bovine α1,6-Man
(XM_606608)

B

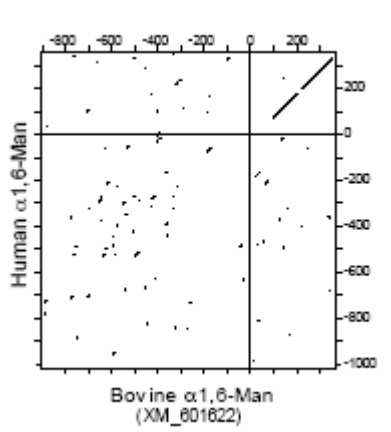
Human α1,6-Man
Bovine α1,6-Man
(XM_601622)

C

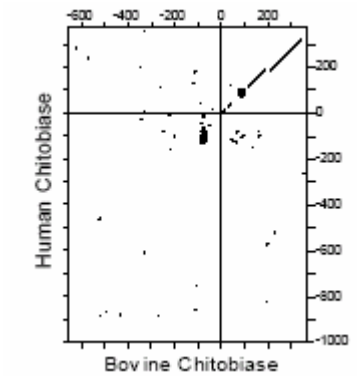
Human Chitobiase
Bovine Chitobiase

D

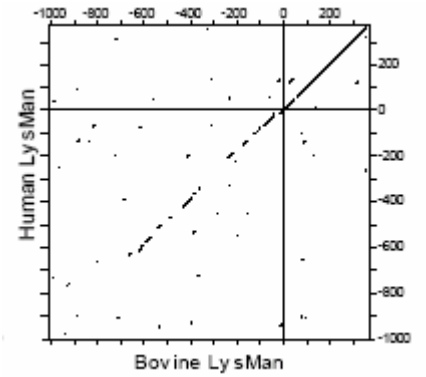
Human LysMan
Bovine LysMan

Table 3: Comparison of total number of species-specific ESTs with identity to chitobiase, LysMan, and core-specific α1-6Man[a].

	Chitobiase		LysMan		Core-specific α1-6Man	
Species	ESTs	Sequence	ESTs	Sequence	ESTs	Sequence
	total number (%)		*total number (%)*		*total number (%)*	
Human	116 *(23)*	NM_004388	502 *(100)*	NM_000528	209 *(42)*	NM_015274
Mouse	36 *(8)*	NM_028836	436 *(100)*	NM_010764	111 *(25)*	NM_008550
Cow	0[b]	XM_602828[b]	74 *(100)*	NM_174561	0[b] 0[b]	XM_606608 XM_601622
Dog	2 *(10)*	XM_547309	20 *(100)*	XM_542048	19 *(95)*	XM_545897
Pig	22 *(88)*	BX671403	25 *(100)*	BP464100	2 *(8)*	NM_213849

[a] cDNA sequences encoding the respective species-specific orthologs of chitobiase, LysMan, and core-specific α1-6mannnosidase were identified by TBLASTN sequence searches (40) using the respective protein sequences for the human orthologs of each enzyme as query sequences (GenBank accession numbers NP_004379, NP_000519, and NP_056089 for chitobiase, LysMan, and core-specific α1-6mannnosidase protein sequences, respectively). The GenBank accession numbers for the respective cDNA reference sequences are shown in the "Sequence" column for each enzyme. Pig chitobiase and LysMan, reference sequences were not available, so EST sequences of the corresponding coding region were used for subsequent analyses. For bovine chitobiase and core-specific α1-6mannnosidase cDNA sequences were not available. In these instances coding region sequences from the corresponding genes were used in subsequent analyses. Two bovine α1-6mannnosidase gene homologs were identified in the sequence

search and the corresponding accession numbers are shown. BLASTN searches (www.ncbi.nlm.nih.gov/BLAST) were subsequently performed using the respective DNA sequences identified for each coding region against the GenBank sequence database filtered for EST sequences from the respective species. EST sequences with >98% identity over a span of at least 60 bp were scored as positive "hits" for each coding region. The total number of EST "hits" were tallied and shown in the corresponding column. The relative ratio of the EST "hits" identified for each coding region by comparison to the number of LysMan-specific ESTs for that species were calculated and shown in parenthesis and italics in each column. The total numbers of ESTs sequences in GenBank for each respective species were: human, 6.1×10^6; mouse, 4.3×10^6; cow, 6.1×10^5; dog, 3.5×10^5; and pig, 4.4×10^5.

[b] No EST sequences were identified in the BLASTN searches of the bovine EST database for the chitobiase or α1-6mannnosidase.

Fig. 11: **Summary diagram for the lysosomal degradation of $Man_3GlcNAc_2$ glycans by chitobiase, LysMan, and core-specific α1-6mannosidase**. The arrows in the respective diagram indicate the potential pathways for catabolism of $Man_3GlcNAc_2$ by the chitobiase, LysMan, and core-specific α1-6mannosidase. The order of cleavage by chitobiase and LysMan do not appear to be restricted based on known substrate specificities for the enzymes (16, 52), but the core-specific α1-6mannosidase can act only after chitobiase action. The solid arrows in the diagram indicate the reactions that were demonstrated in this study. The studies described here have not tested the ability of core-specific α1-6mannosidase to cleave Manα1-6Manβ1-4GlcNAc (dotted arrows), but prior data with partially purified human spleen core-specific α1-6mannosidase indicates that this structure can be cleaved by the enzyme (22).

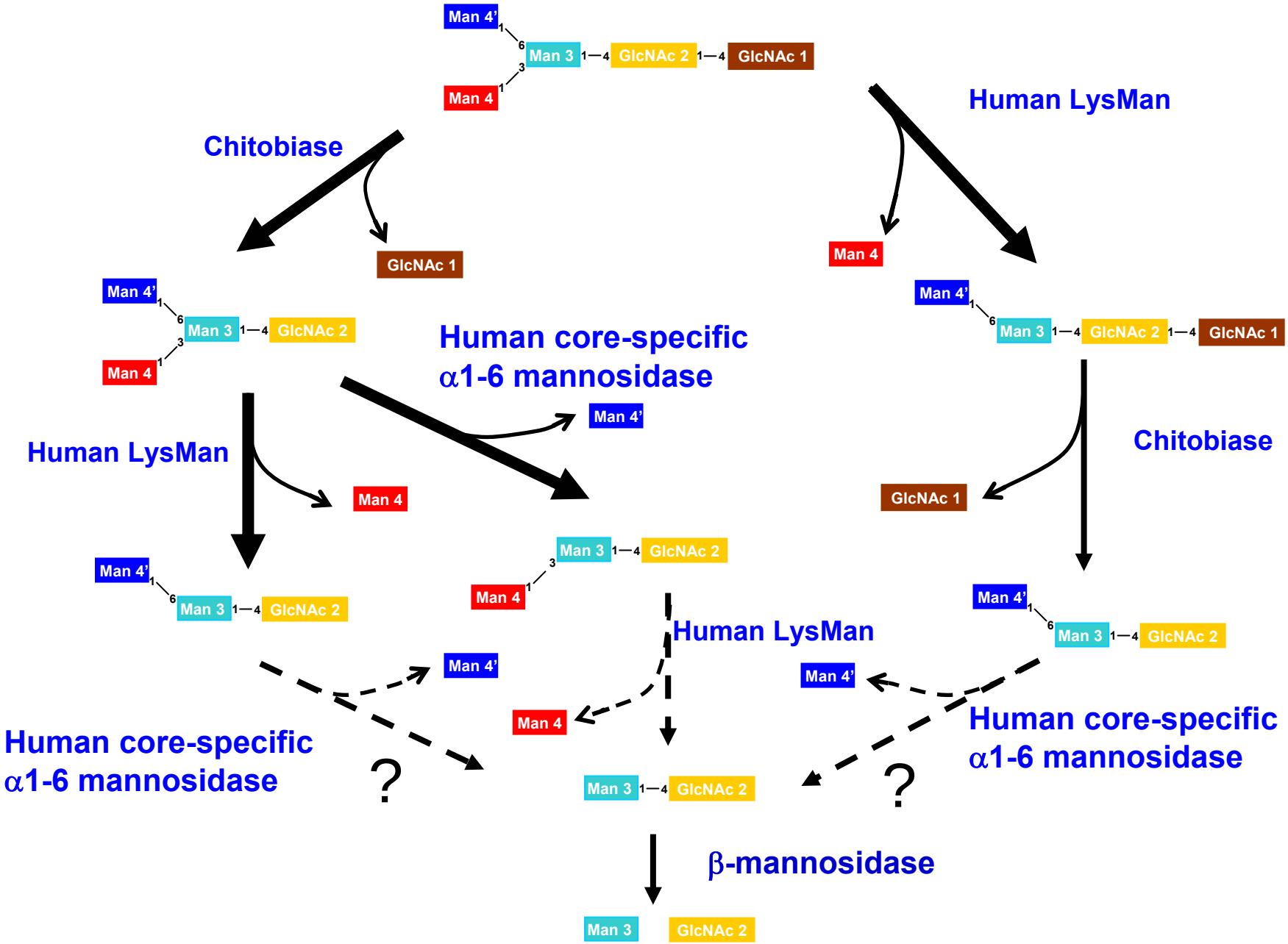
Man 4'
Man 3
GlcNAc 2
GlcNAc 1
Man 4
Chitobiase
Human LysMan
Human core-specific
α1-6 mannosidase
β-mannosidase
?
?

REFERENCE:

1. Moremen, K. W., Trimble, R. B., and Herscovics, A. Glycosidases of the asparagine-linked oligosaccharide processing pathway. Glycobiology, *4:* 113-125, 1994.
2. Moremen, K. in Oligosaccharides in Chemistry and Biology: A Comprehensive Handbook, Vol. II, p. 81-117. New York: John Wiley and Sons, Inc.,, 2000.
3. Henrissat, B. and Bairoch, A. Updating the sequence-based classification of glycosyl hydrolases. Biochem J, *316:* 695-696, 1996.
4. Sousa, M. C., Ferrero-Garcia, M. A., and Parodi, A. J. Recognition of the oligosaccharide and protein moieties of glycoproteins by the UDP-Glc:glycoprotein glucosyltransferase. Biochemistry, *31:* 97-105, 1992.
5. Sousa, M. C. and Parodi, A. J. The interaction of the UDP-GLC:glycoprotein glucosyltransferase with the acceptor glycoprotein. Cell Mol Biol, *42:* 609-616, 1996.
6. Moremen, K. W. Golgi alpha-mannosidase II deficiency in vertebrate systems: implications for asparagine-linked oligosaccharide processing in mammals. Biochim Biophys Acta, *1573:* 225-235, 2002.
7. Liao, Y. F., Lal, A., and Moremen, K. W. Cloning, expression, purification, and characterization of the human broad specificity lysosomal acid alpha-mannosidase. J Biol Chem, *271:* 28348-28358, 1996.
8. Gonzalez, D. S., Kagawa, Y., and Moremen, K. W. Isolation and characterization of the gene encoding the mouse broad specificity lysosomal alpha-mannosidase1. Biochim Biophys Acta, *1445:* 177-183, 1999.

9. Carroll, M., Dance, N., Masson, P. K., Robinson, D., and Winchester, B. G. Human mannosidosis--the enzyme defect. Biochem Biophys Res Commun, *49:* 579-583, 1972.

10. Hocking, J. D., Jolly, R. D., and Batt, R. D. Deficiency of -mannosidase in Angus cattle. An inherited lysosomal storage disease. Biochem J, *128:* 69-78, 1972.

11. Burditt, L. J., Chotai, K., Hirani, S., Nugent, P. G., Winchester, B. G., and Blakemore, W. F. Biochemical studies on a case of feline mannosidosis. Biochem J, *189:* 467-473, 1980.

12. Berg, T., Tollersrud, O. K., Walkley, S. U., Siegel, D., and Nilssen, O. Purification of feline lysosomal alpha-mannosidase, determination of its cDNA sequence and identification of a mutation causing alpha-mannosidosis in Persian cats. Biochem J, *328:* 863-870, 1997.

13. Stinchi, S., Lullmann-Rauch, R., Hartmann, D., Coenen, R., Beccari, T., Orlacchio, A., von Figura, K., and Saftig, P. Targeted disruption of the lysosomal alpha-mannosidase gene results in mice resembling a mild form of human alpha-mannosidosis. Hum Mol Genet, *8:* 1365-1372, 1999.

14. Crawley, A. C., Jones, M. Z., Bonning, L. E., Finnie, J. W., and Hopwood, J. J. Alpha-mannosidosis in the guinea pig: a new animal model for lysosomal storage disorders. Pediatr Res, *46:* 501-509, 1999.

15. al Daher, S., de Gasperi, R., Daniel, P., Hall, N., Warren, C. D., and Winchester, B. The substrate-specificity of human lysosomal alpha-D-mannosidase in relation to genetic alpha-mannosidosis. Biochem J, *277:* 743-751, 1991.

16. Daniel, P. F., Winchester, B., and Warren, C. D. Mammalian alpha-mannosidases--multiple forms but a common purpose? Glycobiology, *4:* 551-566, 1994.

17. Michalski, J. C., Haeuw, J. F., Wieruszeski, J. M., Montreuil, J., and Strecker, G. In vitro hydrolysis of oligomannosyl oligosaccharides by the lysosomal alpha-D-mannosidases. Eur J Biochem, *189:* 369-379, 1990.

18. Abraham, D., Blakemore, W. F., Jolly, R. D., Sidebotham, R., and Winchester, B. The catabolism of mammalian glycoproteins. Comparison of the storage products in bovine, feline and human mannosidosis. Biochem J, *215:* 573-579, 1983.

19. Cenci di Bello, I., Dorling, P., and Winchester, B. The storage products in genetic and swainsonine-induced human mannosidosis. Biochem J, *215:* 693-696, 1983.

20. Winchester, B. Role of alpha-D-mannosidases in the biosynthesis and catabolism of glycoproteins. Biochem Soc Trans, *12:* 522-524, 1984.

21. Daniel, P. F., Evans, J. E., De Gasperi, R., Winchester, B., and Warren, C. D. A human lysosomal alpha(1----6)-mannosidase active on the branched trimannosyl core of complex glycans. Glycobiology, *2:* 327-336, 1992.

22. De Gasperi, R., Daniel, P. F., and Warren, C. D. A human lysosomal alpha-mannosidase specific for the core of complex glycans. J Biol Chem, *267:* 9706-9712, 1992.

23. Haeuw, J. F., Grard, T., Alonso, C., Strecker, G., and Michalski, J. C. The core-specific lysosomal alpha(1-6)-mannosidase activity depends on aspartamidohydrolase activity. Biochem J, *297:* 463-466, 1994.

24. Winchester, B. Lysosomal metabolism of glycoproteins. Glycobiology, *15:* 1R-15R, 2005.

25. Liu, B., Ahmad, W., and Aronson, N. N., Jr. Structure of the human gene for lysosomal di-N-acetylchitobiase. Glycobiology, *9:* 589-593, 1999.

26. Okamura, N., Tamba, M., Liao, H. J., Onoe, S., Sugita, Y., Dacheux, F., and Dacheux, J. L. Cloning of complementary DNA encoding a 135-kilodalton protein secreted from porcine corpus epididymis and its identification as an epididymis-specific alpha-mannosidase. Mol Reprod Dev, *42:* 141-148, 1995.

27. Yonezawa, N., Aoki, H., Hatanaka, Y., and Nakano, M. Involvement of N-linked carbohydrate chains of pig zona pellucida in sperm-egg binding. Eur J Biochem, *233:* 35-41, 1995.

28. Hiramoto, S., Tamba, M., Kiuchi, S., Jin, Y. Z., Bannai, S., Sugita, Y., Dacheux, F., Dacheux, J. L., Yoshida, M., and Okamura, N. Stage-specific expression of a mouse homologue of the porcine 135kDa alpha-D-mannosidase (MAN2B2) in type A spermatogonia. Biochem Biophys Res Commun, *241:* 439-445, 1997.

29. Jin, Y. Z., Dacheux, F., Dacheux, J. L., Bannai, S., Sugita, Y., and Okamura, N. Purification and properties of major alpha-D-mannosidase in the luminal fluid of porcine epididymis. Biochim Biophys Acta, *1432:* 382-392, 1999.

30. Tascou, S., Nayernia, K., Engel, W., and Burfeind, P. Refinement of the expression pattern of a mouse homologue of the porcine 135-kDa alpha-d-mannosidase (MAN2B2). Biochem Biophys Res Commun, *272:* 951-952, 2000.

31. Wu, Y., Swulius, M. T., Moremen, K. W., and Sifers, R. N. Elucidation of the molecular logic by which misfolded alpha 1-antitrypsin is preferentially selected for degradation. Proc Natl Acad Sci U S A, *100:* 8229-8234, 2003.

32. Wilkinson, J. M. Fragmentation of Polypeptides by Enzymic Method. New York, N.Y: John Wiley and Sons, 1986.

33. Gharahdaghi, F., Weinberg, C. R., Meagher, D. A., Imai, B. S., and Mische, S. M. Mass spectrometric identification of proteins from silver-stained polyacrylamide gel: a method for the removal of silver ions to enhance sensitivity. Electrophoresis, *20:* 601-605, 1999.

34. Ducret, A., Van Oostveen, I., Eng, J. K., Yates, J. R., 3rd, and Aebersold, R. High throughput protein characterization by automated reverse-phase chromatography/electrospray tandem mass spectrometry. Protein Sci, *7:* 706-719, 1998.

35. Moremen, K. W. and Robbins, P. W. Isolation, characterization, and expression of cDNAs encoding murine alpha-mannosidase II, a Golgi enzyme that controls conversion of high mannose to complex N-glycans. J Cell Biol, *115:* 1521-1534, 1991.

36. Gonzalez, D. S., Karaveg, K., Vandersall-Nairn, A. S., Lal, A., and Moremen, K. W. Identification, expression, and characterization of a cDNA encoding human endoplasmic reticulum mannosidase I, the enzyme that catalyzes the first mannose trimming step in mammalian Asn-linked oligosaccharide biosynthesis. J Biol Chem, *274:* 21375-21386, 1999.

37. Segel, I. Behavior and analysis of rapid equilibrium and steady-state enzyme systems, Vol. pp 100-160. New York: John Wiley & Sons, Inc.,, 1975.

38. McIlvaine, T. C. A buffer siolution for colorimetric comparison. J. Biol. Chem., *49:* 183-186, 1921.

39. Lal, A., Pang, P., Kalelkar, S., Romero, P. A., Herscovics, A., and Moremen, K. W. Substrate specificities of recombinant murine Golgi alpha1, 2-mannosidases IA and IB and comparison with endoplasmic reticulum and Golgi processing alpha1,2-mannosidases. Glycobiology, *8:* 981-995, 1998.

40. Altschul, S. F., Madden, T. L., Schaffer, A. A., Zhang, J., Zhang, Z., Miller, W., and Lipman, D. J. Gapped BLAST and PSI-BLAST: a new generation of protein database search programs. Nucleic Acids Res, *25:* 3389-3402, 1997.

41. Bateman, A., Birney, E., Cerruti, L., Durbin, R., Etwiller, L., Eddy, S. R., Griffiths-Jones, S., Howe, K. L., Marshall, M., and Sonnhammer, E. L. The Pfam protein families database. Nucleic Acids Res, *30:* 276-280, 2002.

42. Thompson, J. D., Higgins, D. G., and Gibson, T. J. CLUSTAL W: improving the sensitivity of progressive multiple sequence alignment through sequence weighting, position-specific gap penalties and weight matrix choice. Nucleic Acids Res, *22:* 4673-4680, 1994.

43. Page, R. D. TreeView: an application to display phylogenetic trees on personal computers. Comput Appl Biosci, *12:* 357-358, 1996.

44. Maizel, J. V., Jr. and Lenk, R. P. Enhanced graphic matrix analysis of nucleic acid and protein sequences. Proc Natl Acad Sci U S A, *78:* 7665-7669, 1981.

45. Moremen, K. W., Touster, O., and Robbins, P. W. Novel purification of the catalytic domain of Golgi alpha-mannosidase II. Characterization and comparison with the intact enzyme. J Biol Chem, *266:* 16876-16885, 1991.

46. Misago, M., Liao, Y. F., Kudo, S., Eto, S., Mattei, M. G., Moremen, K. W., and Fukuda, M. N. Molecular cloning and expression of cDNAs encoding human alpha-mannosidase II and a previously unrecognized alpha-mannosidase IIx isozyme. Proc Natl Acad Sci U S A, *92:* 11766-11770, 1995.

47. McCracken, A. A. and Brodsky, J. L. Evolving questions and paradigm shifts in endoplasmic-reticulum-associated degradation (ERAD). Bioessays, *25:* 868-877, 2003.

48. Heikinheimo, P., Helland, R., Leiros, H. K., Leiros, I., Karlsen, S., Evjen, G., Ravelli, R., Schoehn, G., Ruigrok, R., Tollersrud, O. K., McSweeney, S., and Hough, E. The structure of bovine lysosomal alpha-mannosidase suggests a novel mechanism for low-pH activation. J Mol Biol, *327:* 631-644, 2003.

49. van den Elsen, J. M., Kuntz, D. A., and Rose, D. R. Structure of Golgi alpha-mannosidase II: a target for inhibition of growth and metastasis of cancer cells. Embo J, *20:* 3008-3017, 2001.

50. Riise, H. M., Berg, T., Nilssen, O., Romeo, G., Tollersrud, O. K., and Ceccherini, I. Genomic structure of the human lysosomal alpha-mannosidase gene (MANB). Genomics, *42:* 200-207, 1997.

51. Berg, T., King, B., Meikle, P. J., Nilssen, O., Tollersrud, O. K., and Hopwood, J. J. Purification and characterization of recombinant human lysosomal alpha-mannosidase. Mol Genet Metab, *73:* 18-29, 2001.

52. Aronson, N. N., Jr. and Kuranda, M. J. Lysosomal degradation of Asn-linked glycoproteins. Faseb J, *3:* 2615-2622, 1989.

53. DeGasperi, R., al Daher, S., Daniel, P. F., Winchester, B. G., Jeanloz, R. W., and Warren, C. D. The substrate specificity of bovine and feline lysosomal alpha-D-mannosidases in relation to alpha-mannosidosis. J Biol Chem, *266:* 16556-16563, 1991.

CHAPTER 3

CONCLUSION

The important roles of N-glycan structures in vertebrate development are considered to largely result from the diversity of linkages and branching patterns on complex N-glycans. Each distinctive structure has the potential to encode information that facilitates connections between cells and their surroundings (1). With unique carbohydrate structures anchored to protein or lipid scaffolds on the cell surface, the task of determining the roles of broad classes of oligosaccharide structures in vertebrate systems is a formidable challenge.

Restricted clues about the roles of broad glycosylhydrolase families (i.e. CAZy GH 38 and GH47 α-mannosidases) involved in the biosynthesis and catabolism of oligosaccharide structures have come from studies involving the treatment of cells or animals with inhibitors of processing glycosylhydrolase (2, 3). But inhibitor studies suffer from the fact that they often target multiple glycosylhydrolases and the interpretation of the results can be complicated. The most persuasive techniques to identify the function of individual processing glycosylhydrolases are the studies on experimentally generated or naturally occurring genetic mutations (4). These methods include gene disruptions in yeast (5, 6), mutants in *C. elegans* (7-9) and *D. melanogaster* (10-12), targeted gene disruptions in mice (13, 14), and congenital defects in humans (4, 14). While these approaches can sometimes yield surprising results, their power lies in either the confirmation of the critical contributions of oligosaccharide structures to vertebrate

development and homeostasis or in the identification of novel compensating activities and alternative biosynthetic pathways.

The roles of glycosidases in biosynthesis and degradation of N-linked glycans have been elucidated by the analysis of the specific gene deficiencies and the structures of the corresponding storage products, substrate specificity studies on the respective enzymes *in vitro* and *in vivo*, and the use of selective small molecule inhibitors. It has been recognized that each specific glycosylhydrolase has its unique role in catalyzing the cleavage of different glycosidic linkages in N-glycans. For example, the highly ordered pathways for N-glycan breakdown in lysosomes results from the sequential release of monosaccharides by the glycosylhydrolases from the non-reducing end of the glycan (15-18).

In lysosomes, N-glycan oligosaccharides are hydrolyzed by enzymes with characteristic acidic pH optima and the polypeptide chains of glycoproteins are broken down by lysosomal proteases. The low pH in lysosomes provides the optimal conditions for the lysosomal enzymes. The amino acids derived from lysosomal proteolysis and the monosaccharides derived from digested oligosaccharides are then recycled for further catabolism or biosynthetic reactions by transport into the cytosol (19).

A clear demonstration of the critical function of lysosomal glycosidase degradation of N-glycans can be found in the lysosomal storage diseases. Genetic alterations in coding regions for lysosomal enzymes result in enzymatic defects and subsequently cause alterations in glycan catabolism. The consequences are the severe clinical phenotypes that result from the excessive carbohydrate storage. Therefore, systematic studies on the catabolism of the N-linked glycoproteins have been pursued in the last few decades to identify the enzymes involved in glycan catabolism and to gain an understanding of the nature of the catabolic pathways.

The catabolic pathways for the recycling of N-glycans by human LysMan have been elucidated by a combination of substrate specificity studies employing HPTLC, HPLC and NMR approaches (20). The catabolism of $Man_9GlcNAc$ proceeds through the formation of a $Man_5GlcNAc$ intermediate involving hydrolysis of the four α1-2-linked mannose residues. Subsequently, the $Man_5GlcNAc$ structure is cleaved to a $Man_2GlcNAc$ structure, which retains a single α-linked Man residue that is resistant to further hydrolysis by the enzyme. These data indicate that the broad specificity LysMan can hydrolyze α1-2, α1-3, and α1-6mannosidic linkages, but that this enzyme cannot readily cleave the final α1-6mannosidic linkage from the core glycan structure. The final core α1-6mannosidic linkage is uniquely hydrolyzed in humans and rodents by a separate lysosomal enzyme, the core specific α1-6mannosidase (20-22). While LysMan was shown to cleave the Manα1-3Man linkage from both $Man_3GlcNAc_2$ and $Man_3GlcNAc$ substrates, the core-specific α1-6mannosidase was found to cleave the core α1-6mannosidic linkage only from $Man_3GlcNAc$ structures. If the core chitobiose linkage is intact (i.e. $Man_3GlcNAc_2$ or $Man_3GlcNAc_2$-Asn glycopeptides), the core-specific α1-6mannosidase can not recognize the glycan as a substrate (20).

The α1-6mannosidase has been purified and characterized (22-24). The enzyme was found to be dependent upon the prior action of the lysosomal chitobiase for removal of the GlcNAc from the reducing end of the chitobiose structure (24). Thus, a model was proposed that the chitobiase and core-specific α1-6mannosidase activities work in functional collaboration to provide full and efficient catabolism of N-glycans in the lysosomes of some mammalian species, but the accessory activities of the chitobiase and possible the α1-6mannosidase have been lost in ungulates, cats and dogs (19, 25, 26).

The absence of a clearly identified gene or cDNA encoding the core specific α1-6mannosidae had made it difficult to establish the genetic relationship between the expression of chitobiase and α1-6mannosidase activities (25). This dissertation describes the cloning, expression, purification, and characterization of the human cDNA encoding core-specific α1-6mannosidase with sequence similarity to members of the CAZy GH 38 family and demonstrates that the enzyme is expressed in a similar set of animal species as the chitobiase. These data indicate that the functional collaboration of the chitobiase and the core-specific α1-6mannosidase extends beyond the enzymatic requirement of both enzymes for N-glycan catabolism, but also suggest that the enzymes activity may have been similarly lost in a set of animal species to result in a coordinate down-regulation of the two accessory activities for N-glycan catabolism.

References:

1. Varki, A. Biological roles of oligosaccharides: all of the theories are correct. Glycobiology, *3:* 97-130, 1993.
2. Stanley, P. Lectin-resistant CHO cells: selection of new mutant phenotypes. Somatic Cell Genet, *9:* 593-608, 1983.
3. Stanley, P. Selection of lectin-resistant mutants of animal cells. Methods Enzymol, *96:* 157-184, 1983.
4. Schachter, H. Congenital disorders involving defective N-glycosylation of proteins. Cell Mol Life Sci, *58:* 1085-1104, 2001.
5. Herscovics, A. and Orlean, P. Glycoprotein biosynthesis in yeast. Faseb J, *7:* 540-550, 1993.
6. Burda, P. and Aebi, M. The dolichol pathway of N-linked glycosylation. Biochim Biophys Acta, *1426:* 239-257, 1999.
7. DeBose-Boyd, R. A., Nyame, A. K., Jasmer, D. P., and Cummings, R. D. The ruminant parasite Haemonchus contortus expresses an alpha1,3-fucosyltransferase capable of synthesizing the Lewis x and sialyl Lewis x antigens. Glycoconj J, *15:* 789-798, 1998.
8. Hagen, F. K., Ten Hagen, K. G., Beres, T. M., Balys, M. M., VanWuyckhuyse, B. C., and Tabak, L. A. cDNA cloning and expression of a novel UDP-N-acetyl-D-galactosamine:polypeptide N-acetylgalactosaminyltransferase. J Biol Chem, *272:* 13843-13848, 1997.

9. Chen, S., Zhou, S., Sarkar, M., Spence, A. M., and Schachter, H. Expression of three Caenorhabditis elegans N-acetylglucosaminyltransferase I genes during development. J Biol Chem, *274:* 288-297, 1999.

10. Foster, J. M., Yudkin, B., Lockyer, A. E., and Roberts, D. B. Cloning and sequence analysis of GmII, a Drosophila melanogaster homologue of the cDNA encoding murine Golgi alpha-mannosidase II. Gene, *154:* 183-186, 1995.

11. Rabouille, C., Kuntz, D. A., Lockyer, A., Watson, R., Signorelli, T., Rose, D. R., van den Heuvel, M., and Roberts, D. B. The Drosophila GMII gene encodes a Golgi alpha-mannosidase II. J Cell Sci, *112:* 3319-3330, 1999.

12. Kerscher, S., Albert, S., Wucherpfennig, D., Heisenberg, M., and Schneuwly, S. Molecular and genetic analysis of the Drosophila mas-1 (mannosidase-1) gene which encodes a glycoprotein processing alpha 1,2-mannosidase. Dev Biol, *168:* 613-626, 1995.

13. Marth, J. D. Will the transgenic mouse serve as a Rosetta Stone to glycoconjugate function? Glycoconj J, *11:* 3-8, 1994.

14. Dennis, J. W., Granovsky, M., and Warren, C. E. Protein glycosylation in development and disease. Bioessays, *21:* 412-421, 1999.

15. Abraham, D., Blakemore, W. F., Jolly, R. D., Sidebotham, R., and Winchester, B. The catabolism of mammalian glycoproteins. Comparison of the storage products in bovine, feline and human mannosidosis. Biochem J, *215:* 573-579, 1983.

16. Aronson, N. N., Jr. Aspartylglycosaminuria: biochemistry and molecular biology. Biochim Biophys Acta, *1455:* 139-154, 1999.

17. Baussant, T., Strecker, G., Wieruszeski, J. M., Montreuil, J., and Michalski, J. C. Catabolism of glycoprotein glycans. Characterization of a lysosomal endo-N-acetyl-beta-

D-glucosaminidase specific for glycans with a terminal chitobiose residue. Eur J Biochem, *159:* 381-385, 1986.

18. Kuranda, M. J. and Aronson, N. N., Jr. A di-N-acetylchitobiase activity is involved in the lysosomal catabolism of asparagine-linked glycoproteins in rat liver. J Biol Chem, *261:* 5803-5809, 1986.

19. Winchester, B. Lysosomal metabolism of glycoproteins. Glycobiology, *15:* 1R-15R, 2005.

20. al Daher, S., de Gasperi, R., Daniel, P., Hall, N., Warren, C. D., and Winchester, B. The substrate-specificity of human lysosomal alpha-D-mannosidase in relation to genetic alpha-mannosidosis. Biochem J, *277:* 743-751, 1991.

21. Cenci di Bello, I., Dorling, P., and Winchester, B. The storage products in genetic and swainsonine-induced human mannosidosis. Biochem J, *215:* 693-696, 1983.

22. Daniel, P. F., Evans, J. E., De Gasperi, R., Winchester, B., and Warren, C. D. A human lysosomal alpha(1----6)-mannosidase active on the branched trimannosyl core of complex glycans. Glycobiology, *2:* 327-336, 1992.

23. De Gasperi, R., Daniel, P. F., and Warren, C. D. A human lysosomal alpha-mannosidase specific for the core of complex glycans. J Biol Chem, *267:* 9706-9712, 1992.

24. Haeuw, J. F., Grard, T., Alonso, C., Strecker, G., and Michalski, J. C. The core-specific lysosomal alpha(1-6)-mannosidase activity depends on aspartamidohydrolase activity. Biochem J, *297:* 463-466, 1994.

25. Daniel, P. F., Winchester, B., and Warren, C. D. Mammalian alpha-mannosidases--multiple forms but a common purpose? Glycobiology, *4:* 551-566, 1994.

26. Liu, B., Ahmad, W., and Aronson, N. N., Jr. Structure of the human gene for lysosomal di-N-acetylchitobiase. Glycobiology, *9:* 589-593, 1999.

APPENDIX

NEUTRAL GLYCOLIPIDS OF THE FILAMENTOUS FUNGUS *N. CRASSA*: ALTERED EXPRESSION IN PLANT DEFENSIN-RESISTANT MUTANTS

Park C, Bennion B, Francois IE, Ferket KK, Cammue BP, Thevissen K, Levery SB. (2005) J Lipid Res. 2005 Apr;46(4):759-68. Reprinted here with permission of publisher, ©The American Society of Biochemistry and Molecular Biology

Abstract

To defend themselves against fungal pathogens, plants produce numerous antifungal proteins and peptides, including defensins, some of which have been proposed to interact with fungal cell surface glycosphingolipid components. Although not known as a phytopathogen, the filamentous fungus *Neurospora crassa* possesses numerous genes similar to those required for plant pathogenesis identified in fungal pathogens (Galagan, J. E., et al. 2003. *Nature* **422:** 859–868), and it has been used as a model for studying plant-phytopathogen interactions targeting fungal membrane components (Thevissen, K., et al. 2003. *Peptides.* **24:** 1705–1712). For this study, neutral glycolipid components were extracted from wild-type and plant defensin-resistant mutant strains of *N. crassa*. The structures of purified components were elucidated by NMR spectroscopy and mass spectrometry. Neutral glycosphingolipids of both wild-type and mutant strains were characterized as ß-glucopyranosylceramides, but those of the mutants were found with structurally altered ceramides. Although the wild type expressed a preponderance of *N*-2'-hydroxy-(*E*)-Δ^3-octadecenoate as the fatty-*N*-acyl component attached to the long-chain base (4*E*,8*E*)-9-methyl-4,8-sphingadienine, the mutant ceramides were found with mainly *N*-2'-hydroxyhexadecanoate instead. In addition, the mutant strains expressed highly increased levels of a sterol glucoside identified as ergosterol-ß-glucoside.

Introduction

Plants possess an impressive arsenal of antimicrobial compounds that are either constitutively arrayed within certain tissues or synthesized in direct response to attack by pathogens. Among these compounds are defensins, a class of evolutionarily and structurally related small, highly basic, cysteine-rich peptides, many of which display antifungal activity (reviewed in 1–3). Defensins are also found in other types of organisms, including insects and humans, as important components of innate immunity (4–6). The structures of human, insect, and plant defensins, which include a conserved amphipathic ß-sheet motif, are consistent with a membranolytic mode of action, but plant defensins, unlike those of humans and insects, have not been shown to induce ion-permeable pores in artificial membranes composed of phospholipids or to change the electrical properties of artificial lipid bilayers (3). Nevertheless, some plant defensins have been shown to induce rapid increases in potassium efflux and calcium uptake in *Neurospora crassa* hyphae (7), and plant defensin-induced membrane permeabilization of *N. crassa* and *Saccharomyces cerevisiae* cells, as measured by SYTOX green uptake, was correlated with the inhibition of growth (8). In addition, using the *N. crassa* and *S. cerevisiae* model systems, high-affinity binding of plant defensins to fungal cells and membrane fractions has been demonstrated and also correlated with their antifungal activity (9, 10).

Recent investigations have implicated sphingolipids as targets of defensin binding to the fungal membrane (11–13). The sensitivity of *S. cerevisiae* to DmAMP1, a defensin isolated from the seeds of *Dahlia merckii* (14), was shown to be dependent on *IPT1* (15), a gene required for the final step in the biosynthesis of the complex yeast sphingolipid mannose-(inositol-phosphate)$_2$-ceramide (16). Moreover, using an ELISA, DmAMP1 was found to interact in a dose-dependent manner with *S. cerevisiae* sphingolipids, and this interaction was enhanced in the

presence of ergosterol, the major sterol component of fungi (12). More recently, the sensitivity of the yeasts *Pichia pastoris* and *Candida albicans* toward RsAFP2, a defensin isolated from seeds of *Raphanus sativus* (radish) (17), was found to be dependent on *GCS* (13), the gene encoding glucosylceramide synthase (UDP-Glc:ceramide ß-glucosyltransferase) (18). In that study, interaction of RsAFP2 was observed with ß-glucopyranosylceramide (GlcCer) isolated from *P. pastoris* but not from soybean or human (13), which differ in the structures of their ceramide moieties. Finally, chemically mutagenized *N. crassa* strains selected for resistance to RsAFP2 were found to have dramatically altered glycolipid/sphingolipid expression profiles (11). Although a number of these differences are obvious from even superficial glycolipid profiling by thin-layer chromatography, as described previously (11), the true nature of some alterations, particularly with respect to neutral glycolipid expression, required detailed structural analysis to become apparent. The structural characterization of these neutral glycolipid components, isolated from wild-type and defensin-resistant mutant *N. crassa* strains, is described in this report.

Material and Method

Fungal isolate and growth conditions

N. crassa [(strain 74-OR23-1A; Fungal Genetics Stock Center (FGSC) number 987, American Type Culture Collection number 24698; termed wild type (WT)] and its mutants were grown on half-strength potato dextrose broth agar (12 g/l potato dextrose broth, 15 g/l agar; Difco, Detroit, MI). For the purposes of lipid extraction, cultures of *N. crassa* WT, MUT16, and MUT24, grown on solid yeast peptone dextrose agar plates at room temperature, were transferred to 1.2 g/l liquid potato dextrose broth medium in 2.5 liter Fernbach flasks and shaken for 3 days at 25°C or 37°C at 250 rpm. Mycelia were harvested by filtration through cheesecloth, washing

off excess media with water. Excess water was removed by gentle pressure, and mycelia were either stored at –80°C until extraction or processed immediately as described below.

Solvents for extraction, anion-exchange chromatography, and high-performance thin-layer chromatography

Solvent A is chloroform-methanol (1:1, v/v); solvent B is isopropanol-hexane-water (55:25:20, v/v/v; upper phase discarded). Solvent C consists of chloroform-methanol-water (30:60:8, v/v/v), and solvent D consists of isopropanol-hexane-water (55:40:5, v/v/v). Solvent E is chloroform-methanol-2 N ammonium hydroxide (40:10:1, v/v/v); solvent F is chloroform-methanol-water [50:47:14, v/v/v; containing 0.035% (w/v) $CaCl_2$].

Extraction and purification of glycosphingolipids

Extraction and purification of glycosphingolipids were carried out as described previously (19–21). Briefly, glycosphingolipids were extracted by homogenizing mycelia (40–80 g wet weight) in a glass-walled blender once with 200 ml of solvent A, two times with 200 ml of solvent B, and once more with 200 ml of solvent A. The four extracts were pooled, dried on a rotary evaporator, dialyzed against water, lyophilized, resuspended in solvent C, and applied to a column of DEAE-Sephadex A-25 (Ac^- form). Neutral glycosphingolipids were eluted with five volumes of solvent C. The neutral fraction was then dried and taken up in solvent D before analytical or preparative high-performance thin-layer chromatography (HPTLC) as described below. Acidic glycosphingolipids were eluted with five volumes of 0.5 M sodium acetate in

methanol. The acidic fraction was dried, dialyzed exhaustively against deionized water, and redried. Analyis of acidic components will be described elsewhere.

HPTLC

Both analytical and preparative HPTLC were performed on silica gel 60 plates (E. Merck, Darmstadt, Germany) using chloroform-methanol-water [60:40:9, v/v/v; containing 0.02% (w/v) $CaCl_2$ (solvent D)] as mobile phase. Lipid samples were dissolved in solvent B and applied by streaking from 5 µl Micro-caps (Drummond, Broomall, PA). For analytical HPTLC, detection was performed with Bial's orcinol reagent [0.55% (w/v) orcinol and 5.5% (v/v) H_2SO_4 in ethanol-water 9:1 (v/v); the plate is sprayed and heated briefly to ~200–250°C; violet staining is positive for the presence of hexose]. For preparative HPTLC, samples were streaked lengthwise on 10 x 20 cm plates, and separated glycosphingolipid bands were visualized under ultraviolet light after spraying with primulin (Aldrich; 0.01% in 80% aqueous acetone). Bands were marked by pencil and individually scraped from the plate. Glycosphingolipids were then isolated from the silica gel by repeated sonication in solvent A followed by centrifugation. After concentration of the extract, primulin was removed by passage through a short column of DEAE-Sephadex A-25 in solvent C.

^{1}H-nuclear magnetic resonance spectroscopy

Samples of underivatized lipids (~0.5–1.0 mg) were deuterium-exchanged by repeated evaporation from $CDCl_3/CD_3OD$ (2:1, v/v) under an N_2 stream at 35–40°C and then dissolved in 0.5 ml of DMSO-d_6/2% D_2O (22–24) for NMR analysis. One-dimensional ^{1}H-NMR spectra, two-

dimensional ^{1}H-^{1}H-gradient-enhanced correlation spectra and total correlation spectra, and two-dimensional ^{1}H-detected ^{1}H-^{13}C-gradient-enhanced heteronuclear single-quantum correlation spectra were acquired at 35°C on Varian Unity Inova 500 MHz (University of New Hampshire, Durham) or 600 or 800 MHz (University of Georgia/Complex Carbohydrate Research Center, Athens) spectrometers using standard acquisition software available in the Varian VNMR software package. Proton chemical shifts are referenced to internal tetramethylsilane (δ = 0.000 ppm), carbon chemical shifts to the natural abundance ^{13}C-methyl resonance of solvent DMSO-d_6 (δ = 40.00 ppm).

Positive ion mode electrospray ionization mass spectrometry

Mass spectrometry was performed in the positive ion mode on a Micromass (Manchester, UK) hybrid electrospray ionization-Qq/oa-time-of-flight (ESI-Q-TOF)-MS instrument, with sample introduction via direct infusion in 100% methanol (~100 ng/μl; flow rate, 0.5 μl/min). As described previously (25, 26), to generate $[M+Li]^+$ adducts of GlcCer molecular species, LiI (10 mM) in methanol was added to the analyte solution until the observed ratio of $[M+Li]^+$ adducts to mixed Na^+/Li^+ adducts in MS profile mode was >5:1; the necessary LiI concentration was generally in the range 2–3 mM. Resolution was generally 4,000 (5% valley) for positive ion mode ESI ($^+$ESI)-Q-TOF-MS molecular adduct profile spectra and 3,000 for MS/collision-induced dissociation (CID)-TOF-MS experiments. Extraction cone voltage (analogous to orifice-to-skimmer potential in Sciex API series instruments) was 35 V for MS profile spectra and MS/CID-MS experiments. Nominal monoisotopic *m/z* values are used in the labeling and

description of $^{+}$ESI-MS results. Interpretation of spectra derived from $[M+Li]^{+}$ adducts of GlcCer molecular species was essentially as described previously (25–27).

Results

Detection and isolation of glycolipids from WT and mutant strains of *N. crassa*

Glucosylceramides were initially detected in all of the neutral lipid fractions from *N. crassa* strains, recognized in HPTLC analysis by their orcinol staining and comigration with an authentic standard (11) (**Fig. 1**) . There did not appear to be any striking quantitative differences between the WT and mutant strains. In addition, a second orcinol-positive band with relative migration (Rf) higher than GlcCer was detectable in both mutants; this band was also detected in the WT, albeit at significantly lower intensity. It was tentatively proposed to be a sterol glycoside (11), based on its orcinol staining and Rf, compared with recent literature (28, 29). No significant dependence of band intensity on culture temperature (25°C versus 37°C) was apparent for either of the putative glycolipids. Both putative glycolipid components were isolated from the crude neutral lipid fractions of each *N. crassa* strain by preparative HPTLC and characterized by ^{1}H-NMR spectroscopy and ESI-MS. Interestingly, a non-hexose-containing lipid migrating near the solvent front (Fig. 1, band c, staining brown with orcinol) appeared to have a reciprocal quantitative relationship with the putative sterol glycoside band; although its behavior did not appear to be typical of a free sterol or *O*-acyl-sterol, it was also isolated and examined for any potential structural or biosynthetic relationship to the glycosidic components of interest. As this did not appear to be the case (data not shown), its analysis was not pursued further in this study. For similar reasons, detailed analysis of a second component staining brown with orcinol (band

b), which appeared in all three strains, was not carried out. An orcinol-positive band with lower Rf (band a) was also detected in all three strains but did not stain with primulin, which detects lipids. ^{1}H-NMR spectroscopy confirmed the absence of resonances characteristic for a lipid component (data not shown).

^{1}H-NMR spectroscopic analysis of *N. crassa* glucosylceramides

Both ^{1}H- and ^{13}C-NMR spectra for several fungal cerebrosides have been previously acquired in DMSO-d_6/2% D_2O at 35°C and all resonances assigned by homonuclear and heteronuclear two-dimensional correlation methods (20, 26). Therefore, it was sufficient for the present work to obtain one-dimensional ^{1}H-NMR spectra from the putative GlcCer components, isolated by preparative HPTLC from each of the three *N. crassa* strains (WT, MUT16, MUT24), to characterize them with respect to monosaccharide identity and key ceramide structural features.

The ^{1}H-NMR spectra confirmed the identity of all three putative GlcCer components (**Fig. 2** ; panels A, B, and C correspond to bands marked GlcCer in Fig. 1, lanes 5, 6, and 7, respectively). Each exhibited a set of resonances with chemical shifts and coupling patterns characteristic of the seven proton ß-glucopyranosyl spin system (see **Scheme 1** for structures and numbering). Additional resonances in each spectrum identified (4*E*,8*E*)-9-methyl-4,8-sphingadienine along with *N*-2"-hydroxy-(*E*)-3"-alkenoate and/or *N*-2"-hydroxyalkanoate. Interestingly, however, the WT and mutant GlcCer clearly differ with respect to unsaturation of the fatty-*N*-acyl moiety. Key resonances for this feature are those from fatty acyl-3" (Fa-3") and Fa-4", which generally appear at ~5.42–5.44 and 5.66–5.68 ppm, respectively, and from Fa-2", which is shifted significantly downfield to ~4.28–4.30 ppm, where the unsaturation is present; these signals are clearly visible

in the WT GlcCer spectrum (Fig. 2A) but absent in those of the mutants (Fig. 2B, C). Thus, although the WT GlcCer exhibits a high level of (*E*)-Δ^3-unsaturation, which can be estimated from the relative integrals of the Fa-4" and sphingosine-5 resonances, this structural modification appears to be completely ablated in the corresponding mutant fractions.

Note that two resonances are observed at slightly different chemical shifts for the ß-Glc H-2' in the WT GlcCer spectrum, as a result of the long-range influence of the (*E*)-Δ^3-unsaturation in ~70% of the ceramide. An additional key upfield resonance for these compounds is that of the sphingadienine 9-methyl group, which was observed in all three spectra as a singlet at 1.545 ± 0.002 ppm (data not shown). Remaining glycosphingolipid structural features, not conveniently assessed by NMR analysis, are the chain lengths of the Fa and sphingosine moieties. These were determined unambiguously by mass spectrometric methods, which in addition provided confirmation of most of the features discussed above.

Characterization of *N. crassa* glucosylceramides by ESI-MS and tandem MS

In $^{+}$ESI-Q-TOF-MS, lithiated molecular ions were observed primarily at *m/z* 760 for the WT GlcCer (**Fig. 3A**) , consistent with a monohexosylceramide containing (4*E*,8*E*)-9-methyl-4,8-sphingadienine attached to *N*-2"-hydroxy-(*E*)-3"-octadecenoate. In some fractions (data not shown), ion abundance at *m/z* 762 was clearly observed above the theoretical level of the $^{13}C_2$ isotope peak for the major species, consistent with the additional presence of a minor GlcCer component containing saturated *N*-2"-hydroxyoctadecanoate, as noted in the ^{1}H-NMR spectra. Minor components were also observed at *m/z* 746, 734, and 732 (the ion at *m/z* 776 primarily representing residual Na^+ adduct). Details about the ceramide structure of the major and minor components were provided by tandem ESI-MS/CID-TOF-MS experiments (**Fig. 4**). As found

previously with MS/CID-MS spectra acquired on a triple quadrupole instrument (25, 26), key ions diagnostic for fatty-*N*-acyl and sphingoid carbon number and level of unsaturation can be observed at high abundance in the hybrid Q-TOF spectra, but with the expected increases in overall sensitivity, resolution, and mass accuracy. In the CID spectrum of the major $[M+Li]^+$ at *m/z* 760, an O ion, corresponding to loss of the fatty-*N*-acyl chain (**Scheme 2**), is observed abundantly at *m/z* 480, characteristic for a monohexosyl-(4*E*,8*E*)-9-methyl-4,8-sphingadienine (25). Additional loss of the hexose moiety yields a confirming N ion, appearing in this spectrum at *m/z* 318. A T ion, derived from loss of the hexose and most of the sphingoid, is observed abundantly at *m/z* 330, providing complementary information about the carbon number and the level of unsaturation of the fatty-*N*-acyl chain, in this case *N*-2"-hydroxy-(*E*)-3"-octadecenoate. This is confirmed by the appearance of a corresponding W ion, particularly characteristic for 2-hydroxy-fatty-*N*-acylation and composed of the acyl C_2-C_{17} in the form of an aldehyde, at *m/z* 259. Assignments for other product ions are listed in **Table 1**. Tandem CID product spectra of minor GlcCer components were also obtainable, enabling in most cases characterization of minor structural variations responsible for the decrements in their molecular masses. For example, in the CID spectrum of the minor $[M+Li]^+$ at *m/z* 746 (Fig. 4B), 14 u decrements are observed almost exclusively for the O and N ions (*m/z* 466 and 304, respectively) but not for the T and W ions, consistent with lack of the branching methyl group on the sphingoid but not with h17:1 fatty-*N*-acylation [this is not always the case (25, 26)]. On the other hand, in the CID spectrum of $[M+Li]^+$ at *m/z* 732 (Table 1), O and N ions are again observed at *m/z* 480 and 318, respectively, but the T and W ions are decremented to *m/z* 302 and 231, respectively, consistent with h16:1 fatty-*N*-acylation. In the CID spectrum of $[M+Li]^+$ at *m/z* 734 (Table 1), the T and W ions are

observed at *m/z* 304 and 233, respectively, consistent with saturation of the shorter chain fatty-*N*-acyl moiety (h16:0).

Significantly, in the $^{+}$ESI-Q-TOF-MS profile of GlcCer from MUT16 (Fig. 3B), the major $[M+Li]^{+}$ was observed at *m/z* 734, consistent with *N*-2"-hydroxyhexadecanoyl-(4*E*,8*E*)-9-methyl-4,8-sphingadienine as the most abundant ceramide component. This ceramide composition was confirmed by acquisition of a tandem CID spectrum (**Fig. 5A**) , which exhibited O and N product ions at *m/z* 480 and 318, respectively, and T and W product ions at *m/z* 304 and 233, respectively, as observed before for the minor WT GlcCer component. A minor $[M+Li]^{+}$ was also observed in the $^{+}$ESI-Q-TOF-MS profile of the MUT16 GlcCer at *m/z* 720 (Fig. 3B), decremented 14 u with respect to the major component; the CID product ion spectrum of this $[M+Li]^{+}$ (Fig. 5B) exhibited corresponding 14 u decrements to the O and N ions, now observed at *m/z* 466 and 304, respectively (the latter isobaric to the h16:0 T ion).

The $^{+}$ESI-MS data for the MUT24 strain GlcCer (data not shown) were essentially identical to those described above for the MUT16 component, and together they supported the somewhat surprising conclusion that the underlying mutation(s) has in each case resulted not only in ablation of the (*E*)-Δ^3-unsaturation of the fatty-*N*-acyl moiety but also in a virtually 100% shift in the dominant fatty-*N*-acyl chain length, shorter than that found in the WT GlcCer by two CH_2 units.

NMR spectroscopic analysis of *N. crassa* sterol glycosides

The one-dimensional ^{1}H-NMR spectrum of the putative sterol glycoside component isolated from *N. crassa* MUT24 is shown in **Fig. 6** . As with the GlcCer spectra analyzed above, a seven proton ß-glucopyranosyl spin system is recognizable from the same characteristic set of

resonances observed with similar chemical shifts and coupling patterns (resonances marked H-1' to H-6a' and H-6b'). The remaining resonances and their connectivities were assigned (see supplementary table) by acquisition and analysis of two-dimensional ^{1}H-^{1}H-gradient-enhanced correlation and -total correlation spectra (data not shown) along with a ^{1}H-detected ^{13}C-^{1}H-gradient-enhanced heteronuclear single-quantum correlation spectrum (see supplementary figure). Based on this analysis, along with comparison with published NMR spectral data (28), the glycolipid was identified as ergosterol-ß-glucoside (Scheme 2), which was previously identified as the major sterol glycoside component of *P. pastoris* (29) and of transgenic *S. cerevisiae* expressing a UDP-Glc:sterol ß-D-glucosyltransferase (*UGT*) gene from *P. pastoris* (28). The NMR data are indeed comparable with those published for 3ß-(2,3,4,6-tetra-*O*-acetyl-ß-D-glucopyranosyloxy) ergosta-5,7,22*E*-triene (28), allowing for somewhat predictable chemical shift increments attributable to that group's analytical choice of per-*O*-acetylating the ß-D-glucosyl moiety, as well as for smaller differences resulting from the use of a different solvent and acquisition temperature in that work. NMR spectra obtained on the corresponding components from MUT16 and WT *N. crassa* were essentially identical to those shown for the MUT24 component, although the amount isolated from the WT strain was sufficient only for the acquisition of a one-dimensional ^{1}H-NMR spectrum.

Discussion

In this work, we isolated and characterized two neutral glycolipid components from *N. crassa* not previously identified in this species; more significantly, we detected changes in their expression patterns in mutant strains selected for resistance to a radish defensin, RsAFP2 (11). These consisted of *i*) structural changes to the fatty-*N*-acyl moiety of GlcCer found in both WT

and mutant *N. crassa* strains [shortening of the dominant chain length from C18 to C16, and ablation of (*E*)-Δ^3-unsaturation], and *ii*) increased accumulation of GlcSte, identified as ergosterol-ß-D-glucoside. Together with previously noted changes in the expression of acidic glycosphingolipids (11), which are still under investigation, it is apparent that the mutant strains exhibit a complex set of phenotypic alterations at the biochemical level. Whether these result from a single underlying mutation or from combinations of several mutations, and whether these mutations are actually in the genes coding for enzymes directly involved in the synthesis of the glycolipids in question, remain to be determined.

Previous studies have provided evidence that a variety of plant defensins interact with fungal sphingolipids as a primary step leading to growth arrest and that fungal GlcCer is a particular target of RsAFP2 (13). Moreover, selectivity with respect to ceramide structural features was displayed in ELISA-based binding assays, because RsAFP2 showed little interaction with GlcCer from plant or human sources, which lack one or more of the structural modifications found in fungal GlcCer (13). This suggests, on the one hand, that the observed changes in GlcCer structure between the WT and mutant *N. crassa* strains, such as the loss of fatty-*N*-acyl (*E*)-Δ^3-unsaturation, could have a direct effect on the binding interaction with RsAFP2. On the other hand, this hypothesis is not fully supported by the earlier biological assays of RsAFP2-GlcCer interactions, which were carried out using a *P. pastoris* system, or by the ELISA-based measurements of binding specificity, made with purified GlcCer from *P. pastoris* (13), because GlcCer from *P. pastoris* and other hemiascomycetous yeasts do not display the (*E*)-Δ^3-unsaturation under any circumstances. Thus, this feature is probably not essential for the interaction; therefore, it is unlikely that its ablation could by itself account for the loss of susceptibility to RsAFP2 displayed by the *N. crassa* mutants. Alternatively, it is possible that the

shortening of the fatty-*N*-acyl chain in the mutant GlcCer could have an effect on its interaction with RsAFP2. There is evidence that such alterations in ceramide structure, even as subtle as a two carbon difference in fatty-*N*-acyl chain length, can modify the presentation of glycosphingolipids on the cell membrane surface, affecting their interactions with peptide and protein ligands (30, 31).

A third possibility is suggested by the increase in GlcSte levels observed in the mutant strains. There is evidence suggesting that fungal sterols could modulate the interaction of some defensins with their glycosphingolipid targets on the membrane surface, as addition of ergosterol was found to increase the interaction of another plant defensin, DmAMP1, with *S. cerevisiae* glycosylinositol phosphorylceramides in an ELISA (12). In addition, Ferket et al. (11) observed reduced sensitivity of the MUT16 and MUT24 mutants to the plant defensin HsAFP1; consistent with this, a *P. pastoris* mutant strain, Δ*ugt51*, lacking UGT activity, was found to be 4-fold more sensitive toward HsAFP1 (K. Thevissen, unpublished data). On the other hand, HsAFP1 does not appear to interact with sphingolipids, either GlcCer or glycosylinositol phosphorylceramides (K. Thevissen, unpublished data). Moreover, no significant change was observed in the sensitivity of the *P. pastoris* Δ*ugt51* mutant toward RsAFP2 (K. Thevissen, unpublished data). Although this does not completely rule out a relationship between increased GlcSte expression and decreased RsAFP2 sensitivity in the *N. crassa* mutants, considerably more work will be required to clarify whether it is a significant factor. It should be noted here that the apparent accumulation of GlcSte in the *N. crassa* mutants could also result from downregulation of an as yet unknown ß-glucosidase or other GlcSte-metabolizing enzyme.

In any case, GlcSte biosynthesis has been strongly implicated as a factor contributing to fungal phytopathogenicity and could be involved in the sensitivity of fungi to other plant defensins, as appears to be the case with HsAFP1. Functional characterization of *UGT* genes from a number of fungi, including *S. cerevisiae*, *C. albicans*, and *P. pastoris*, has been carried out by Warnecke et al. (28); they pointed out a highly similar sequence in a gene from *Magnaporthe grisea*, *pth8*, the disruption of which had previously been correlated with reduced pathogenicity (32). More recently, Kim et al. (33) also identified a putative factor in fungal disease virulence displaying strong homology to the *UGT* family through its deduced peptide sequence, the *chip6* gene from *Colletotrichum gloeosporioides* (*Glomerella cingulata* group), and demonstrated that its product expressed in *Escherichia coli* possessed UGT activity. Disruption of *chip6* in *C. gloeosporioides* resulted in an apparent reduction of UGT activity to 45% of the WT level and correlated with reduced pathogenicity toward its natural host, avocado fruit. In light of results described by Ferket et al. (11) and herein, it would be of interest to determine if the reduced pathogenicity of the *M. grisea* and *C. gloeosporioides ugt* mutants can be further correlated with increased binding and susceptibility to plant defensins such as RsAFP2 and HsAFP1.

Accumulation of GlcSte does not appear as widespread in the fungal kingdom as that of GlcCer (for recent discussions of the occurrence, biosynthesis, and possible functional roles of GlcCer in fungi, see 34, 35). Sakaki et al. (29) surveyed GlcSte and GlcCer expression in a number of fungi and found several that produced little or no detectable GlcSte under the culture conditions used; these included *C. albicans* and many strains of *P. pastoris*, both of which had been shown previously to have *UGT* genes (homologs of *S. cerevisiae UGT51*) encoding functional proteins (28). They also showed that GlcSte accumulates in one strain of *P. pastoris* in response to heat or ethanol shock, in contrast to GlcCer, which appears to be constitutively

expressed. The evidence suggests that GlcSte is not essential for viability, although UGT51p-catalyzed biosynthesis of GlcSte was recently shown to be required for oxidative metabolism of small molecules, such as methanol or alkanes, by some fungi (36, 37).

Because the current study establishes that *N. crassa*, an established model fungal species, is capable of GlcSte biosynthesis, it may also prove to be a good system for studies of GlcSte function. As indicated by Sakaki et al. (29), tblastn (Basic Local Alignment Search Tool) queries (38) of the *N. crassa* genome databases (Munich Information Center for Protein Sequences, http://mips.gsf.de/proj/neurospora; and Whitehead Institute, http://www.broad.mit.edu/annotation/fungi/neurospora) (39) show that it contains three candidate genes encoding peptide sequences with a high degree of similarity to those of known fungal and plant *UGT* genes (MIPS codes xnc115_090, 3nc440_840, and 1nc130_180; Whitehead codes NCU093011, NCU002811, and NCU074731, respectively). The closest match for xnc115_090/NCU09301.1 appeared to be the putative *M. grisea pth8 UGT* (29). Kim et al. (33) pointed out the similarity between *chip6* and 1nc130_180/NCU07473.1; the closest match for 3nc440_840/NCU00281.1 also appears to be *chip6*. Systematic disruption or silencing experiments should identify which are active in GlcSte biosynthesis in WT *N. crassa*. Using this information, it would be of interest to determine whether susceptibility to RsAFP2 can be restored by disruption of *UGT* expression in the mutant strains.

Acknowledgements

This work was supported in part by the New Hampshire Biological Research Infrastructure Network-Center for Structural Biology [National Institutes of Health (NIH) P20 RR-16459], by the NIH Resource Center for Biomedical Complex Carbohydrates (NIH P41 RR-05351), and by Grant G.0288.04 from the Fonds voor Wetenschappelijk Onderzoek-Vlaanderen. I.E.J.A.F. is a postdoctoral fellow of the Fonds voor Wetenschappelijk Onderzoek-Vlaanderen (IWT/OZM/030508).

Supplementary key words ergosterol • sphingolipid • sterol • glucoside • ceramide • cerebroside • electrospray ionization • nuclear magnetic resonance spectroscopy • mass spectrometry • collision-induced dissociation • tandem mass spectrometry

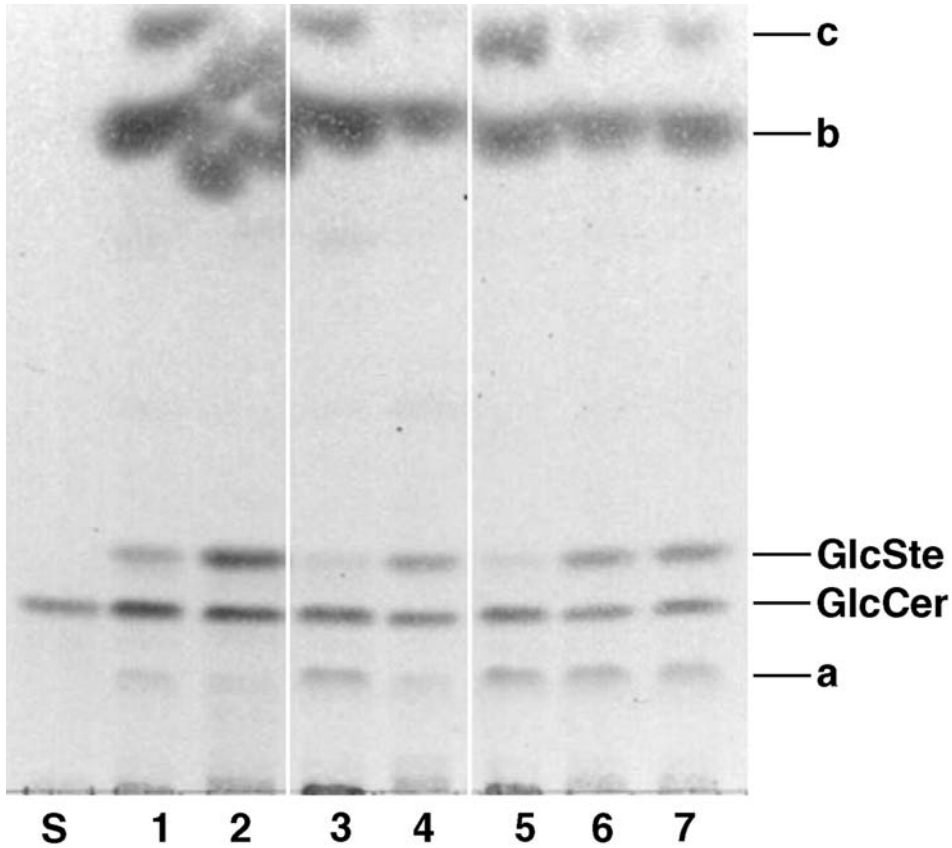

Fig. 1. High-performance thin-layer chromatography profiles of neutral glycolipids from *N. crassa* wild-type (WT), MUT16, and MUT24. Crude neutral lipid fractions, containing steryl-ß-glucopyranoside (GlcSte) and ß-glucopyranosylceramide (GlcCer), were developed with solvent E; hexose-containing bands were visualized with Bial's orcinol reagent (all bands on the lower section of the gel stained violet, that is, positive for hexose content; bands on the upper section of the gel stained brown to brownish green, that is, negative for hexose content). Lane S, authentic GlcCer from *Aspergillus nidulans* (21); lanes 1, 3, 5, WT; lanes 2, 4, 6, MUT16; lane 7, MUT24. Lanes 1 and 2, 3 and 4, and 5 to 7 [the third set was adapted from the results of Ferket et al. (11)] show lipids extracted from three different sets of cultures that were cultured 2–5 weeks apart. The first and third sets were cultured at 25°C, and the second set was cultured at 37°C; in the second and third sets, samples applied to the gel were diluted in two times the volume of solvent used in the first set. The identities of components a, b, and c have not been unequivocally established.

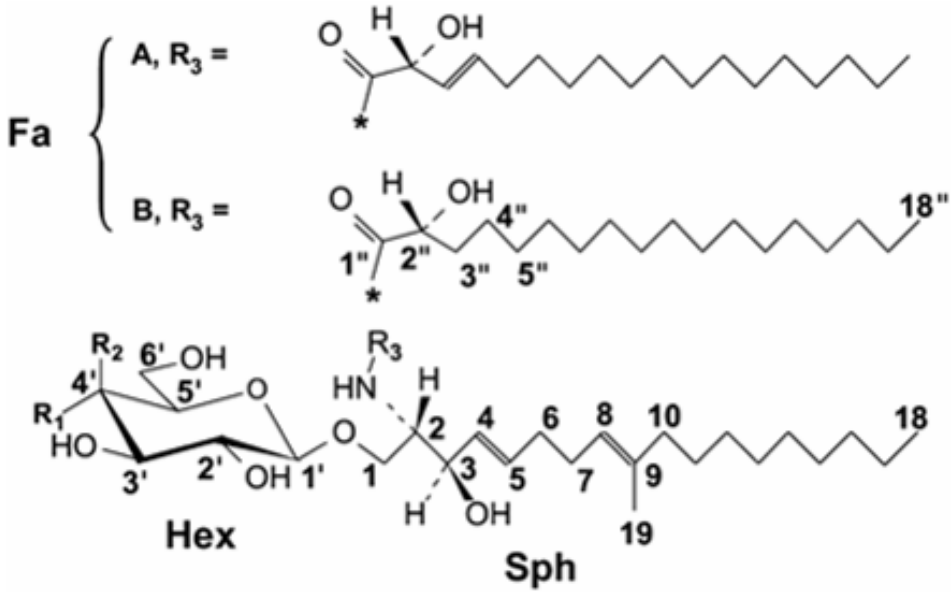

Scheme 1. Structures of prototypical fungal cerebrosides with numbering of sphingosine (Sph), hexose (Hex), and fatty acyl (Fa) moieties: (4*E*,8*E*)-*N*-2"-hydroxyoctadec-(*E*)-3"-enoyl-1-ß-D-glucopyranosyl-9-methyl-4,8-sphingadienine (fatty acid R3 = **A**, R1 = OH, R2 = H); (4*E*,8*E*)-*N*-2"-hydroxyoctadec-(*E*)-3"-enoyl-1-ß-D-galactopyranosyl-9-methyl-4,8-sphingadienine (fatty acid R3 = **A**, R1 = H, R2 = OH); (4*E*,8*E*)-*N*-2"-hydroxyoctadecanoyl-1-ß-D-glucopyranosyl-9-methyl-4,8-sphingadienine (fatty acid R3 = **B**, R1 = OH, R2 = H); and (4*E*,8*E*)- *N*-2"-hydroxyoctadecanoyl-1-ß-D-galactopyranosyl-9-methyl-4,8-sphingadienine (fatty acid R3 = **B**, R1 = H, R2 = OH).

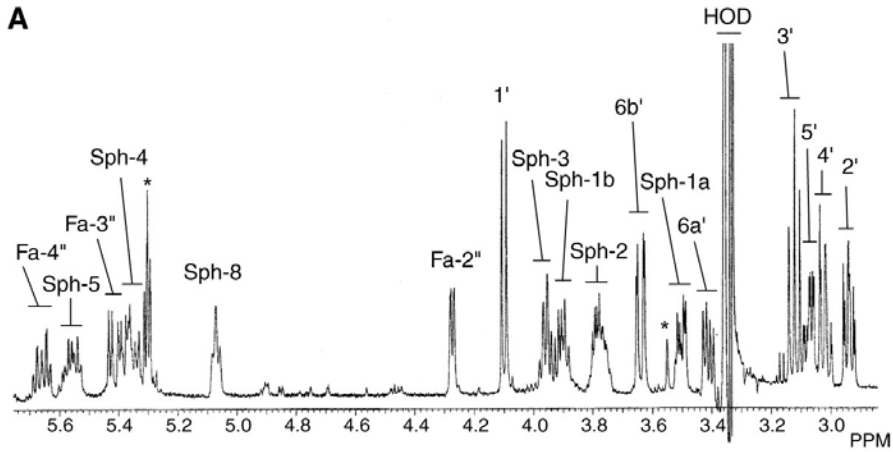

Fig. 2A. Downfield sections of one-dimensional 1H-NMR spectra of GlcCer fractions isolated from *N. crassa* strains. A: WT. B: MUT16. C: MUT24. Resonances from nonexchangeable protons of sphingosine (Sph), fatty acyl (Fa), and hexose (prefix omitted) are designated by Arabic numerals (corresponding to those in Scheme 1). Resonances marked by asterisks are from unknown impurities. Fa-2"+ is H-2" from saturated 2"-hydroxy fatty acid, isochronous with the Sph-2 resonance. HOD, residual monodeuterated water.

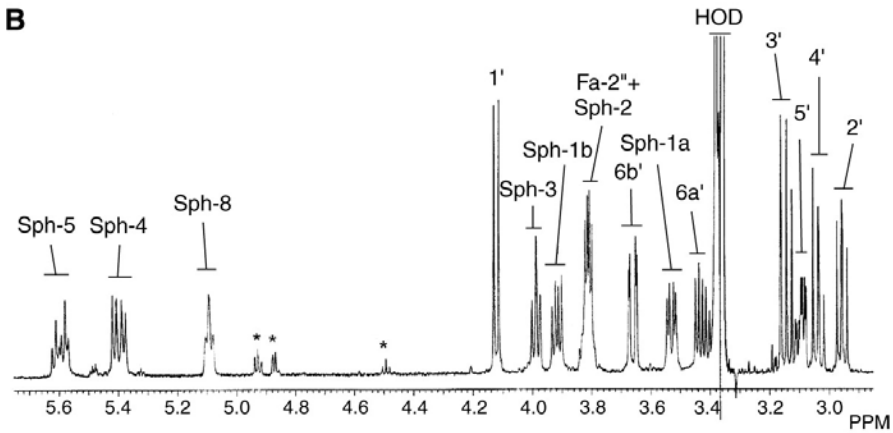

Fig. 2B. Downfield sections of one-dimensional 1H-NMR spectra of GlcCer fractions isolated from *N. crassa* strains. A: WT. B: MUT16. C: MUT24. Resonances from nonexchangeable protons of sphingosine (Sph), fatty acyl (Fa), and hexose (prefix omitted) are designated by Arabic numerals (corresponding to those in Scheme 1). Resonances marked by asterisks are from unknown impurities. Fa-2"+ is H-2" from saturated 2"-hydroxy fatty acid, isochronous with the Sph-2 resonance. HOD, residual monodeuterated water.

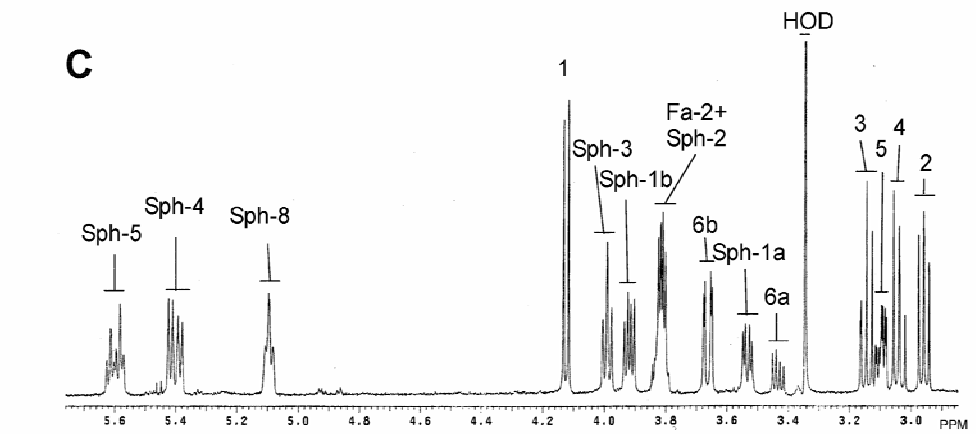

Fig. 3. Downfield sections of 1-D ^{1}H-NMR of neutral fraction from *N. crassa* mutants spont 10 (**B**, GlcCer area) and spont20 (**C**, GlcCer area). Resonances from non-exchangeable protons of sphingosine (Sph), fatty acyl (Fa), and

Fig. 2C. Downfield sections of one-dimensional 1H-NMR spectra of GlcCer fractions isolated from *N. crassa* strains. A: WT. B: MUT16. C: MUT24. Resonances from nonexchangeable protons of sphingosine (Sph), fatty acyl (Fa), and hexose (prefix omitted) are designated by Arabic numerals (corresponding to those in scheme 1). Resonances marked by asterisks are from unknown impurities. Fa-2"+ is H-2" from saturated 2"-hydroxy fatty acid, isochronous with the Sph-2 resonance. HOD, residual monodeuterated water.

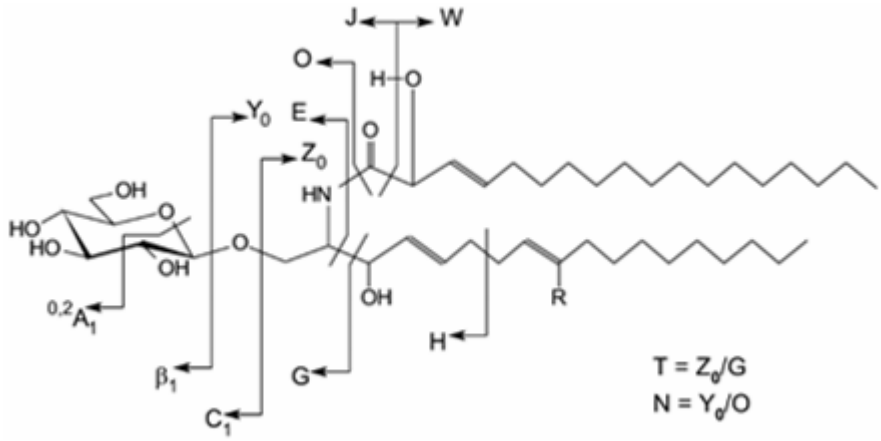

Scheme 2. Fragmentation of a cerebroside with nomenclature of Costello et al. (40–42) as modified by Adams and Ann (43).

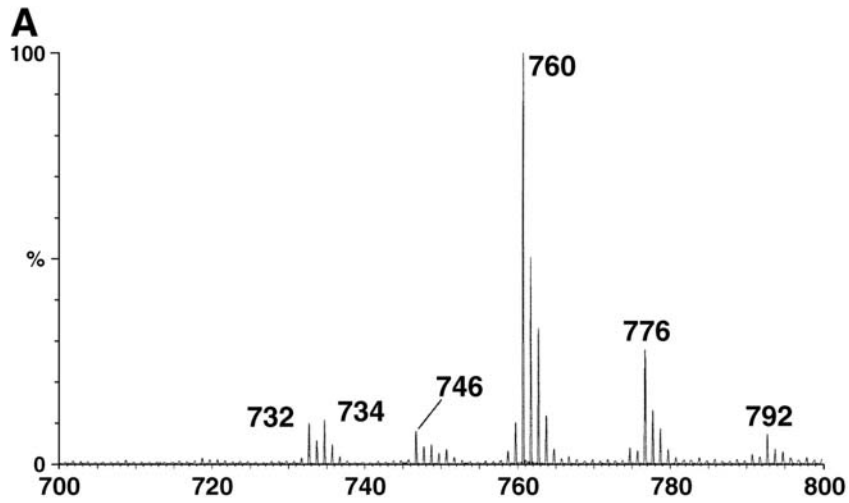

Fig. 3A. Lithium molecular adduct profiles from positive ion mode electrospray ionization (+ESI) mass spectrometry of GlcCer fractions isolated from *N. crassa* strains. A: WT. B: MUT16. Peak labels are nominal, monoisotopic *m/z*.

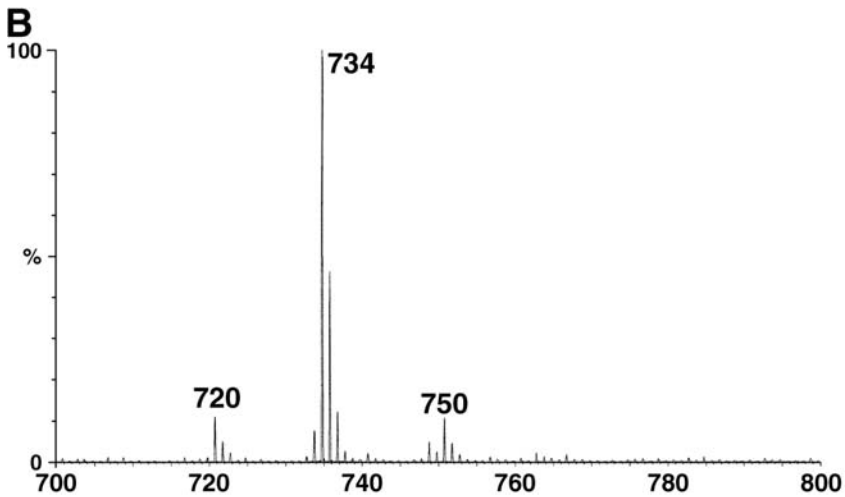

Fig. 3B. Lithium molecular adduct profiles from positive ion mode electrospray ionization (+ESI) mass spectrometry of GlcCer fractions isolated from *N. crassa* strains. A: WT. B: MUT16. Peak labels are nominal, monoisotopic *m/z*.

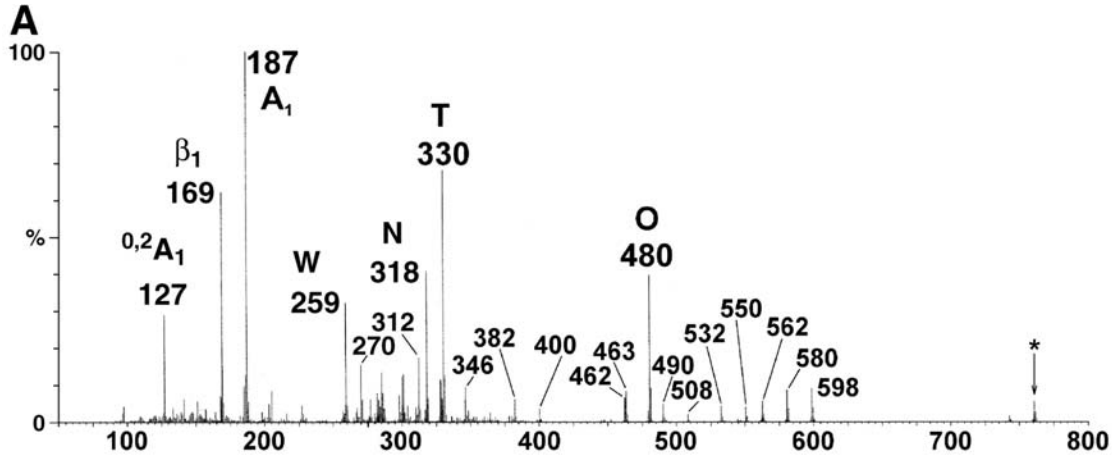

Fig. 4A. Tandem +ESI-MS/collision-induced dissociation (CID)-MS product ion spectra of selected [M+Li]+ from a *N. crassa* WT GlcCer fraction. A: Product ion spectrum from *m/z* 760. B: Product ion spectrum from *m/z* 746.

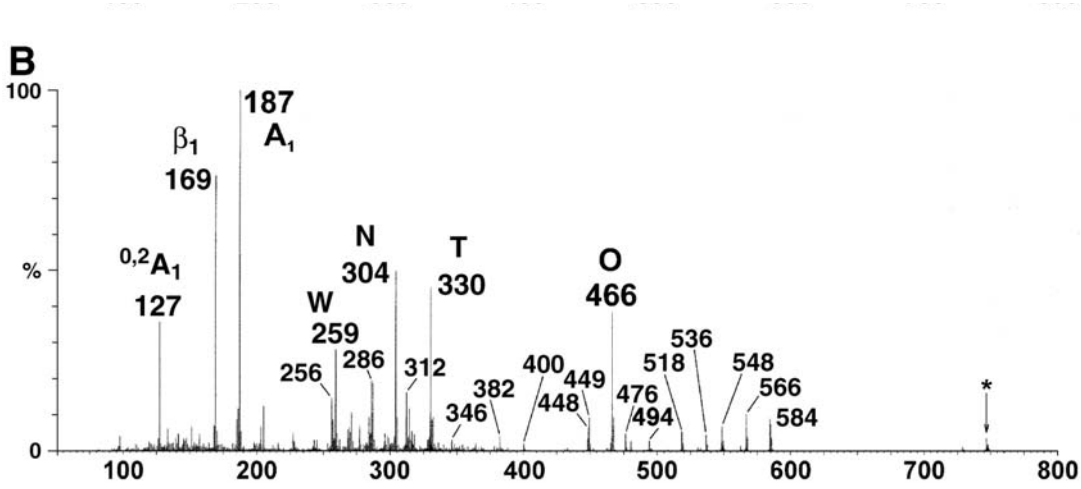

Fig. 4B. Tandem +ESI-MS/collision-induced dissociation (CID)-MS product ion spectra of selected [M+Li]+ from a *N. crassa* WT GlcCer fraction. A: Product ion spectrum from *m/z* 760. B: Product ion spectrum from *m/z* 746.

TABLE 1. Positive ion mode electrospray ionization-mass spectrometry/collision-induced dissociation-mass spectrometry data (all fragments •Li+ except where noted) for *N. crassa* wild-type ß-glucopyranosylceramide (major component, Nc1; minor components, Nc3, Nc4, and Nc5) and mutant ß-glucopyranosylceramide (major component, Nc4; minor components, Nc2 and Nc6), with proposed interpretations of fragments
All values are nominal, monoisotopic *m/z*. Fragment nomenclature is after Costello et al. (40–42) as modified and expanded by Adams and Ann (43) (see **Scheme 3**), with additional designations given by Hsu and Turk (27). The six to seven most abundant fragments in each spectrum are shown in boldface.

	Wild type				Mutant		
	Major	Minor			Major	Minor	
	Nc1	Nc3	Nc4	Nc5	Nc4	Nc2	Nc6
Fatty acid	h18:1	h18:1	h16:0	h16:1	h16:0	h18:0	h16:0
Sphingosine	d19:2	d18:2	d19:2	d19:2	d19:2	d18:2	d18:2
M	760	746	734	732	734	748	720
Y_0	598	584	572	570	572	586	558
Z_0	580	566	554	552	554	568	540
H' (H–H_2O)	562	562	536	534	536	564	536
Z_0–H_2O (Z_0' b_2)	562	548	536	534	536	564	522
Z_0–CH_2O (a_2)	550	536	524	522	524	538	510
Z_0–CH_2O–H_2O	532	518	—	504	—	—	—
J (M–acyl C_2-C)	508	494	508	508	508	494	496
J' (J–H_2O)	490	476	490	490	490	476	478
O (M–acyl)	**480**	**466**	**480**	**480**	**480**	**466**	**466**
O'a (M–acyl –NH_3)	463	449	463	463	463	449	449
O' (M–acyl –H_2O)	462	448	462	462	462	448	448
Z_0/H	400	400	374	372	374	402	—
Z_0/H' (Z_0/H–H_2O)	382	382	356	354	356	384	—
Z_0/H'' (Z_0/H–2H_2O)	364	364	338	336	338	—	—
S (Y_0/G)	346	346	320	318	320	348	348
T (Z_0/G)	**330**	**330**	**304**	**302**	**304**	**332**	**304**
N (Y_0/O)	**318**	**304**	**318**	**318**	**318**	**304**	**304**
T' (T–H_2O)	312	312	286	284	286	314	314
U (T–C_2H_2)	304	304	278	278	278	306	306
N'	300	286	300	300	300	286	286
d_{3b}	285	271	285	285	285	271	271
N'' [Li^+]	282	268	282	282	282	268	270
N'–CH_2O (e_{3b})	270	256	270	270	270	256	256
W (acyl C_2-C)	**259**	**259**	**233**	**231**	**233**	**261**	**233**
E	227	227	227	227	227	227	227
C_1	**187**	**187**	**187**	**187**	**187**	**187**	**187**
ß$_1$	**169**	**169**	**169**	**169**	**169**	**169**	**169**
$^{0,2}A_1$	127	127	127	127	127	127	127
$^{0,2}A_1$–CH_2O	97	97	97	97	97	97	97

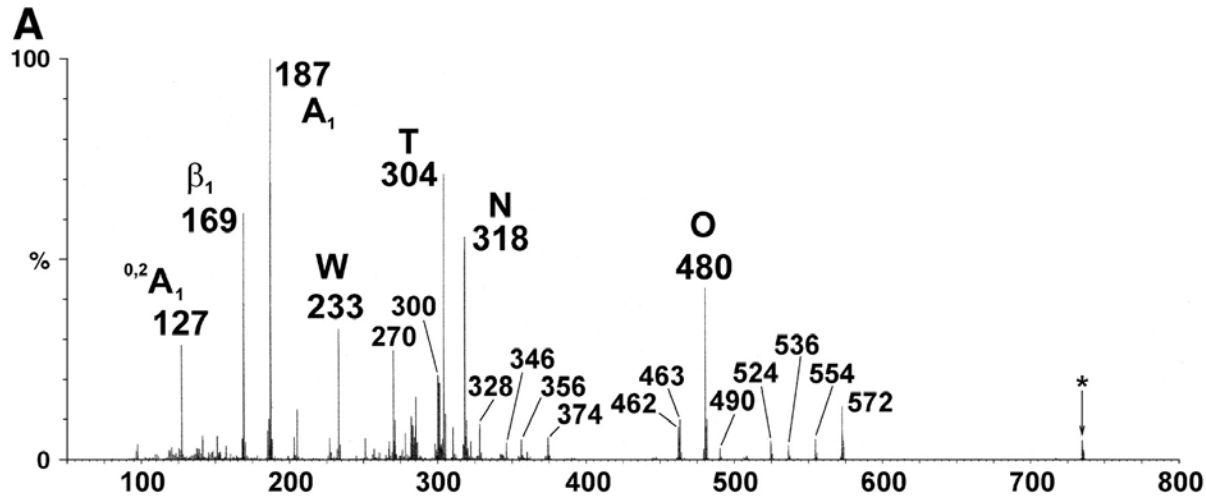

Fig. 5A. Tandem +ESI-MS/CID-MS product ion spectra of selected [M+Li]+ from a *N. crassa* MUT16 GlcCer fraction. A: Product ion spectrum from *m/z* 734. B: Product ion spectrum from *m/z* 720.

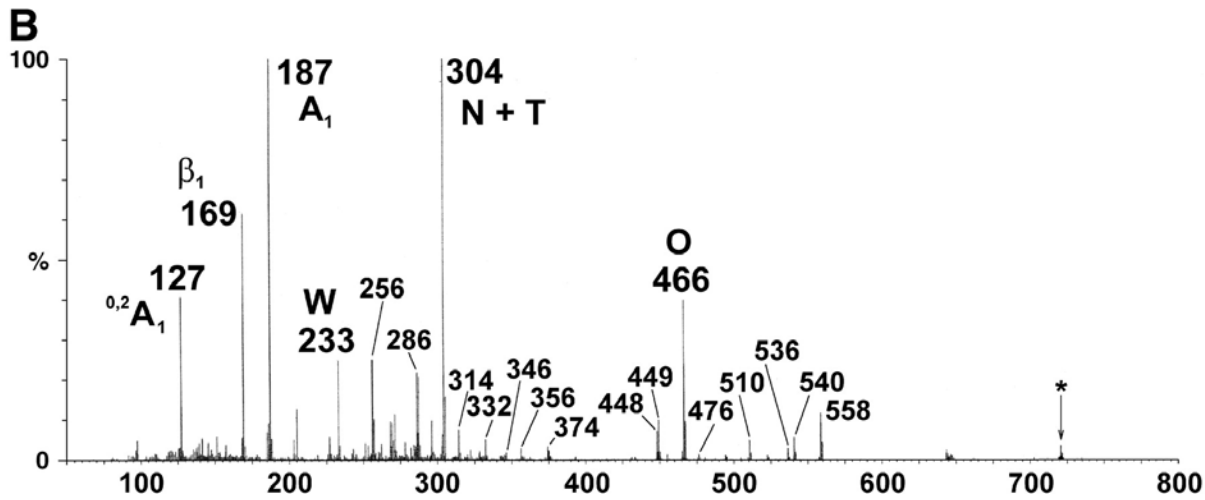

Fig. 5B. Tandem +ESI-MS/CID-MS product ion spectra of selected [M+Li]+ from a *N. crassa* MUT16 GlcCer fraction. A: Product ion spectrum from *m/z* 734. B: Product ion spectrum from *m/z* 720.

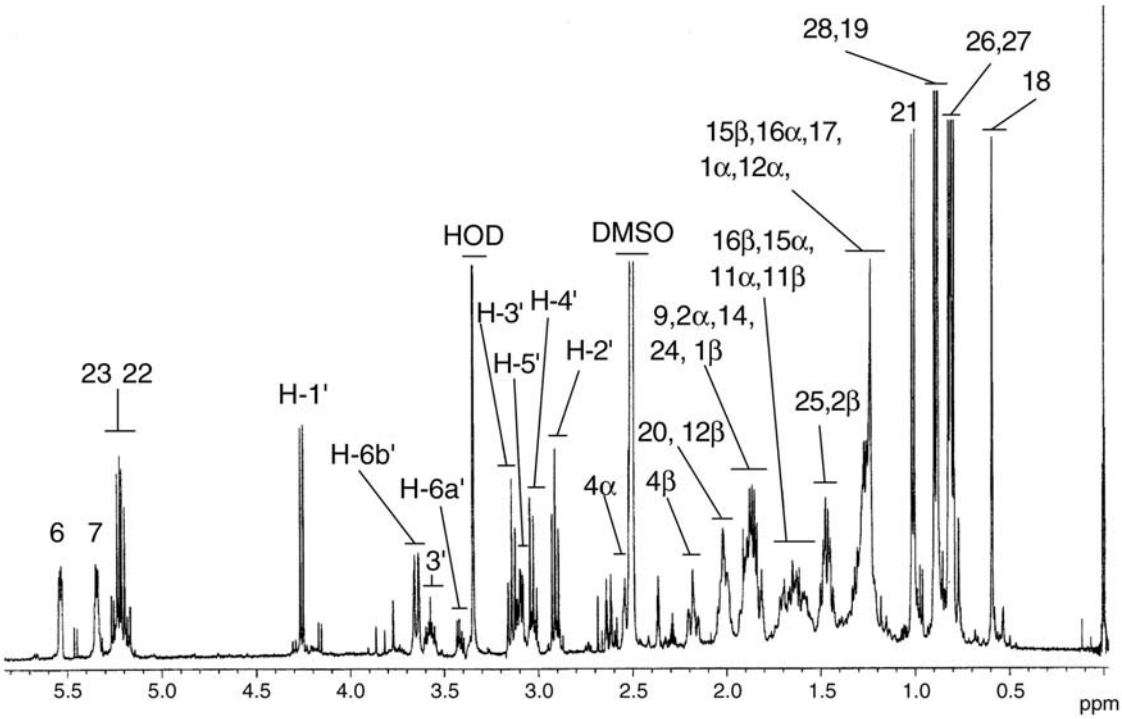

Fig. 6. One-dimensional 1H-NMR spectrum of a GlcSte fraction isolated from *N. crassa* MUT24. Resonances from nonexchangeable protons of sterol (prefix omitted) and hexose (H) are designated by Arabic numerals, and those of the latter are primed. The corresponding structure and numbering are depicted in Scheme 2. HOD, residual monodeuterated water.

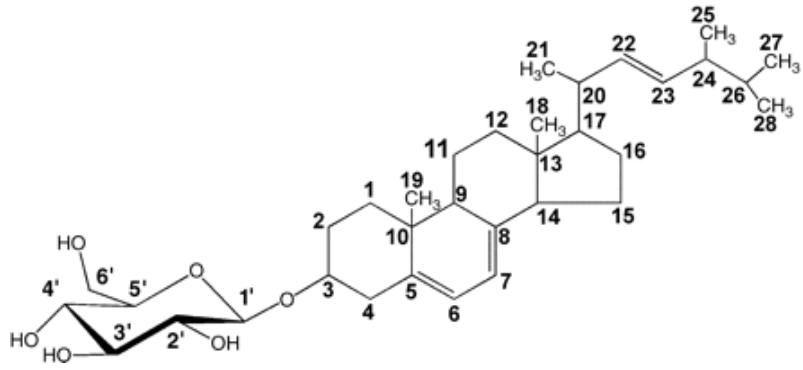

Scheme 3. Structure of ergosterol-ß-D-glucopyranoside with numbering of sterol and hexose moieties.

Reference

1. Thomma, B. P. H. J., B. P. A. Cammue, and K. Thevissen. 2002. Plant defensins. *Planta.* **216:** 193–202.

2. Broekaert, W. F., B. P. A. Cammue, M. F. C. De Bolle, K. Thevissen, G. W. De Samblanx, and R. W. Osborn. 1997. Antimicrobial peptides from plants. *Crit. Rev. Plant Sci.* **16:** 297–323.

3. Thevissen, K., K. K. Ferket, I. E. Francois, and B. P. Cammue. 2003. Interactions of antifungal plant defensins with fungal membrane components. *Peptides.* **24:** 1705–1712.

4. Hoffmann, J. A. 1995. Innate immunity of insects. *Curr. Opin. Immunol.* **7:** 4–10.

5. Ganz, T. 2003. Defensins: antimicrobial peptides of innate immunity. *Nat. Rev. Immunol.* **3:** 710–720.

6. Bulet, P., C. Hetru, J. L. Dimarcq, and D. Hoffmann. 1999. Antimicrobial peptides in insects. Structure and function. *Dev. Comp. Immunol.* **23:** 329–344.

7. Thevissen, K., A. Ghazi, G. W. De Samblanx, C. Brownlee, R. W. Osborn, and W. F. Broekaert. 1996. Fungal membrane responses induced by plant defensins and thionins. *J. Biol. Chem.* **271:** 15018–15025.

8. Thevissen, K., F. R. Terras, and W. F. Broekaert. 1999. Permeabilization of fungal membranes by plant defensins inhibits fungal growth. *Appl. Environ. Microbiol.* **65:** 5451–5458.

9. Thevissen, K., R. W. Osborn, D. P. Acland, and W. F. Broekaert. 1997. Specific, high affinity binding sites for an antifungal plant defensin on *Neurospora crassa* hyphae and microsomal membranes. *J. Biol. Chem.* **272:** 32176–32181.

10. Thevissen, K., R. W. Osborn, D. P. Acland, and W. F. Broekaert. 2000. Specific binding sites for an antifungal plant defensin from dahlia (*Dahlia merckii*) on fungal cells are required for antifungal activity. *Mol. Plant Microbe Interact.* **13:** 54–61.

11. Ferket, K. K. A., S. B. Levery, C. Park, B. P. A. Cammue, and K. Thevissen. 2003. Isolation and characterization of *Neurospora crassa* mutants resistant to antifungal plant defensins. *Fungal Genet. Biol.* **40:** 176–185.

12. Thevissen, K., I. E. Francois, J. Y. Takemoto, K. K. Ferket, E. M. Meert, and B. P. Cammue. 2003. DmAMP1, an antifungal plant defensin from dahlia (*Dahlia merckii*), interacts with sphingolipids from *Saccharomyces cerevisiae*. *FEMS Microbiol. Lett.* **226:** 169–173.

13. Thevissen, K., D. C. Warnecke, I. E. Francois, M. Leipelt, E. Heinz, C. Ott, U. Zahringer, B. P. Thomma, K. K. Ferket, and B. P. Cammue. 2004. Defensins from insects and plants interact with fungal glucosylceramides. *J. Biol. Chem.* **279:** 3900–3905.

14. Osborn, R. W., G. W. De Samblanx, K. Thevissen, I. Goderis, S. Torrekens, F. Van Leuven, S. Attenborough, S. B. Rees, and W. F. Broekaert. 1995. Isolation and characterisation of plant defensins from seeds of Asteraceae, Fabaceae, Hippocastanaceae and Saxifragaceae. *FEBS Lett.* **368:** 257–262.

15. Thevissen, K., B. P. Cammue, K. Lemaire, J. Winderickx, R. C. Dickson, R. L. Lester, K. K. Ferket, F. Van Even, A. H. Parret, and W. F. Broekaert. 2000. A gene encoding a sphingolipid biosynthesis enzyme determines the sensitivity of *Saccharomyces cerevisiae* to an antifungal plant defensin from dahlia (*Dahlia merckii*). *Proc. Natl. Acad. Sci. USA.* **97:** 9531–9536.

16. Dickson, R. C., E. E. Nagiec, G. B. Wells, M. M. Nagiec, and R. L. Lester. 1997. Synthesis of mannose-(inositol-P)$_2$-ceramide, the major sphingolipid in *Saccharomyces cerevisiae*, requires the *IPT1* (*YDR072c*) gene. *J. Biol. Chem.* **272:** 29620–29625.

17. Terras, F. R., H. M. Schoofs, M. F. De Bolle, F. Van Leuven, S. B. Rees, J. Vanderleyden, B. P. Cammue, and W. F. Broekaert. 1992. Analysis of two novel classes of plant antifungal proteins from radish (*Raphanus sativus* L.) seeds. *J. Biol. Chem.* **267:** 15301–15309.

18. Leipelt, M., D. Warnecke, U. Zahringer, C. Ott, F. Muller, B. Hube, and E. Heinz. 2001. Glucosylceramide synthases, a gene family responsible for the biosynthesis of glucosphingolipids in animals, plants, and fungi. *J. Biol. Chem.* **276:** 33621–33629.

19. Toledo, M. S., E. Suzuki, A. H. Straus, and H. K. Takahashi. 1995. Glycolipids from *Paracoccidioides brasiliensis*. Isolation of a galactofuranose-containing glycolipid reactive with sera of patients with paracoccidioidomycosis. *J. Med. Vet. Mycol.* **33:** 247–251.

20. Toledo, M. S., S. B. Levery, A. H. Straus, E. Suzuki, M. Momany, J. Glushka, J. M. Moulton, and H. K. Takahashi. 1999. Characterization of sphingolipids from

mycopathogens: factors correlating with expression of 2-hydroxy fatty acyl (*E*)-Δ^3-unsaturation in cerebrosides of *Paracoccidioides brasiliensis* and *Aspergillus fumigatus*. *Biochemistry*. **38:** 7294–7306.

21. Levery, S. B., M. Momany, R. Lindsey, M. S. Toledo, J. A. Shayman, M. Fuller, K. Brooks, R. L. Doong, A. H. Straus, and H. K. Takahashi. 2002. Disruption of the glucosylceramide biosynthesis pathway in *Aspergillus nidulans* and *Aspergillus fumigatus* by inhibitors of UDP-Glc:ceramide glucosyltransferase strongly affects spore germination, cell cycle, and hyphal growth. *FEBS Lett.* **525:** 59–64.

22. Dabrowski, J., P. Hanfland, and H. Egge. 1980. Structural analysis of glycosphingolipids by high-resolution ^{1}H nuclear magnetic resonance spectroscopy. *Biochemistry.* **19:** 5652–5658.

23. Yamada, A., J. Dabrowski, P. Hanfland, and H. Egge. 1980. Preliminary results of *J*-resolved, two-dimensional ^{1}H-NMR studies on glycosphingolipids. *Biochim. Biophys. Acta.* **618:** 473–479.

24. Dabrowski, J., H. Egge, and P. Hanfland. 1980. High resolution nuclear magnetic resonance spectroscopy of glycosphingolipids. I. 360 MHz ^{1}H and 90.5 MHz ^{13}C NMR analysis of galactosylceramides. *Chem. Phys. Lipids.* **26:** 187–196.

25. Levery, S. B., M. S. Toledo, R. L. Doong, A. H. Straus, and H. K. Takahashi. 2000. Comparative analysis of ceramide structural modification found in fungal cerebrosides by electrospray tandem mass spectrometry with low energy collision-induced dissociation of Li^+ adduct ions. *Rapid Commun. Mass Spectrom.* **14:** 551–563.

26. Toledo, M. S., S. B. Levery, E. Suzuki, A. H. Straus, and H. K. Takahashi. 2001. Characterization of cerebrosides from the thermally dimorphic mycopathogen *Histoplasma capsulatum*: expression of 2-hydroxy fatty *N*-acyl (*E*)-Δ^3-unsaturation correlates with the yeast-mycelium phase transition. *Glycobiology.* **11:** 113–124.

27. Hsu, F-F., and J. Turk. 2001. Structural determination of glycosphingolipids as lithiated adducts by electrospray ionization mass spectrometry using low-energy collisional-activated dissociation on a triple stage quadrupole instrument. *J. Am. Soc. Mass Spectrom.* **12:** 61–79.

28. Warnecke, D., R. Erdmann, A. Fahl, B. Hube, F. Muller, T. Zank, U. Zahringer, and E. Heinz. 1999. Cloning and functional expression of UGT genes encoding sterol glucosyltransferases from *Saccharomyces cerevisiae*, *Candida albicans*, *Pichia pastoris*, and *Dictyostelium discoideum*. *J. Biol. Chem.* **274:** 13048–13059.

29. Sakaki, T., U. Zahringer, D. C. Warnecke, A. Fahl, W. Knogge, and E. Heinz. 2001. Sterol glycosides and cerebrosides accumulate in *Pichia pastoris*, *Rhynchosporium secalis* and other fungi under normal conditions or under heat shock and ethanol stress. *Yeast.* **18:** 679–695.

30. Kiarash, A., B. Boyd, and C. A. Lingwood. 1994. Glycosphingolipid receptor function is modified by fatty acid content. Verotoxin 1 and verotoxin 2c preferentially recognize different globotriaosyl ceramide fatty acid homologues. *J. Biol. Chem.* **269:** 11138–11146.

31. Lingwood, C. A. 1996. Aglycone modulation of glycolipid receptor function. *Glycoconj. J.* **13:** 495–503.

32. Sweigard, J. A., A. M. Carroll, L. Farrall, F. G. Chumley, and B. Valent. 1998. *Magnaporthe grisea* pathogenicity genes obtained through insertional mutagenesis. *Mol. Plant Microbe Interact.* **11:** 404–412.

33. Kim, Y. K., Y. Wang, Z. M. Liu, and P. E. Kolattukudy. 2002. Identification of a hard surface contact-induced gene in *Colletotrichum gloeosporioides* conidia as a sterol glycosyl transferase, a novel fungal virulence factor. *Plant J.* **30:** 177–187.

34. Warnecke, D., and E. Heinz. 2003. Recently discovered functions of glucosylceramides in plants and fungi. *Cell. Mol. Life Sci.* **60:** 919–941.

35. Barreto-Bergter, E., M. R. Pinto, and M. L. Rodrigues. 2004. Structure and biological functions of fungal cerebrosides. *An. Acad. Bras. Cienc.* **76:** 67–84.

36. Stasyk, O. V., T. Y. Nazarko, O. G. Stasyk, O. S. Krasovska, D. Warnecke, J. M. Nicaud, J. M. Cregg, and A. A. Sibirny. 2003. Sterol glucosyltransferases have different functional roles in *Pichia pastoris* and *Yarrowia lipolytica*. *Cell Biol. Int.* **27:** 947–952.

37. Oku, M., D. Warnecke, T. Noda, F. Muller, E. Heinz, H. Mukaiyama, N. Kato, and Y. Sakai. 2003. Peroxisome degradation requires catalytically active sterol glucosyltransferase with a GRAM domain. *EMBO J.* **22:** 3231–3241.

38. Altschul, S. F., W. Gish, W. Miller, E. W. Myers, and D. J. Lipman. 1990. Basic local alignment search tool. *J. Mol. Biol.* **215:** 403–410.

39. Galagan, J. E., S. E. Calvo, K. A. Borkovich, E. U. Selker, N. D. Read, D. Jaffe, W. FitzHugh, L.-J. Ma, S. Smirnov, S. Purcell et al. 2003. The genome sequence of the filamentous fungus *Neurospora crassa*. *Nature* **422:** 859–868.

40. Domon, B., and C. E. Costello. 1988. Structure elucidation of glycosphingolipids and gangliosides using high-performance tandem mass spectrometry. *Biochemistry.* **27:** 1534–1543.

41. Domon, B., J. E. Vath, and C. E. Costello. 1990. Analysis of derivatized ceramides and neutral glycosphingolipids by high-performance tandem mass spectrometry. *Anal. Biochem.* **184:** 151–164.

42. Costello, C. E., and J. E. Vath. 1990. Tandem mass spectrometry of glycolipids. *Methods Enzymol.* **193:** 738–768.

43. Adams, J., and Q. Ann. 1993. Structure determination of sphingolipids by mass spectrometry. *Mass Spectrom. Rev.* **12:** 51–85.